THE UNIVERSITY *of* EDINBURGH

An investigation of murine cytomegalovirus modulation of TLR/IL-1β signalling pathways

Tali Pechenick Jowers

s0454275

A thesis presented in fulfilment of requirements for the degree of
Doctor of Philosophy,
The University of Edinburgh

2012

Supervisors:

Prof. Peter Ghazal, Prof. Jürgen Haas, Prof. Keith Fox

Declaration of Authorship

I hereby declare that this thesis is of my own composition, and that it contains no material previously submitted for the award of any other degree. The work reported in this thesis has been executed by myself, except where due acknowledgement is made in the text.

Tali Pechenick Jowers

Abstract

Cytomegaloviruses (CMV), the prototypical β-herpesviruses, have co-evolved with their hosts and thus acquired multiple strategies for modulation of the immune response. Viral engagement of pattern recognition receptors (PRR), such as toll-like receptors (TLRs) and cytosolic nucleic acids sensors, initiates the host immune response through activation of elaborate signalling programs. The ensuing inflammatory response is further sustained and amplified through cytokines, such as IL-1β, activating signalling pathways greatly overlapping those utilized by TLRs. The central hypothesis of this thesis is that a viral counter-measure by murine CMV (MCMV) involves specific targeting of TLR- and IL-1β-induced signalling along the MyD88 to NF-κB pathway. To test this hypothesis MCMV inhibition of IL-1β signalling was initially investigated in a fibroblast cell line. It was demonstrated that in MCMV infected cells IL-1β-induced IκBα degradation is largely inhibited. Comparison of productive and non-productive infection showed this modulation requires de-novo viral gene expression beyond the immediate early region. Further investigations utilising a ORF M45 deletion mutant identified viral gene M45 as necessary for mediating the observed modulation of IL-1β-induced IκBα degradation. To further test the hypothesis, studies were extended to include TLR stimulation in the context of bone marrow-derived macrophages (BMDM) infection. It was found that TLR7/9-induced NF-κB activation is inhibited in MCMV infected BMDM. Overall, data presented in this study demonstrate a previously unrecognised MCMV inhibition of IL-1β- and TLR7/9-induced NF-κB activation, and indicate a role for viral gene M45 in mediating this effect.

Acknowledgements

Firstly, thank you to Prof Peter Ghazal for providing scientific and financial support for this thesis and for his encouragement throughout. I would also like to thank Dr Paul Dickinson whose scientific opinion I value greatly and who was always available for discussions. Thank you also goes to Prof Jürgen Haas for guidance at the beginning of the work and for the opportunity to work with his group, especially Dr Even Fosum, who was extremely helpful.

Thank you to the Welcome Trust for the generous financial support including during my maternity leave.

Special thanks to Marilyn Horne, Marie Craigon and Alan Ross for providing support in many different forms. Thank you to many other members of the DPM for creating a lovely work environment. Special thanks to Dr Kevin Robertson from whom I have learned a lot and have always enjoyed working with.

Diwakar Santha Kumar and Nouf Nasser Mohammad Laqtom for always being there to help (evening, Christmas and coming especially back to lab from home). Your welcoming smiles always make me feel better.

To Kim Martin for being a friend and partner for afternoon walks.

To Dr Samantha Griffiths for invaluable feedback on this manuscript, encouragement and for being a dear friend and colleague.

To my friends in Israel including Taly Fiegenbaum Peri, Renana Petoka, Dorit Cohen and Oren Carmeli. Even with the geographical distance and not so frequent talks I feel you encouraging me in what ever I do.

Most importantly thank you to my parents who always believe in me and support me to follow my dreams. You are amazing parents. This also goes to my sisters and brother – I am blessed to have you.

Last, but contrary to least, thank you to the love of my life, my husband Christian Jowers, and to the light of my life, my son Gabriel Pechenick Jowers. Gabriel- the fundamental experiment which started this work was performed on the weekend I found out I was pregnant with you. This thesis is at least partially yours, after all you worked with me in the lab for 9 months. You are the most amazing child. My dear husband, I have put you through a lot while working on this PhD and you were always there amazingly supportive. Mi amor, no words exist to describe my feelings for you and how amazing you are.

Table of Contents

List of Figures

List of Tables

Chapter 1- Introduction

Chapter 2: Materials and Methods

Abbreviations

AIDS	Acquired immune deficiency syndrome
AIM2	Absent in melanoma 2
ASC	Apoptosis-associated speck-like protein containing a CARD
APS	Ammonium persulfate
BAC	Bacterial artificial chromosome
BSA	Bovine serum albumin
BMDM	Bone marrow-derived macrophage
°C	Degrees Celsius
C57BL/6	C57 black 6 laboratory mouse strain
cDCs	Conventional dendritic cells
CHX	Cyclohexmide
CMV	Cytomegalovirus
CNS	Central nervous system
CPE	Complete cytopathic effect
CS	Calf serum
CSF-1	Colony-stimulating factor-1
DAI	DNA-dependent activator of IFN-regulatory factors
DC	Dendritic cell
DMEM	Dulbecco's Modified Eagle Medium
DMSO	Dimethyl sulfoxide
DNA	Deoxyribonucleic acid

ds	Double stranded
ECL	Enhanced chemiluminescence
EDTA	Ethylenediaminetetraacetic acid
EGFP	Enhanced green fluorescent protein
ELISA	Enzyme-linked immunosorbent assay
FACS	Fluorescence-activated cell sorting
FCS	Fetal calf serum
HA	Hemagglutinin
HI	Heat-inactivated
HIV	Human immunodeficiency virus
HCMV	Human cytomegalovirus
hpi	Hours post infection
HRP	Horseradish peroxidase
HSPGs	Heparan sulfate proteoglycans
HSV	Herpes simplex virus
IE	Immediate early
IFN	Interferon
IL-1β	Interleukin-1β
IL-1F	Interleukin-1 family
IL-1R	Interleukin-1 receptor
IL-1RAP	IL-1R Accessory protein
IL-6	Interleukin-6
IKK	IκB kinase

iMO	Inflammatory monocytes
IRAK	IL-1R Associated kinase
IRF3	Interferon regulatory factor 3
JNK	c-Jun amino (N)-terminal kinase
Kb	Kilobase
kDa	Kilodalton
LB	Luria-Bertani
LPS	Lipopolysaccharide
LRR	Leucine-rich repeat domain
MAPKs	Mitogen-activated protein kinases
MCMV	Murine cytomegalovirus
MEF	Mouse embryonic fibroblasts
MIEP	Major immediate-early promoter
ml	Millilitre
MOI	Multiplicity of infection
MW	Molecular weight
MyD88	Myeloid differentiation primary response protein 88
NF-κB	Nuclear Factor-KappaB
NLR family	Nucleotide-binding domain leucine-rich repeats family
ODN	Oligodeoxynucleotide
ORF	Open reading frame
PAMP	Pathogen associated molecular pattern
PBS	Phosphate buffered saline

pDC	Plasmacytoid dendritic cells
PFA	Paraformaldehyde
PFU	Plaque forming unit
Pg	Picogram
PRR	Pattern recognition receptor
PYHIN family	Pyrin and NIH domain-containing protein family
RHIM	RIP homotypic interaction motif
RIP	Receptor interacting protein
RNA	Ribonucleic acid
Rpm	Revolutions per minute
SDS	Sodium dodecyl sulphate
SDS-PAGE	Sodium dodecyl sulfate polyacrylamide gel electrophoresis
ss	Single stranded
TAB1	Adaptor proteins TAK1-binding protein 1
TAK1	TGF-β-activated kinase 1
TBS	Tris buffered saline
TBS-T	Tris-buffered saline-Tween
TE	Tris-EDTA
TIR domain	Toll/IL (interleukin)-1 domain
TIRAP	TIR domain-containing adapter protein
TLR	Toll-like receptor
TNF	Tumor necrosis factor
TRAM	TRIF-related adaptor molecule

TRIF	TIR domain-containing adaptor inducing IFN-β
UBD	Ubiquitin binding domain
UV	Ultraviolet
v/v	volume/volume
WT	Wild-type
w/v	weight/volume
µg	Microgram
µl	Microlitre
µM	Micromolar

1 Chapter 1

Introduction

1.1 Family *Herpesviridae*: A brief overview

Herpesviridae is a large family of viruses, with over 200 members identified thus far, highly disseminated in nature. Inclusion in the family *Herpesviridae* has been historically based on virion architecture consisting of: a linear double-stranded DNA (varying in length from 124 to 230 kb), icosahedral capsid (approximately 125 nm in diameter), tegument (amorphous, sometime asymmetric material surrounding the capsid) and an envelope. Members of this family share four key biological properties:

a) Their genome encodes enzymes involved in nucleic acid metabolism, DNA synthesis and protein processing.

b) DNA replication as well as capsid assembly takes place in the nucleus.

c) Lytic infection results in destruction of the infected cells.

d) Establishment of latency following primary infection of the natural host.

The family *Herpesviridae* is further divided into three subfamilies, *alpha/beta/gamma-herpesvirinae*, with human pathogens represented in each (Table 1.1).

Table 1.1: Biological characteristics of the three subfamilies of herpesviruses *

Characteristic	*Alphaherpesvirinae*	*Betaherpesvirinae*	*Gammaherpesvirinae**
Host range	Variable, often broad	Restricted	Limited to family of natural host
Reproductive cycle	Short	Long	Relatively long
Infection in cell culture	Spreads rapidly, Infects many cell types	Progresses slowly	Infects primarily lymphoblastoid cells
Cytotoxicity	Much cell destruction	Enlarged cells form	Some lytic infections of the epithelial and fibroblasts cells
Latency	Primarily in sensory cells	Maintained in many cells including secretory glands, lymphoreticular cells, kidneys, and others	Specific for either B or T lymphocytes
Viruses pathogenic in humans **	-- HHV-1 (Herpes simplex virus 1 (HSV-1)) -- HHV-2 (Herpes simplex virus 2 (HSV-2)) -- HHV-3 (Varicella-zoster virus (VZV)	-- HHV-5 (Cytomegalovirus) -- HHV-6 -- HHV-7	-- HHV-4 (Epstein-Barr virus (EBV)) -- HHV-8 (Kaposi's sarcoma-associated HV (KSHV))

* Adapted from: (James H. Strauss, 2008) (Philip E. Pellett, 2006)

** For each virus both the official designation (HHV = Human herpes virus + number) and vernacular name are given.

1.2 Cytomegaloviruses (CMVs)

1.2.1 Human CMV (HCMV) overview and pathogenesis

HCMV, a characteristic betaherpesvirus, is ubiquitously present in the human population. Overall prevalence of infection, however, varies greatly in accordance with socioeconomic circumstances. Worldwide prevalence of HCMV among women of child bearing age varies from 45 to 100% (Cannon et al., 2010). Horizontal transmission of the virus occurs via direct contact with bodily secretions such as blood, saliva and urine, semen and cervical secretions, and as a result of solid-organ transplantation or haematopoietic stem-cell transplantation. Additionally, HCMV can also be vertically transmitted from mother to fetus or new born (Gandhi and Khanna, 2004). Primary infection of an immunocompetent host is usually asymptomatic, however, may present clinically as mononucleosis syndrome with persistent fever, myalgia, and cervical adenopathy (Gandhi and Khanna, 2004). Importantly, following the resolution of acute infection life-long viral latency is established. Reactivation from latency under conditions of immunosuppression (for example following organ transplant) or immunodeficiency (as in the case of acquired immune deficiency syndrome (AIDS) patients) is a major contributor to HCMV-related disease burden. As a result, much research effort is directed at understanding latency including identification of cells serving as latent virus reservoirs, mapping latency at a molecular level, understanding the factors (at the cellular and immune system level) that maintain latency or promote reactivation (Mocarski, 2006) (Reddehase et al., 2002). In contrast to immunocompetent hosts, primary infection or reactivation in immunocompromised individuals can result in

serious morbidity or death. Manifestation of HCMV-associated disease differs and depends on the particular clinical setting. Pneumonitis and gastrointestinal disease are the most common complications of cytomegalovirus infection following haematopoietic stem-cell transplantation. In solid-organ transplant recipients HCMV-related morbidity can be caused by (a) an acute, systemic, febrile illness (sometimes referred to as CMV syndrome), (b) effects on specific organs, or (c) indirect effects including graft rejection, accelerated coronary artery atherosclerosis (heart transplant) and enhanced susceptibility to other opportunistic infections. In the case of AIDS patients the most frequent clinical manifestation of HCMV disease is retinitis. HCMV has also been suspected of accelerating the time to AIDS and death in patients with Human Immunodeficiency Virus (HIV) infection (Mocarski, 2006). Additional substantial and severe disease burden is caused by congenital HCMV infection. Congenital HCMV infection is symptomatic in about 5% to 10% of newborns of which about 10% suffer from severe and even fatal disease. Moreover, congenital CMV infection results in damage to the central nervous system (CNS) and organs of perception in 50% to 90% of symptomatic newborns. Importantly, CNS sequelae, mainly hearing loss, also develops in 7% to 25% of infants who are asymptomatic at birth (Pass, 2001). Finally, a correlation between HCMV and diseases such as immunosenescence and athrosclerosis has been suggested, however more research is required to establish the role, if any, of the virus in the pathogenesis of these conditions (Mocarski, 2006) (Boeckh and Geballe, 2011).

1.2.2 Murine CMV (MCMV) as a model for HCMV

Experimental studies of HCMV pathogenesis are limited by the strict species specificity of the virus. Despite considerable evolutionary divergence within the betaherpesvirinae family, MCMV has proven an invaluable model for the study of HCMV (McGeoch et al., 2006) (Mocarski, 2004). MCMV and HCMV share roughly 80 homologous open reading frames (ORFs), about half of the estimated number of ORFs encoded by these viruses. Approximately 40 of these are conserved across the herpesvirus family (Brocchieri et al., 2005) (Rawlinson et al., 1996). More importantly, pathogenesis of MCMV infection of mice resembles that of HCMV in its natural host (Krmpotic et al., 2003) (Price and Olver, 1996) (Scalzo et al., 2007). Therefore, this model system allows the of study virus/host interactions in a physiologically relevant context. However, it is important to consider that conserved viral strategies for modulation of host response may be mediated by different viral products of the two viruses as well as differ in underlying mechanisms (Mocarski, 2004).

1.2.3 HCMV and MCMV virion structure and replication

Key features of HCMV and MCMV virion structure and replication are shared across the herpesvirus family. The following overview focuses on HCMV however the principles described apply to MCMV.

1.2.3.1 Virion structure

As mentioned above herpesviruses all share a characteristic virion structure. The approximately 235 kbp, double-stranded DNA genome of HCMV is packaged in a linear form within a 125 nm icosahedral nucleocapsid (Mocarski, 2006). The nucleocapsid is embedded within a protein matrix termed the tegument. Upon infection tegument proteins are released into the cytoplasm of the infected cell and play a role in multiple viral processes including delivery of viral genomes to the nucleus, regulation of gene expression and modulation of host immune responses (Kalejta, 2008). Finally, the nucleocapsid and tegument are engulfed by a lipid bilayer envelope, derived from cellular membranes, containing virus-encoded glycoproteins (Mocarski, 2006). HCMV particles have also been shown to contain cellular and viral RNA (Bresnahan and Shenk, 2000) (Terhune et al., 2004). The overall size of the HCMV virion is 200 to 300 nm in diameter (Figure 1.1).

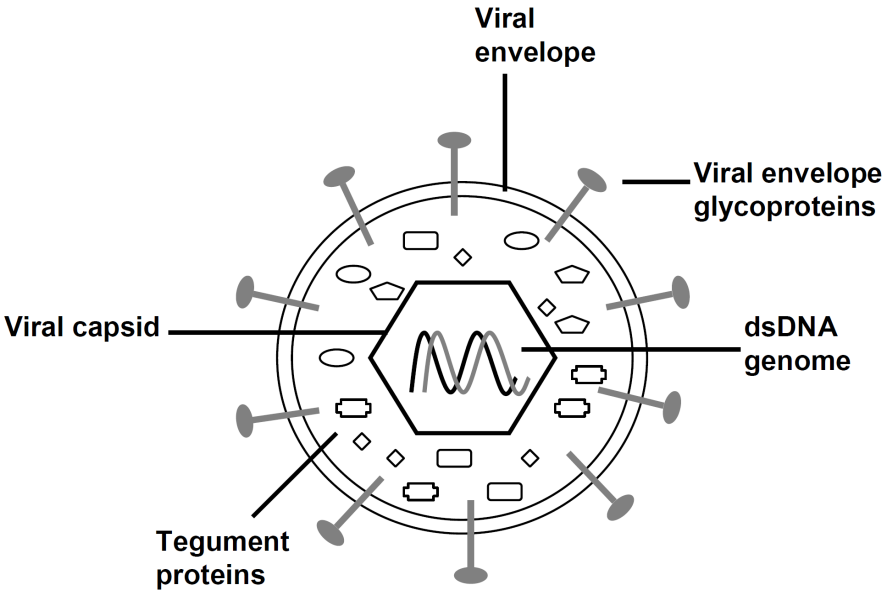

Figure 1.1: The CMV virion. A schematic representation (not to scale) of an average CMV virion.

1.2.3.2 Replication

For the purposes of this overview the replication cycle will be divided into following steps: a) attachment and entry, b) gene expression and DNA replication, c) capsid assembly, egress and release (Figure 1.2).

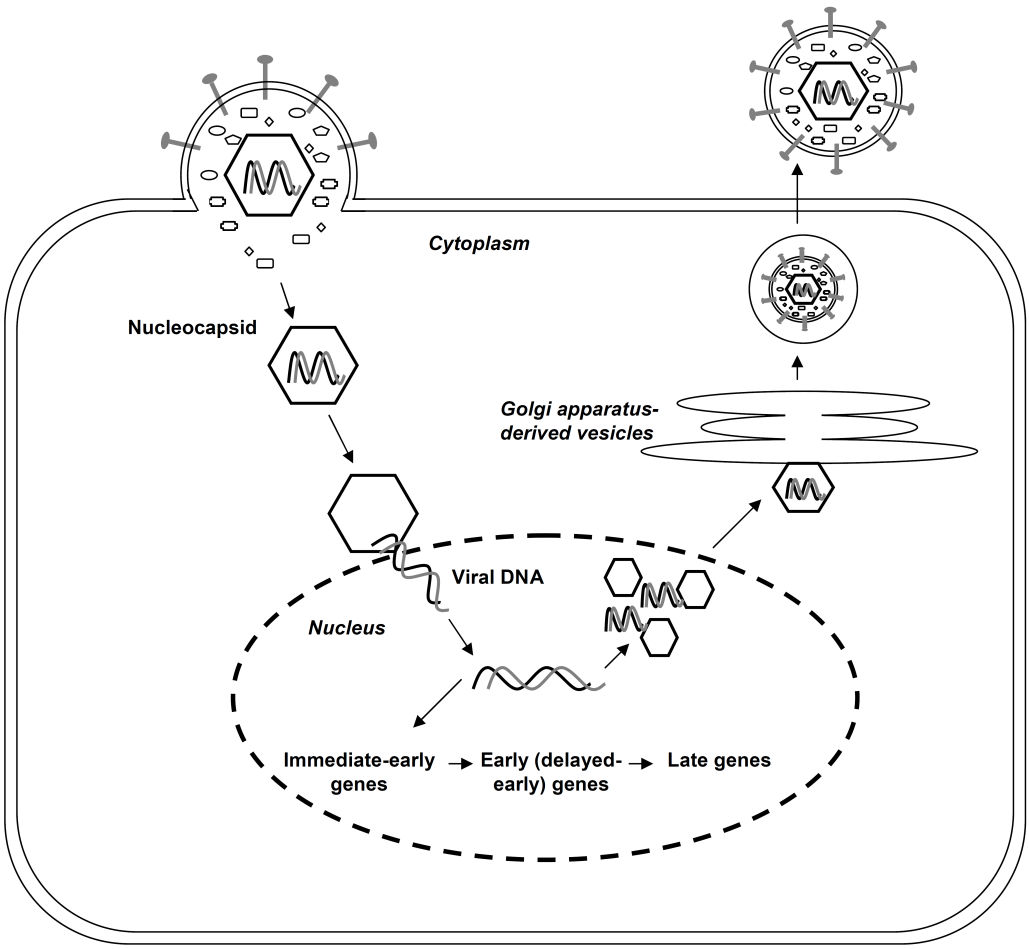

Figure 1.2: A schematic representation of key features of CMV replication. The virus enters the cell via direct fusion of viral envelope and cellular plasma membrane leading to the release of nucleocapsid and tegument proteins into the cytoplasm. The capsid is then shuttled, along microtubules, to the nuclear pore complex and viral DNA is delivered into the nucleus. Transcription of viral genes begins immediately with immediate-early (IE) genes are transcribed first, followed by early (E, also called delayed-early) genes and finally late (L) genes (cytoplasmic translation is not depicted). Viral DNA is replicated and encapsidated in the nucleus. Initially a procapsid shell is formed to which genome-length segment of viral DNA is inserted to produce a filled nucleocapsid. Nucleocapsids egress from the nucleus through sequential budding and fusion with the inner and outer nucleic membranes, respectively (not depicted). This results in non-enveloped nucleocapsids in the cytoplasm which then re-enveloped as they bud into Golgi apparatus-derived vesicles containing viral glycoproteins. A cellular vesicle engulfing a fully formed virion is thus formed. Release of the virion is completed through shuttle of the virion-containing vesicle to the cell surface followed by fusion of vesicle and plasma membranes. This resulted in the release of a mature virion from the cell (variation in capsid or virion sizes appearing in the figure are due to presentation needs only).

Attachment and Entry

Herpesviruses enter the cell via direct fusion of viral envelope and cellular plasma membrane. In the case of HCMV this process is mediated by binding of viral envelope glycoproteins to cell surface receptors. This allows the fusion of viral and cellular membranes resulting in introduction of the nucleocapsid and tegument proteins into the cytoplasm. The following model has been suggested for HCMV entry into fibroblasts: 1) An initial tethering step of the virion to the cell surface involves interaction of viral homodimers of glycoprotein (g)B (a dimer this complex is referred to as gB) and heterodimers of gM:gN with cellular heparan sulfate proteoglycans (HSPGs). 2) A more stable binding step follows, probably mediated by gB through interaction with an unidentified cellular receptor. 3) Fusion of viral and cellular membranes is mediated by a gH:gL:gO complex along with gB. Cellular integrin heterodimers (α2β1, α6β1, αVβ3) are thought to play a role in both binding and binding/fusion steps of viral entry in a manner depending on gB and gH (Isaacson et al., 2008). Homologous glycoproteins of MCMV have not been investigated with respect to their role in viral attachment and entry. The exception being the positional homolog of HCMV gO, m74 of MCMV, which has recently been shown to function similarly to its HCMV counterpart (Scrivano et al., 2010). HCMV has also been shown to enter specific cells types, such as endothelial and epithelial cells, via endocytosis (Bodaghi et al., 1999) (Ryckman et al., 2006) (Sinzger, 2008).

Gene expression and DNA replication

Following fusion of virion and cell membranes the capsid and tegument proteins are directly released into the cytoplasm. The capsid is then shuttled, likely assisted by tegument proteins, along microtubules to the nuclear pore complex. Viral DNA is then delivered into the nucleus and transcription begins (Kalejta, 2008). CMVs gene transcription occurs in a cascading manner such that immediate-early (IE or α) genes are transcribed first, followed by early (E, also called delayed-early or β) genes and finally late (L or γ) genes (Mocarski, 2006). IE genes are expressed immediately upon entry, independently of de novo synthesis of viral proteins and function in regulating further viral gene transcription. The major IE gene regions of HCMV and MCMV are highly similar. A complex regulatory sequence- the major IE enhancer promoter (MIEP) - controls the transcription of major IE transcripts. Located down-stream of MIEP is a transcriptional unit which gives rise to the alternatively spliced ie1 and ie2 or ie1 and ie3 transcripts in HCMV and MCMV, respectively. The MCMV major immediate-early region also includes an ie2 gene positioned on the opposite side of the enhancer elements and transcribed in the opposite direction in relation to the ie1/ie3 genes (it should not be confused with the HCMV ie2 which is the functional homologue of MCMV ie3) (Busche et al., 2008). Early gene expression requires prior expression of IE functional proteins. Early gene products play a role in diverse processes including viral DNA synthesis and capsid maturation as well as altering host cell and host animal response to infection. L genes are expressed last and can be further subdivided into γ1 (or leaky L) genes, when expression begins after 24 hpi and is resistant to inhibition of

DNA synthesis, and γ2 genes (or true L), when expression is dependent on viral DNA synthesis. Early and late gene products contribute to capsid maturation, DNA encapsidation, virion maturation, and egress from the cell (Mocarski, 2006).

Capsid assembly egress and release

Viral DNA is replicated and encapsidated in the nucleus. Initially a procapsid shell is formed to which genome-length segment of viral DNA is inserted to produce a filled nucleocapsid, the DNA entry portal is then covered by portal capping protein (PCP, encoded by UL75). Nucleocapsids egress and release from the nucleus and cell is a complex process. Initially nucleocapsids undergo envelopment by budding through the inner nuclear membrane. It is thought that this is followed by fusion with the outer nuclear membrane results in deenvelopment and release of nucleocapsids into the cytoplasm. Nucleocapsids are then re-enveloped as they bud into Golgi apparatus-derived vesicles containing viral glycoproteins. A cellular vesicle engulfing a fully formed virion is thus formed. Release of the virion is completed through shuttle of the virion-containing vesicle to the cell surface followed by fusion of vesicle and plasma membranes. This results in the release of a mature virion from the cell (Mettenleiter et al., 2009).

1.3 Pattern recognition receptors and sensing of CMV

Innate immune recognition of pathogens is mediated by germline encoded receptors which detect conserved and invariant features of microorganisms. These receptors are known as pattern recognition receptors (PRRs). Their targets are often referred to as pathogen-associated molecular patterns (PAMPs) although they may be equally present on non-pathogenic microorganisms. Sensing of pathogens via PRRs initiates innate immune activation as well as stimulates and regulates the adaptive immune response (Janeway and Medzhitov, 2002) (Medzhitov, 2007). PRRs, namely members of the Toll-like receptor (TLR) family, Absent in melnoma 2 (AIM2) and DNA-dependent activator of IFN-regulatory factors (DAI), shown to play a role in HCMV/MCMV detection are discussed below.

1.3.1 Toll-like receptors- overview and role in CMV detection

1.3.1.1 Toll-like receptors- overview

TLRs are type I integral membrane glycoproteins with an extracellular leucine-rich repeat domain (LRR) and a cytoplasmic region, conserved also in interleukin-1 receptors (IL-1Rs), known as a Toll/IL (interleukin)-1 (TIR) domain (Akira and Takeda, 2004). To date 10 TLRs are known in humans while 13 TLRs have been identified in mice, although mouse TLR10 is not functional. TLR1-9 are conserved between both species. Collectively TLRs have been shown to detect PAMPs from bacteria, viruses, parasites and fungi (see summary in Table 1.2) (Kawai and Akira, 2010). TLRs are presents both

on the cell surface (TLR1, TLR2, TLR4, TLR5, TLR6, TLR11) as well in endosomal compartments (TLR3, TLR7-10) (Takeuchi and Akira, 2010).

Table 1.2: TLRs and their Ligands (adapted from (Takeuchi and Akira, 2010))

TLR	Ligand	Origin of the Ligand
TLR1	Traicyl lipoprotein	Bacteria
TLR2	Lipoprotein	Bacteria, viruses, parasites, self
TLR3	dsRNA	Viruses
TLR4	LPS	Bacteria,
TLR5	Flagellin	Bacteria
TLR6	Diacyl lipoprotein	Bacteria, viruses
TLR7 (human TLR8)	ssRNA	Viruses, bacteria, self
TLR9	CpG-DNA	Viruses, bacteria, protozoa, self
TLR10	Unknown	Unknown
TLR11	Profilin-like molecule	Protozoa

1.3.1.2 TLR induced responses

TLR engagement by their cognate PAMPs leads to activation of nuclear factor -κB (NF-κB) and mitogen-activated protein kinases (MAPKs) resulting in the secretion of inflammatory cytokines. In addition, secretion of type I interferons (IFN) is stimulated in a TLR and cell specific manner (Figure 1.3) (Kawai and Akira, 2011). TLRs signal via their cytoplasmic TIR domain which mediates the recruitment of TIR-domain-containing adaptor proteins (i.e., myeloid differentiation primary response protein 88 (MyD88), TIR domain-containing adaptor inducing IFN-β (TRIF), TIR domain-containing adapter protein (TIRAP, also known as MAL), TRIF-related adaptor molecule (TRAM)). TLR signalling is often divided into MyD88-dependent and TRIF-

dependent signalling cascades (O'Neill and Bowie, 2007). All TLRs, except TLR3, require MyD88 for signal transduction i.e. signal in a MyD88-dependent way. MyD88-mediated signalling culminates in NF-κB and MAPKs activation and induction of inflammatory cytokines (Kawai and Akira, 2011). This pathway, which is investigated in this thesis in the context of viral infection, is described in some detail in the next section. In addition, TLR2, TLR7 and TLR9 activate MyD88-dependent, but distinct pathways, to induce type I IFN secretion. Induction of type I IFN responses is cell type restricted. To date TLR7/TLR9 and TLR2 have been shown induce an IFN response in plasmacytoid dendritic cells (pDC) and inflammatory monocytes (iMO), respectively (Barbalat et al., 2009) (Gilliet et al., 2008). TRIF-mediated signalling is induced by TLR3 and TLR4 (TLR4 uniquely utilises both MyD88 and TRIF-dependent signalling). Recruitment of TRIF leads to activation of both interferon regulatory factor 3 (IRF3) and NF-κB. Thus inducing the expression of both inflammatory cytokines and type I IFN (Kawai and Akira, 2010).

Despite great overlap in signalling pathways and transcriptional responses induced by different TLRs, it is thought that the generation of a pathogen tailored response is enabled by multiple mechanisms including: - Selective recruitment of one or more TIR-domain-containing adaptor proteins; - Cell type specific signalling at least partially due to differential expression patterns of TLR as well as signalling modules utilised by them; - Intracellular translocation of TLRs following ligand binding resulting in initiation of distinct signalling pathways or differential response kinetics; - Crosstalk within the TLR

family as well as with other PRRs (Ishii et al., 2008) (Barton, 2008) (O'Neill and Bowie, 2007).

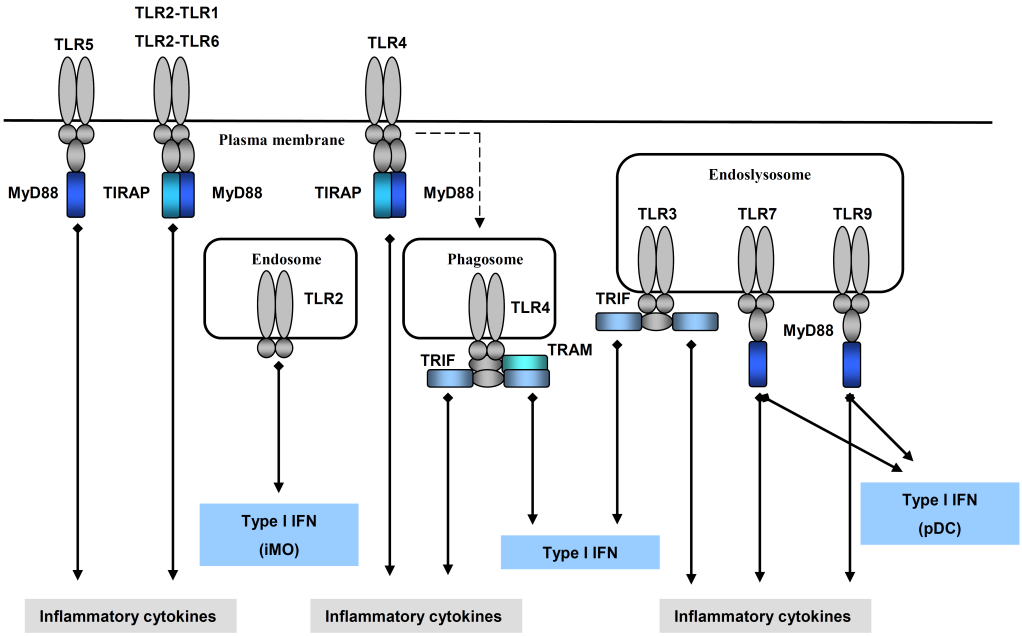

Figure 1.3: TLR induced responses. TLR engagement by their cognate PAMPs leads to recruitment of TIR-domain-containing adaptor proteins: MyD88, TRIF, TIRAP (MAL) and TRAM. All TLRs, except TLR3, signal in a MyD88-dependent way which culminates in NF-κB and MAPKs activation and thus induction of inflammatory cytokines. Stimulation of TLR2, TLR7 and TLR9 additionally results in secretion of type I IFN. This response is cell type restricted- TLR7/TLR9 and TLR2 induce an IFN response in plasmacytoid dendritic cells (pDC) and inflammatory monocytes (iMO), respectively. TLR4, expressed at the cell surface, initially signals in a TIRAP/MyD88 to induce inflammatory cytokines. It is then translocated into phagosomes where it recruits signal adaptors TRAM/TRIF resulting in upregulation of both inflammatory cytokines and type I IFN. TLR3 signals exclusively via TRIF to induce both inflammatory cytokine and type I IFN responses (figure is based on (Kawai and Akira, 2010) (Kawai and Akira, 2011)

1.3.1.3 MyD88-dependent activation of NF-κB and MAPKs

Engagement of all TLRs (except TLR3) by their cognate PAMPs leads to direct or adaptor-protein mediated binding of MyD88. MyD88 serves as a recruitment platform for IL-1R associated kinase 4 (IRAK) followed by IRAK2 and IRAK1 (Kawai and Akira, 2010). Activation of IRAK4 is necessary for NF-κB and MAPK activation, while IRAK1 and IRAK2 are required for the initiation of a robust and sustained TLR response (Suzuki et al., 2002) (Kawagoe et al., 2008). IRAKs form a family of serine/threonine kinases however the exact role of their kinase activity in the context of TLR signalling is complex. Phosphorylation of IRAK1, and possibly IRAK2, results in their dissociation from the receptor complex and subsequent binding to TRAF6 (Flannery and Bowie, 2010). TRAF6 is a ubiquitin E3 ligase which, together with the ubiquitin E2 complex Ubc13/Uev1A, synthesises K63 polyubiquitin chains (Cao et al., 1996) (Deng et al., 2000) (Lomaga et al., 1999) (for overviews of ubiquitination see (Liu and Chen, 2011) (Carpenter and O'Neill, 2009)). This leads to binding and activation of a preformed complex consisting of the kinase TGF-β-activated kinase 1 (TAK1) and adaptor proteins TAK1-binding protein 1 (TAB1), TAB2 or TAB3 (Wang et al., 2001) (Liu and Chen, 2011). This is followed by TAK1 activation of the IκB kinase (IKK) complex (through phosphorylation of its IKKβ subunit) resulting in NF-κB activation (see below). Several proteins have been shown to be poly-ubiquitinated by TRAF6 including TRAF6 itself, IRAK1, IRAK2, TAK1, TAB2 and NEMO. TAB2 and TAB3 contain an ubiquitin binding domain (UBD), which preferentially binds K63 polyubiquitin chains. This binding promotes the autophosphorylation and therefore

activation of TAK1 (Liu and Chen, 2011). However, the exact manner in which K63 polyubiquitin chains regulate TRAF6-TAK1-NEMO interactions is not fully understood (Liu and Chen, 2011). TAK1 also functions initiate a MAPKs activation cascade. It phosphorylates MAPK kinases which in turn phosphorylate and activate the MAPKs-p38 and c-Jun amino (N)-terminal kinases (JNKs). p38 and JNKs then activate various transcription factors and well as influence translation (Cargnello and Roux, 2011) (Kawai and Akira, 2010) (Figure 1.4).

The mammalian nuclear factor-κB (NF-κB) family includes five members: RelA (p65), RelB and c-Rel, and the precursor proteins NF-κB1 (p105) and NF-κB2 (p100), which are processed into p50 and p52, respectively. NF-κB transcription factors form homo- and heterodimers to bind κB sites in promoters or enhancers of targets genes. Transcription of target genes is then regulated through the recruitment of transcriptional co-activators and transcriptional co-repressors (Ghosh and Hayden, 2008). The immediate regulatory circuit of NF-κB consists of IκB proteins and the IκB kinase (IKK) complex. The IKK complex is composed of two catalytically active kinases, IKKα and IKKβ, and the regulatory subunit IKKγ (NEMO). Under resting conditions members of the IκB family, namely IκBα, IκBβ and IκBε, bind and sequester NF-κB dimmers in the cytoplasm. Stimulation, for example by TLRs or cytokines such as IL-1β, leads to activation of the IKK complex which in turn phosphorylates the IκB proteins. This targets IκB proteins for ubiquitination and proteasomal degradation thus releasing NF-κB dimers for nuclear translocation. IKKβ and IKKγ dependent activation of NF-κB is also known as the canonical NF κB activation pathway (Oeckinghaus et al., 2011)

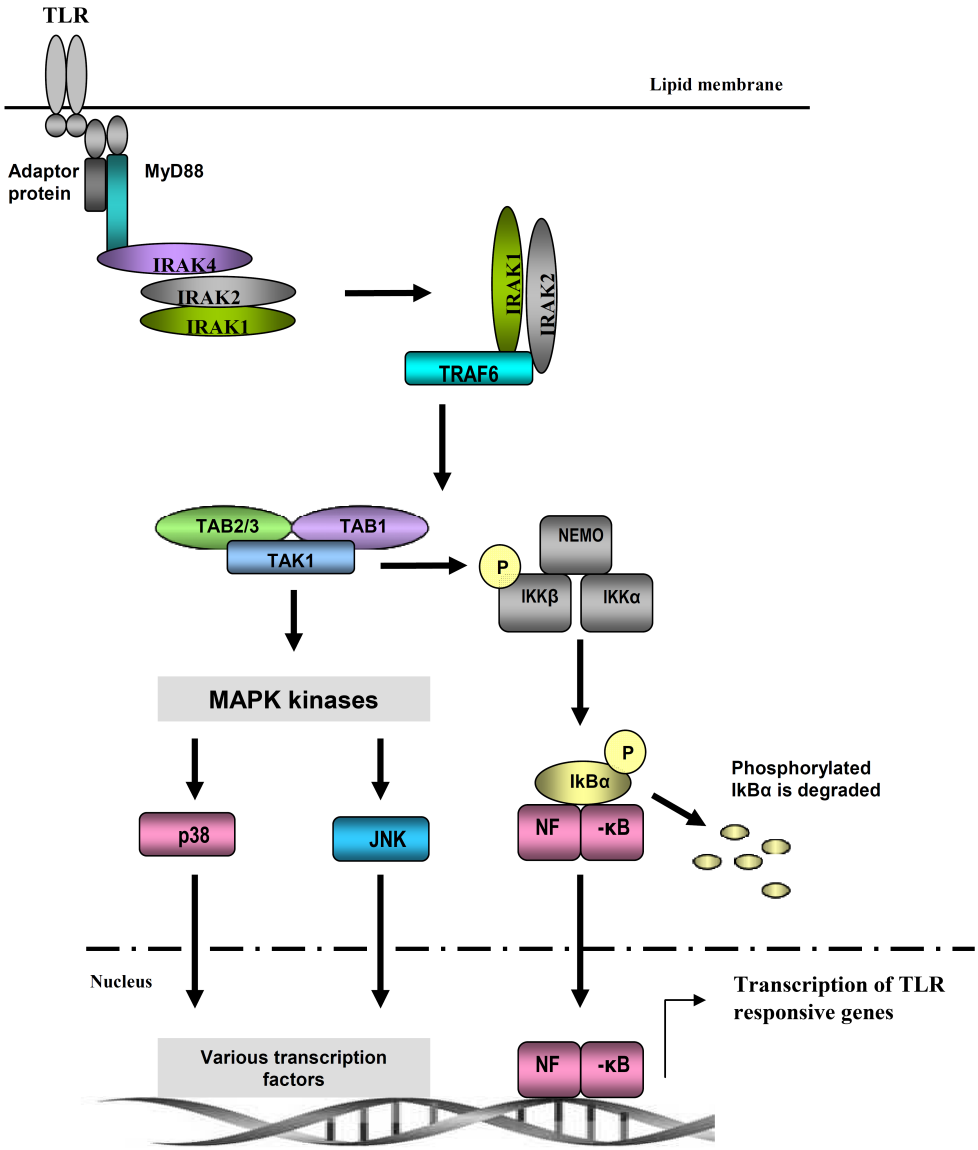

Figure 1.4: MyD88-dependent activation of NF-κB and MAPKs. TLR ligation leads to direct or adaptor-protein mediated binding of MyD88 which serves as a recruitment platform for IRAK4, IRAK2 and IRAK1. Subsequently IRAK1and IRAK2 dissociate from the receptor complex and bind to TRAF6. Next a preformed complex consisting of the TAK1 and adaptor proteins TAB1and TAB2 or TAB3 is recruited. This results in activation of the kinase function of TAK1 which phosphorylates IKKβ and thus activates the IKK complex and subsequently NF-κB. NF-κB translocates to the nucleus where it upregulates the expression of cytokine genes. TAK1 also functions to initiate MAPKs activation cascades leading to further transcription-factor activation.

1.3.1.4 TLRs in CMV detection

Liver transplant patients with a TLR2 polymorphism, which in-vitro shows impaired recognition of viral-envelope protein gB, exhibited significantly higher viral load and increased susceptibility to HCMV disease (Brown et al., 2009) (Kijpittayarit et al., 2007). These findings corroborate earlier studies which suggested that TLR2, probably acting as a heterodimer with TLR1, recognises HCMV resulting in NF-κB activation and cytokine secretion. TLR2 activation by the virus was attributed to recognition of envelope proteins gH and gB (Compton et al., 2003) (Boehme et al., 2006). Earlier studies on the role of TLR2 in MCMV biology failed to detect a difference in viral load in the spleen and it was reported, although the data was not provided, that TLR2 deficiency did not affect mouse resistance to infection (Delale et al., 2005). However, Szomolanyi-Tsuda et al found significantly increased viral load in spleen and liver of TLR2 knock-out mice in comparison to wild type animals. Elevated viral load correlated with reduced cytokine expression and a decrease in numbers of NK cells, but normal functionality, in the organs examined (Szomolanyi-Tsuda et al., 2006). Interestingly, pro-inflammatory cytokine secretion by macrophages and DCs in response to MCMV infection was shown to depend on TLR2 (Barbalat et al., 2009) (Compton et al., 2003). Moreover, TLR2 recognition of MCMV contributed to type I IFN secretion from pDCs (Barbalat et al., 2009).

MCMV systemic infection of TLR9 knock-out (TLR9-/-) animals or mice lacking a functional TLR9 receptor results in increased mortality and elevated viral titres in the

spleen in comparison to wild type animals. In TLR9-/- animals an impaired cytokine response to infection was observed (variation regarding the effect on specific cytokines exists between reports, possibly due to differences in the genetic background of animals used). This correlated with diminished activation of NK cells (key effector cells in innate immunity to CMV (Stipan Jonjic, 2006)) in the absence of TLR9 (Delale et al., 2005) (Krug et al., 2004) (Tabeta et al., 2004). Importantly, TLR9, but not MyD88, was found redundant for anti-viral defence in the liver. Cytokine production (including IFNα) as well as NK cells and macrophage accumulation in the liver were un-affected in TLR9-/- mice. Moreover, viral replication and general virus-induced liver disease were comparable to wild type animals. This was in contrast to finding in spleen suggesting a site specific contribution of TLR9 to localised response to MCMV infection (Hokeness-Antonelli et al., 2007). TLR7 was also found to play a role in host immunity to MCMV. Zucchini et al found higher susceptibility to MCMV-induced death, increased viral load in the spleen and significantly lower serum levels of IFNα in TLR9-/-TLR7-/- in comparison to TLR9 or TLR7 only knock-out animals. Indeed, the phenotype of TLR9-/-TLR7-/- animals with regards to susceptibility to MCMV-induced death recapitulated that of MyD88-/- mice. Thus, suggesting an overlapping function for TLR7 and TLR9 detection of MCMV in host response to infection (Zucchini et al., 2008). It is important to note that while a role for TLR9 and TLR7 in MCMV detection has been demonstrated it is not clear exactly which viral determinants are sensed or what is the mechanism responsible for delivering them into the endosomal compartment in which these TLRs reside (Rathinam and Fitzgerald, 2011).

Finally, TLR3 was found to contribute to the innate immune response to MCMV. Tabeta et al found that in comparison to wild type mice infection of TLR3-/- results in a highly significant increase in viral titres in the spleen and reduced systemic levels of cytokines including type I IFN (Tabeta et al., 2004). Although a study by Delale et al failed to find a role for TLR3 in host response to MCMV (Delale et al., 2005).

1.3.2 AIM2 - overview and role in CMV detection

AIM2, a member of the pyrin and NIH domain-containing protein family (PYHIN family), is a cytosolic dsDNA sensor (Schattgen and Fitzgerald, 2011) (Paludan et al., 2011). Following binding of dsDNA AIM2 initiates the formation of inflammasomes - intracellular multiprotein complexes responsible for cleavage of pro-IL 1β and pro IL-18 into active IL-1β and IL-18, respectively (Rathinam and Fitzgerald, 2010). A role for AIM2 in innate immune sensing of MCMV was demonstrated by Rathinam *et al* (Rathinam et al., 2010). This study found that in comparison to control animals MCMV-infected AIM2-deficient mice exhibited reduced levels of serum IL-18 and lower spleen IFNγ production as well as elevated viral loads in this organ (Rathinam et al., 2010).

1.3.3 DAI - overview and role in CMV detection

DAI (also known as ZBP1 or DLM-1) is a cytoplasmic DNA sensor. It activates the interferon regulatory factor (IRF) and NF-κB transcription factors, leading to type-I interferon production (Takaoka et al., 2007) (Kaiser et al., 2008) (Rebsamen et al.,

2009). Recent studies have implicated DAI in mediating type I IFN production by HCMV-infected fibroblasts (DeFilippis et al., 2010a) (DeFilippis et al., 2010b).

1.4 IL-1β – overview and role in CMV biology

1.4.1 IL-1β overview

Interleukin-1β (IL-1β) is a member of the IL-1 family (IL-1F) of immune-modulators of which 11 members are currently known in humans including IL-1β, IL-1α, IL-1 receptor antagonist (IL-1Ra), IL-18 and IL-33 (Dinarello, 2009). IL-1β and IL-1α are often referred to as IL-1 as both signal through the same receptor complex- IL-1 type I receptor (IL-1RI). However, these two cytokines differ in several ways: 1) IL-1β circulates systemically while IL-1α acts locally; 2) Pattern of expression- IL-1β is mainly produced by monocytes and macrophage while IL-1α is more widely expressed; 3) Transcription of these two genes is differentially regulated both during development and in response to environmental cues; 4) IL-1α can also localise to the nucleus and act as a transcriptional activator (Sims and Smith, 2010). The major source of IL-1β is monocytes, macrophages and dendritic cells. B lymphocytes and NK cells can also produce this cytokine while fibroblasts and epithelial cells generally do not (Dinarello, 2009). Multiple cell types including endothelial and epithelial cells, fibroblasts, dendritic cells and T lymphocytes are stimulated by IL-1β (Weber et al., 2010) (Dinarello, 1996).

IL-1β is a master regulator of the inflammatory response through synergetic action with TNF α to activate proinflammatory responses in a wide range of cells (such as induced

secretion of cytokine and chemokines especially interleukin (IL)-6, increased expression of adhesion molecules in endothelial cells and promotion of diapedesis and the acute phase response (Barksby et al., 2007) (Dinarello, 2011a). The key role played by IL-1β in initiation and mediation of inflammation is underscored by the growing number of non-infectious inflammatory diseases (also known as autoinflammatory diseases) which are now treated as standard by blocking IL-1β function (Dinarello, 2011a) (Masters et al., 2009). In addition, IL-1β contributes to the shaping of adaptive immune responses through direct and indirect effects on T and B cell responses (Dinarello, 2011b).

IL-1β is produced as an inactive precursor (pro- IL-1β, 33 kDa in size) which is cleaved into the bioactive cytokine (17 kDa). The best understood mechanism for IL-1β processing is mediated by the protease caspase-1 in the context of multimeric protein platforms called inflammasomes. Inflammasomes are categorised by the PRR that initiates their formation. To date, four inflammasome complexes have been defined. Three are assembled upon activation of NLRP1, NLRP3 and IPAF- members of the nucleotide-binding domain leucine-rich repeats (NLRs) family of PRRs. The forth inflammasome is recruited to AIM2, a member of the pyrin and NIH domain-containing protein family (PYHIN family), which senses dsDNA in the cytoplasm (Bauernfeind et al., 2011). The AIM2 inflammasome is described below as AIM2 has been shown to play a role in host response to MCMV (Rathinam et al., 2010). Similar principles apply to the other inflammasomes. Following binding of dsDNA AIM2 engages the apoptosis-associated speck-like protein containing a CARD (ASC) protein. This allows for the recruitment of pro-caspase-1 and the production of active caspase-1. Caspase-1 then

cleaves pro- IL-1β into active IL-1β (Bauernfeind et al., 2011). Alternative, caspase-1 independent, IL-1β processing mechanisms exist including neutrophil-derived serine proteases or proteases released from microbial pathogens (Netea et al., 2010). Finally, IL-1β is secreted via an unknown mechanism (Sims and Smith, 2010).

IL-1β signals through a receptor heterodimer composed of IL-1 receptor type I (IL-1R1) and IL-1R accessory protein (IL-1RAP). IL-1β initially binds to IL-1R1 followed by IL-1RAP recruitment. Both receptor sub-units have extracellular immunoglobulin domains and a TIR domain in the cytoplasmic portion (O'Neill, 2008). Formation of the receptor heterodimer allows for recruitment MyD88. The ensuing signalling cascade greatly overlaps MyD88-dependent TLR signal transduction as described in section 1.3.1.3 (O'Neill, 2008). In brief MyD88 mediated the recruitment of IRAKs and TRAF6 leading to activation of the IKK complex followed by activation of NF-κB and MAPK pathways.

1.4.2 IL-1β role in CMV biology

Monocytes, a major source of IL-1β, have been shown in-vitro (using isolated peripheral blood monocytes) to secrete IL-1β in response to HCMV infection (Dudding et al., 1989) (Yurochko and Huang, 1999). Additionally, IL-1β has been shown to inhibit the growth of HCMV in primary fibroblasts and marrow stromal cell lines (Iwata et al., 1999) (Randolph-Habecker et al., 2002). End-point assay of viral replication in primary fibroblasts similarly found IL-1β to inhibit MCMV growth (van der Meer et al., 1989).

In-vivo administration of IL-1R1, thus blocking both IL-1α and IL-1β signalling via the endogenous receptor, resulted in an initial trend towards increased virus titres but decreased titres at later time-points in both C57BL/6 and BALB/c mice (Yerkovich et al., 1997). In a different study, a single administration of recombinant IL-1β prior to infection with MCMV, did not alter survival (van der Meer et al., 1989). Interestingly, in an in-vivo study of serum cytokine levels following MCMV infection of C57BL/6 mice, no IL-1β was detected while IL-1α levels were elevated in infected animals in comparison to controls (Ruzek et al., 1997). A better understanding of the role IL-1β plays during MCMV infection awaits an examination in IL-1β knock-out animals.

1.5 Crosstalk between TLRs, IL-1β and inflammasomes

TLRs and the IL-1β receptor (IL-1RI) sub-units ((IL-1R1) and (IL-1RAP)) are members of the interleukin-1 receptor/Toll-like receptor superfamily (O'Neill, 2008). A conserved Toll/IL (interleukin)-1 (TIR) domain is present in the cytoplasmic end of both TLRs and IL-1RI subunits. Following ligand binding these TIR domains allow for recruitment of TIR-domain-containing cellular signalling adaptors (i.e. MyD88, TRIF, TIRAP (MAL) and TRAM) and initiation of signalling. Thus, IL-1RI and TLRs activate many overlapping signal transduction events (O'Neill, 2008). Importantly, TLR activation induces the expression of pro-IL-1β which, following independent inflammasome activation, is processed and secreted. Secreted IL-1β goes on to activate, both locally and systemically, similar signalling pathways to those initially induced by TLRs. This can be viewed as a system for signal amplification (locally) and broadcasting (systemically or otherwise activation of cells not directly exposed to

microbial products). The requirement for inflammasome activation, for IL-1β processing, integrates signals for inflammasome-forming PRRs (Figure 1.5) (Barton, 2008) (Ishii et al., 2008) (Sims and Smith, 2010).

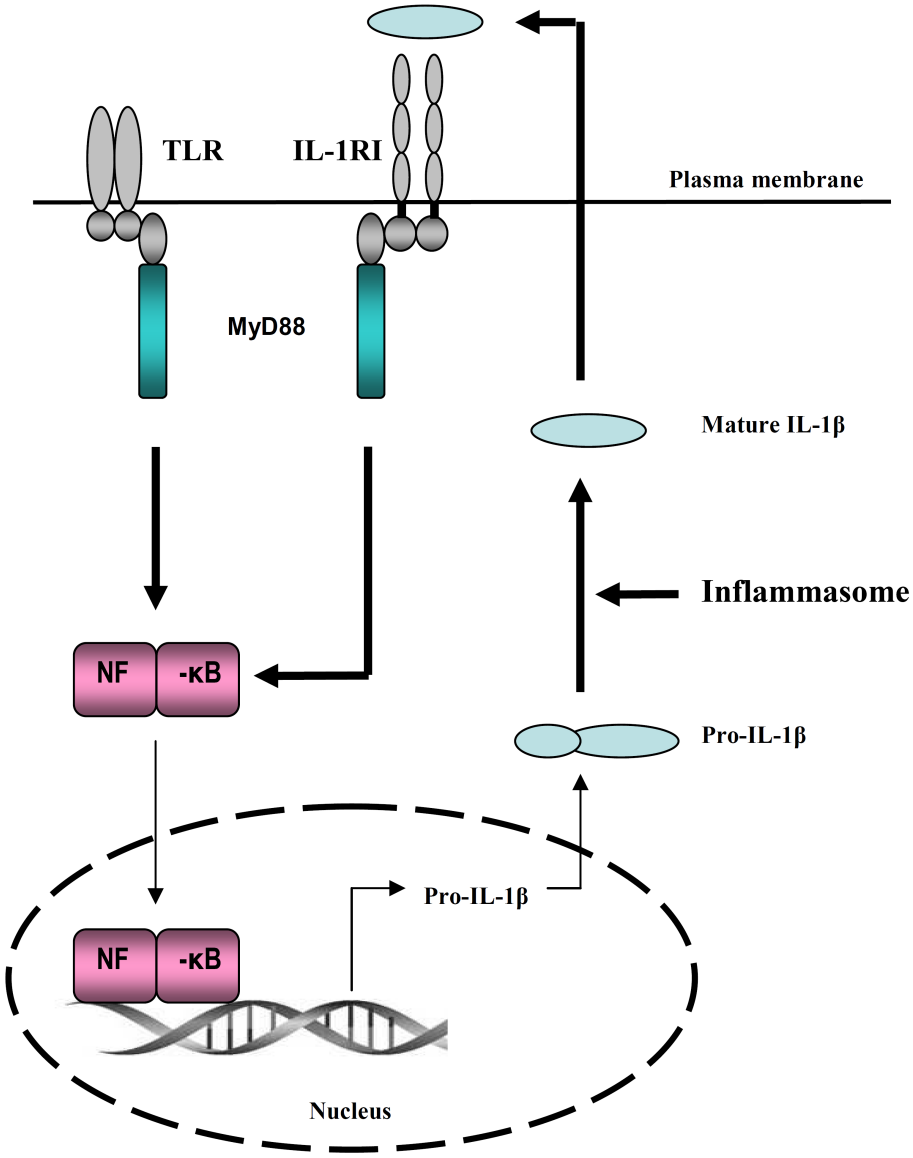

Figure 1.5: Crosstalk between TLRs, IL-1β and inflammasomes. TLRs and IL-1β activate many of the same signal transduction events. TLR activation induces the expression of pro-IL-1β which, following independent inflammasome activation, is processed and secreted. Secreted IL-1β goes on to activate, both locally and systemically, similar signalling pathways to those initially induced by TLRs (Figure adapted from (Barton, 2008)).

1.6 Thesis rationale and central hypothesis

Viral engagement of pattern recognition receptors, such as TLRs and cytosolic nucleic acid sensors, initiates the host immune response through activation of elaborate signalling programs. The ensuing response is further sustained and amplified through cytokines such as IL-1β activating signalling pathways greatly overlapping those utilized by TLRs. Several TLRs detect MCMV and play an important role in host immunity to this pathogen. These include TLR9, TLR7 and TLR2, which signal in a MyD88-dependent manner resulting in NF-κB and MAPKs activation. The pro-inflammatory cytokine IL-1β also activates this MyD88 to NF-κB and MAPKs axis. CMVs are known for the multiple mechanisms by which they evade and modulate the host immune-response to infection (Mocarski, 2002) (Loewendorf and Benedict, 2010). It would therefore be anticipated that CMVs modulate TLR/ IL-1β activation of NF-κB and MAPK responses.

The central hypothesis of this thesis is that a viral counter-measure by MCMV involves specific targeting of TLR- and IL-1β-induced signalling along the MyD88 to NF-κB pathway.

The main objectives of the study are:

a) Determine whether MCMV modulates IL-1β induced NF-κB activation, more specifically the degradation of IκBα – the quintessential NF-κB inhibitor (Chapter 3).

b) Identify the viral product/s mediating the modulation of IL-1β induced IκBα degradation (Chapter 4).

c) Extend studies to include members of the TLR family (Chapter 5)

2 Chapter 2

Materials and Methods

2.1 Cell culture

2.1.1 General methods for cell culture

All cells were maintained in humidified incubator at a 5% CO2 atmosphere, 37°C. Tissue culture flasks and plates were obtained from Nunc (Copenhagen, Denmark). Cells were cultured according to sterile technique and routinely tested for Mycoplasma using the MycoSensorTM PCR Assay Kit (Stratagene) (testing was preformed by Alan Ross, Division of Pathway Medicine, The University of Edinburgh, UK). Reagents used for cell culture were additionally tested for endotoxin using the The Endosafe -PTS™ System (Charles River) (testing was preformed by staff at the Clinical Research Imaging Centre (CRIC), The University of Edinburgh, UK).

2.1.2 Cell lines

The murine embryonic fibroblast-derived immortalized cell line NIH/3T3 was obtained from American Type Culture Collection (ATCC, USA, catalogue number CRL-1658). The NIH/3T3-Bam25 cell line (referred to as Bam25 in this manuscript) was derived from NIH/3T3 cells by transfection of the pBAM25 plasmid (a plasmid containing the MCMV ie1 and ie3 genes) as described previously (Angulo et al., 2000). Mouse

embryonic fibroblasts (MEFs) P53 -/- (ATCC, catalogue number CRL2645), were originally derived from mouse embryos with null mutations in the p53 gene. L929 cells were obtained from Sigma (catalogue number 85011425). This cell line is a subclone of the parental strain L, which was derived from normal subcutaneous areolar and adipose tissue. NIH/3T3 and Bam25 cells were grown in Dulbecco's modified Eagle medium (DMEM) (Lonza) supplemented with 10% heat-inactivated (HI) calf serum (CS) (Invitrogen), 2 mM glutamine (Lonza) and 50 U of Penicillin/Streptomycin (Lonza) per ml. For MEFs P53 -/- HI CS was replaced with HI Fetal Bovine Serum (FBS) (Lonza). The L929 cell line was grown in DMEM/F-12 media with GlutaMAX (Invitrogen) containing 10% HI FBS and antibiotics as described above. Medium (DMEM or DMEM/F-12) supplemented with CS or FCS, glutamine and Penicillin/Streptomycin is hereafter referred to as complete growth medium. For isolation and culture bone marrow-derived macrophages (BMDM) see section 2.2.

2.1.3 Serum (CS or FBS) heat inactivation

Serum was thawed overnight at 4°C followed by equilibration to 37°C in a water bath. Heat inactivation was achieved by incubation of serum at 56°C for 30 min. Heat inactivated serum was then filtered using a Stericup vacuum filtration unit (Millipore) aliquoted and stored at -20°C.

2.1.4 Passaging cells lines

Cells at 70-80% confluence were washed once with phosphate buffered saline (PBS) and then incubated with trypsin/EDTA (Lonza) at room temperature until detached (the volume of trypsin/EDTA used dependent on the flask size). They were then mixed with fresh medium (1:1 ratio of trypsin/EDTA to medium) and centrifuged at ~250g for 5 min at room-temperature. The supernatant was discarded and cell pellets re-suspended in appropriate amount of fresh medium and re-seeded at a split ratio of 1:2 to 1:8 depending on cell line and experimental needs. This process was repeated every 2-3 days up to a maximum of 25-30 passages.

2.1.5 Cell counting and seeding plates

To count cells after trypsinization and re-suspension (as described in section 2.1.4), 10 µl of cell suspension was placed onto a haemocytometer (Bright-line Hemacytometer, Hausser Scientific, USA) under a cover slip and viable cells counted in the central 25 marked squares. The number or cells per ml was calculated by multiplying the number of cells counted by 10^4 (as specified for the haemocytometer used). Cell counts were kept between 10-90 cells. If required, a portion of cell suspension was diluted and the dilution factor incorporated into calculation of cell number. This process was repeated 2-4 times for each sample and an average count was used. Counted cells were then further diluted as needed in medium and seeded at specific densities in different sized tissue culture flasks, dishes or plates (Table 2.1).

Table 2.1: Cell seeding densities

Plate type	***96 well***	***48 well***	***24 well***	***6 well***
Medium volume (µl/ well)				
---	100	500	1000	3000
Cells/well (seeding density)				
NIH/3T3 or NIH/3T3-Bam25	$1.5x10^4$	N/A	$3x10^4$	$3x10^5$
(MEFs) P53 -/-	N/A	$2x10^4$		
BMDM	$4x10^4$	N/A	$5x10^5$	$1x10^6$
Inoculum volume (µl/ well)				
---	25-30	100	250	1000

N/A = Non-applicable

2.1.6 Cryopreservation of cells

For long term storage, cells were harvested and counted as described above. This was followed was centrifugation of the cells and re-suspension in freezing medium (50% CS or FCS (as appropriate for the cell type in question), 40% DMEM and 10% dimethyl sulfoxide (DMSO)) adjusted so that each 1 ml aliquot contained $2\text{-}5x10^6$ cells. Cryovials (Corning) containing aliquots were placed in a Nalgene Cryo 1ºC Freezing Container at –80°C overnight. The next day cells were transferred to liquid nitrogen storage (-170°C).

2.1.7 Thawing cells from liquid nitrogen

For resurrection of frozen cells from liquid nitrogen, individual vials of cells were thawed in a water bath at 37°C and added to 10 ml of fresh warm complete growth

medium (as defined in section 2.1.2). Cells were then centrifuged at ~250g for 5 min. Supernatants were discarded and cell pellets re-suspended in 5 ml fresh complete growth medium and transferred to a 25 cm^2 tissue culture flask to be propagated as described previously.

2.1.8 Cell viability assay

Cell viability assays were performed using the Cell Titer-Blue Cell Viability Assay (Promega) according to manufacturer's instructions. Briefly, cells were grown in a 96 well plate in complete growth medium (as defined in section 2.1.2) at a volume of 100 µl/well. To assess viability 20 µl/well of Cell Titer Blue Reagent pre-adjusted to room temperature was added followed by 1-3 hr incubation at 5% CO_2 atmosphere, 37ºC. Finally, fluorescence measurements were taken using the POLARstar OPTIMA microplate Reader (BMG LabTech, UK).

2.1.9 Transfection of plasmids into cells

Attractene Transfection Reagent (Qiagen) was used according to manufacturer's instructions for fast-forward transfection. Briefly, 1.2 µg DNA, dissolved in Tris-EDTA (TE) buffer (pH 7-8), was diluted in medium without serum or antibiotics to a total volume of 100 µl. Attractene Transfection Reagent (4.5 µl) was added and the mixture incubated for 15 min at room temperature. During this time NIH/3T3 cells were trypsinised, counted and cell density adjusted to $1.5x10^5$ cells/ml. In to each well of a 6

well plate 2 ml of cell suspension was added followed by addition of the transfection complexes. Cells were then incubated under normal conditions. Transfection efficiency was evaluated at 24 hr post transfection using GFP expression as a positive readout.

2.2 Bone-Marrow-Derived Macrophages (BMDM)

2.2.1 Preparation of L929 conditioned media

The L929 cell line was used to produce conditioned media containing macrophage colony-stimulating factor-1 (CSF-1) required for differentiating bone marrow myeloid progenitor cells into macrophages. L929 cells were grown in a 175 cm^2 flask. When nearly confluent, cells were harvested and passaged into thirty 175 cm^2 flasks with 50 ml of fresh complete growth medium each (complete growth medium is defined in section 2.1.2). Cells were then cultured for 14 days at which point the supernatant was removed, filtered and aliquoted into 50 ml tubes. Aliquots were stored at -20°C.

2.2.2 Mouse bone marrow progenitor cell isolation and macrophage differentiation

Bone marrow myeloid progenitor cells were extracted from mouse femurs. All animals were 10-12 week old male C57BL/6 mice (BRR, The University of Edinburgh, UK). Mice were sacrificed via cervical dislocation performed by BRR staff. Femurs were then extracted under sterile conditions and any excess tissue removed. Both ends of each femur were then cut off and the marrow cavity flushed using a needle (27G ½inch needle, BD Biosciences) attached to a syringe filled with BMDM complete growth

medium i.e. DMEM/F-12 media with GlutaMAX (Invitrogen) containing 10% HI FBS, 10% L929 conditioned media and 50 U of Penicillin/Streptomycin (Lonza) per ml. Cells were recovered into a 50 ml tube, centrifuged (~250g for 5 min) and re-suspended in fresh BMDM complete growth medium. Cells were then counted and seeded at $7x10^6$ cells/15cm dish. These precursor cells were cultured in BMDM complete growth media for a 7-day differentiation period into BMDM with medium replenished at days 3 and 5. At day 6 adherent cells were scraped in BMDM complete growth medium, centrifuged, counted and seeded as required (seeding densities are specified in Table 2.1). Cells were cultured in DMEM complete growth media overnight and used on day 7 for experiments or for characterisation by FACS analysis (see section 2.2.3).

2.2.3 Characterisation of BMDM by FACS analysis

BMDM cultures were characterised by Flow Cytometry analysis. This technique was used to measure the expression of cell surface protein markers CD11b (expressed by both monocytes and macrophages) and F4/80 (a murine macrophage restricted cell surface marker).

For flow cytometric analysis, bone marrow progenitor cells cultured for 7 days as described above were washed with ice cold PBS and harvested by scraping. The volume of cell suspension was adjusted to 2 ml ice cold PBS. Cells were then counted and aliquoted at 1 $x10^6$ cells/1.5ml tube followed by blocking in 50 µl blocking buffer (1% bovine serum albumin (BSA), 1 mM sodium azide, 10% normal mouse serum (Serotec)

in PBS) for 10min at room temperature. The following antibodies were used for cell staining: Allophycocyanin (APC) conjugated monoclonal rat-anti-mouse F4/80 (IgG2a, Caltag Laboratories) and fluorescein isothiocyanate (FITC) conjugated rat-anti-mouse CD11b (IgG2b, eBiosciences) or their isotype controls. Antibodies were diluted in FACS buffer (PBS + 1% BSA + 1 mM Sodium Azide) to final dilution of 1:200 and 50 µl of antibody dilution was added to cells. Thirty minutes incubation in the dark was followed by 3 washes with ice cold PBS, centrifugation and re-suspension in 400 µl of cold FACS buffer. A BD FACScan™ system (Becton Dickinson), located at the CALM - Confocal and Advanced Light Microscopy Facility, Queens' Medical Research Institute, MRC Centre for Inflammation Research, The University of Edinburgh, was used to perform the flow cytometric analysis of samples. Data were analyzed using FlowJo software (Treestar, USA). Data from a representative experiment is shown in Figure 2.1. Flow cytometric analysis was performed with the kind assistance of Dr Kevin Robertson, data analysis and was done with the kind assistance of Muhamad Fairus .B.N. Hassim, both from The Division of Pathway Medicine, The University of Edinburgh, UK.

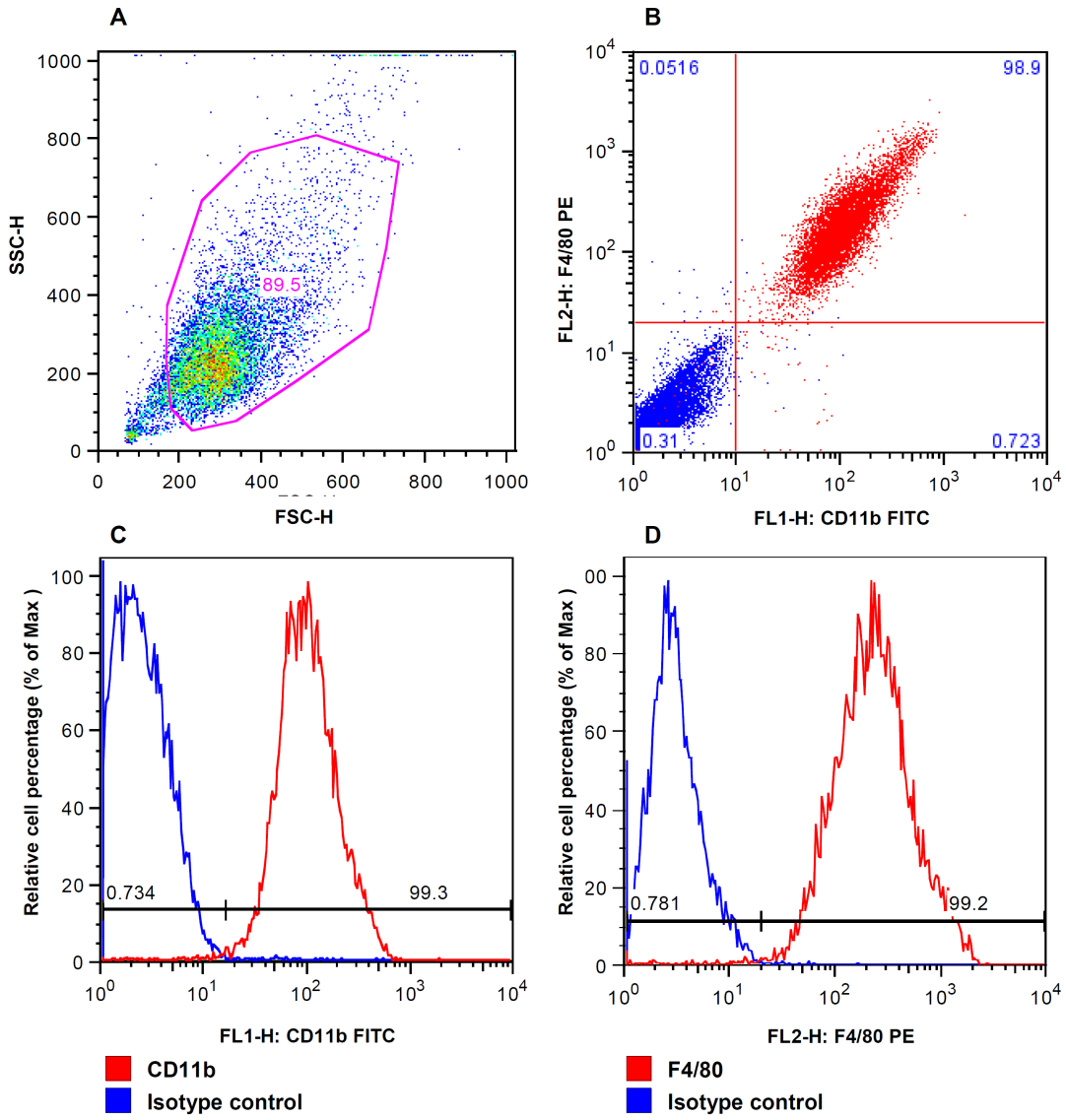

Figure 2.1: Phenotypic characterization of BMDM by flow cytometry. Expression of F4/80 and CD11b was analysed: A) Dot blot showing gating of cells in forward scatter (FSC) and side scatter (SSC). B) Scatter plot showing double-staining signals for F4/80 and CD11b plotted against each other. C + D) Histograms of percentage enrichment of CD11b (C) or F4/80 (D) positive cells within the gated population.

2.3 General methods for virology

2.3.1 Viruses

MCMV wild-type

The parental murine cytomegalovirus (MCMV) strain is derived from bacterial artificial chromosome (BAC) clone pSM3fr, containing the complete MCMV genome, as described previously (Messerle et al., 1997) (Wagner et al., 1999).

MCMVdie3

Construction of the MCMVdie3 has been described previously (Angulo et al., 2000), in short: exon 5 of the ie1/ie3 gene transcription unit was deleted from the MCMV BAC clone pSM3fr (for genomic map see figure 2.2). Gene expression of this virus is limited to immediate-early genes *ie1* and *ie2*, rendering the virus absolutely growth deficient (Angulo et al., 2000) (Lacaze et al., 2011). Replication can be rescued by growing the virus on the complementary cell line (Bam25) expressing both IE1 and IE3 (Angulo et al., 2000).

MCMV-GFP

MCMV-GFP virus is the MCMVdie3 revertant virus as described previously (Angulo et al., 2000) (for genomic map see figure 2.2). It contains a green fluorescent protein (GFP) reporter gene under control of the HCMV MIEP. The GFP expression cassette is located in front of the *ie2* gene spanning the transcription start site of this gene and disrupting its expression (Angulo et al., 2000) (Lacaze et al., 2011). The *ie2*gene has been shown to be

dispensable for viral growth *in vitro and in vivo* (Manning and Mocarski, 1988) (Cardin et al., 1995).

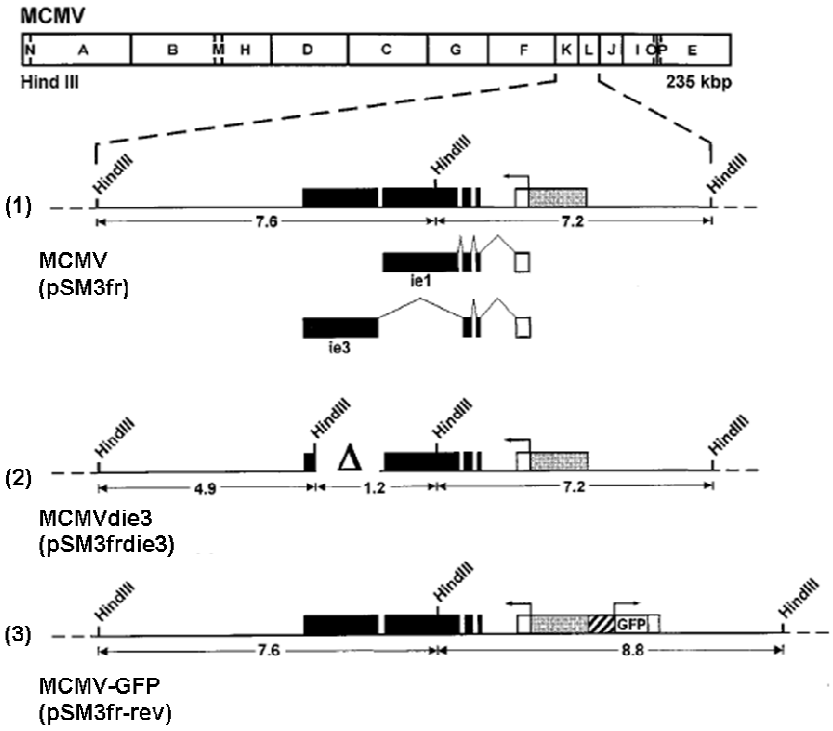

Figure 2.2: Schematic representation of the immediate early gene coding region of MCMV, MCMV-GFP and MCMVdie3 viruses. The HindIII map of the MCMV genome is shown at the top. The expanded map of the HindIII K and L fragments represents the major IE gene region of MCMV. Coding exons are shown in black, and the first noncoding exon of the ie1/ie3 transcription unit is depicted as an open rectangle. The gray box marks the MCMV enhancer ie1/ie3 promoter. The structure of the ie1 and ie3 transcripts is indicated below line 1 of the expanded map. The deletion in the fifth exon of the ie3 transcript is marked by the delta (Δ). The cross-hatched box in front of the GFP ORF represents the HCMV MIEP (Adapted from (Angulo et al., 2000)).

ΔM45

This virus is a kind gift from Professor W. Brune (Leibniz Institute for Experimental Virology, Hamburg, Germany) and has been previously described (Brune et al., 2003), in short: This virus was constructed using a BAC clone of MCMV-GFP which in turn is derived from the MCMV BAC plasmid pSM3fr and contains a enhanced green fluorescent protein (EGFP) reporter gene under control of the HCMV MIEP, inserted into the MCMV *ie2* locus (Brune et al., 2003) and Wolfram Brune, Personal communications). MCMV-GFP BAC clone has the same genomic structure as the above described MCMV-GFP but was constructed independently from the MCMV BAC clone pSM3fr and is not a MCMVdie3 revertant (Wolfram Brune, Personal communications). ORF M45 was deleted from the MCMV-GFP BAC and replaced with a zeocin resistance gene (Brune et al., 2003).

CM45 (in previous publications referred to as revertant M45 (RM45))

A kind gift from Professor W. Brune (Leibniz Institute for Experimental Virology, Hamburg, Germany), has been previously described (Mack et al., 2008), in short: the nonessential genes m02 to m06 are replaced with an M45 gene tagged with an influenza virus hemagglutinin (HA) epitope, under the control of a murine pgk promoter (Mack et al., 2008) (Jurak and Brune, 2006).

2.3.2 Viral stock preparation

For each virus strain a seed stock was initially produced from an existing low passage stock and this was used for generation of bulk stocks. NIH/3T3 cells were used for all viruses except MCMVdie3 for which the Bam25 complementary cell line was used. For preparation of bulk stock cells were infected at MOI of 0.001 in suspension (total volume 5 ml) for 30 min at 37°C with occasional tapping. Allowing for 4.5- $5x10^6$ cells/175cm^2 flask cells were seeded and flasks were topped up to 20 ml with DMEM supplemented with 3% HI CS, glutamine and Penicillin/Streptomycin (as detailed in section 2.1.2). Infected cultures were grown under normal condition for 5-7 days until a nearly complete cytopathic effect (CPE) was observed. Supernatant and cells were harvested from multiple flasks and combined. When possible, viral stock was concentrated immediately, if this was not possible the harvested stock was aliquoted into 50 ml tubes and these were stored at -80°C.

2.3.3 Concentration of viral stocks

Preferentially the procedure for viral stock concentration was performed immediately upon harvest. However if frozen aliquots were used then these were allowed to thaw gradually at room temperature for about 30min followed by incubation in a 37°C water bath. In order to harvest intracellular as well as extracellular virus fresh or thawed stock was centrifuged (7000g, 4ºC, 20 min, Sorval SLA-1500 rotor). All the following steps were performed on ice. Supernatant was collected into fresh centrifuge tubes and kept on

ice. Cell pellet was re-suspended in 10 ml ice-cold medium and homogenised using a 40 ml homogeniser (Wheaton, USA). Disrupted cells were centrifuged in a 30 ml tube (3600g, 4ºC, 20 ml, SORVAL SS34 rotor) and the supernatant pulled together with total viral stock. This was followed by centrifugation (30,000g, 4ºC, 3 hr, SORVAL rotor SLA-15000). The supernatant was discarded and the virus-containing pellet was incubated in residual fluid overnight on ice in a cold room (4°C). The next day pellets were re-suspended by pipetting up and down using a 1000 µl micropipette and pooled. Virus suspension was then homogenised using a 25 ml homogeniser (Wheaton, USA) and gently pipetted onto a 20% sorbitol solution (sorbitol solution was prepared in Tris buffered saline (TBS), pH = 7.8; sorbitol was purchased from Sigma) in 30 ml centrifugation tubes (at a ratio of 10 parts sucrose to 1 part virus suspension). These were then centrifuged (30,000g, 4ºC, 3 hr, SORVAL SS34 rotor). The supernatant was discarded and 500 µl 3% FCS DMEM medium was added per tube followed by 2 hr incubation on ice and final re-suspension using 1000 µl micropipette. Total volume was adjusted to 3 ml and further homogenised using a 5 ml homogeniser (Wheaton, USA). Aliquots of 50 µl, 100 µl and 200 µl were prepared and stored at -80ºC.

2.3.4 Titration of virus by plaque assay

Plaque assays were used to measure the concentration of virus in a sample i.e. virus titre. Plaque assays were performed on MEFs P53 -/- for all viruses except MCMVdie3 in which case the Bam25 cell line was used. Cells were seeded in 24 or 48 well plates and incubated overnight at 5% CO_2 atmosphere, 37°C (for seeding densities see Table 2.1).

On the day of the assay, 10 fold serial dilutions (usually 10^{-1} to 10^{-6}) of the virus-containing sample were prepared in duplicate. Culture medium supplemented with 3% serum was used to dilute the virus. When using 48 well plates 100 µl of virus inoculum was transferred onto the cells, 200 µl were used for 24 well plates. This was followed by 1h incubation at 5% CO_2 atmosphere 37°C at which time the monolayer was washed once with medium. To cover the cells a 0.25% agarose-medium mixture was prepared by: heating to boiling point pre-made 2.5% agarose solution (2.5% agarose in distilled water) and diluting it 1:10 in 3% serum supplemented medium. Wash medium was then removed from the monolayers and the agarose-medium mixture added carefully. Cells were then incubated for 3-4 days under normal conditions at which point plaques were counted. To calculate the virus titre measured in plaque forming units to ml (PFU/ml) the following equation was used:

PFU/ml = number of plaques counted * individual dilution factor * 10 (in the case of 48 well plates) or *5 (in the case of 24 well plates)

2.3.5 Infection of cells

Once the titre of a given viral stock was known it was possible to calculate the amount of viral stock needed to achieve a desired multiplicity of infection (MOI). The MOI corresponds to the number of PFUs delivered per cell. To infect cells, viral inoculum was prepared by mixing the required amount of viral stock with 3% serum supplemented media. The total volume of inoculum used for different plate formats is specified in

Table 2.1. Cells were incubated with the viral inoculum for an absorption period of 1 hr at 5% CO_2 atmosphere, 37°C. Monolayers were then washed three times with media and replenished with normal growth media. Time zero (T0) or zero hours post infection (0 hpi) corresponds to the end of the viral adsorption period. For mock infections the same medium used for preparation of viral inoculum was used only with no virus added. All wash steps and medium replenishing steps were followed as per infected wells.

2.3.6 Viral growth curves

2.3.6.1 Plaque assay based growth curves

Growth curves were used to analyse viral replication. This allowed to compare the effect of different treatments on viral growth or to compare growth characteristics of wild type versus mutant viruses. To perform growth curve analysis, cells were seeded in a 24 well plate and incubated over night at 5% CO_2 atmosphere, 37°C. The next day infection at a low MOI (in this study MOI of 0.2) or high MOI (in this study MOI of 2) was used. For infection procedure see section 2.3.5. Supernatants of cultures were sampled at 24 hr intervals on days 1 to 5 or 6 post infection. Collected supernatants were titrated using plaque assays.

2.3.6.2 Fluorescence based growth curves of GFP-reporter virus

Viral growth was evaluated by measuring GFP expression by the MCMV-GFP virus (described in section 2.3.1).To ensure that MCMV-GFP characteristics of replication

reflect that of the wild type virus, the growth kinetics of MCMV and MCMV-GFP were analysed using plaque assay based growth curves (Figure 2.3). MCMV-GFP replication was effectively indistinguishable from that of MCMV. This is in accordance with previously published data (Angulo et al., 2000). A strong correlation between GFP signal and PFU/ml measurements has been previously demonstrated (Dr M. Blanc, DPM, Personal communications). Fluorescence based growth curves were performed as follows: NIH/3T3 cells were seeded in black (clear bottom) 96-well plates and incubated overnight at 5% CO_2 atmosphere, 37°C. Phenol red-free DMEM was used. The next day cells were infected at a MOI = 0.2. GFP signal over time was measured using a POLARstar OPTIMA microplate Reader (BMG LabTech, UK). Excitation and emission wave lengths were set at 485 nm 520 nm, respectively.

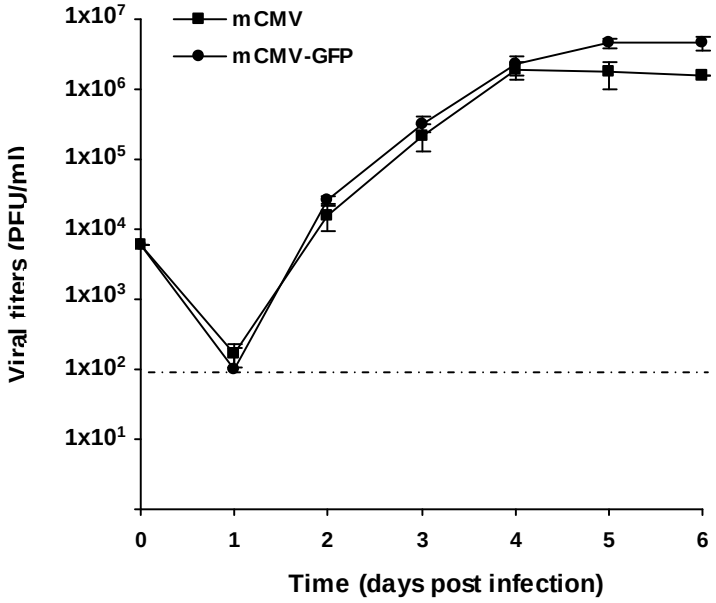

Figure 2.3: Comparison of growth kinetics of MCMV and MCMV-GFP in NIH/3T3 cells. NIH/3T3 cells were infected at an MOI = 0.05 with MCMV or MCMV-GFP. At indicated time points post infection (days post infection) supernatants from the infected cultures were harvested and titered on MEFp53 $^{-/-}$ monolayers. Error bars indicate the standard deviation from three separate wells. Dotted line represents the limit of detection (100 PFU/ml).

2.4 Cytokines and agonists

Recombinant mouse IL-1β (Thermo Scientific, catalogue number RMIL1BI) and recombinant mouse TNFα (Thermo Scientific, catalogue number RMTNFAI) were re-constituted in 0.5 ml dH_2O and diluted in 10% FCS supplemented DMEM to a concentration of 1 μg/ml. Recombinant mouse IFNβ was purchased from Stratech Scientific (catalogue number 12400-1). Aliquots of these cytokines were kept at -80°C.

TLR9 ligand ODN 1668 (InvivoGen, catalogue number tlrl-modnb) and TLR9 ligand control (InvivoGen, catalogue number tlrl-modnbc) were re-constituted in sterile endotoxin-free water, aliquoted and stored at -20°C.

TLR7 ligand R-848 ((4-Amino-2-(ethoxymethyl)-a,a-dimethyl-1H-imidazo[4,5-c]quinoline-1-ethanol, S 28463, Resiquimod), Enzo Life Sciences, catalogue number ALX-420-038) was re-constituted in DMSO aliquoted and stored at -20°C.

2.5 Protein methods

2.5.1 Buffers and solutions used for protein methods

Lysis buffer: 50 mM Tris-Cl pH 7.5, 100 mM NaCl, 1% (w/v) NP40 (also known as IGEPAL CA-630 (Sigma)). Shortly before use the required amount of lysis buffer was supplemented with protease inhibitors (Roche, Complete tablets, catalogue number 04

693 116 001) and phosphatase inhibitors (Roche, PhosStop, catalogue number 04 906 837 001)).

Laemmli sample loading buffer: 2 x sample loading buffer was bought from Sigma (catalogue number S3401).

Laemmli Running Buffer (Tris-Glycine): 25 mM Tris, 192mM glycine, 0.1% SDS, pH 8.3.

Transfer buffer (Towbin buffer): 25 mM Tris, 192 mM glycine, 20% (v/v) methanol, 0.025% SDS, pH 8.3.

Tris-Buffered Saline (TBS): 10 mM Tris; 100 mM NaCl, pH 7.8.

Tris-buffered saline- Tween (TBS-T): 10 mM Tris-HCl, 100 mM NaCl, 0.2% Tween-20.

10% Ammonium Persulfate (APS): 1 gr of APS was added to 10 ml dH_2O, aliquoted and stored at -20°C.

1 M Tris-HCl pH 6.8: 120 g Tris were added to 800 ml of dH_2O, pH was adjusted using HCl and total volume made up to 1 litre with dH_2O.

1.5 M Tris- HCl pH 8.8: 181 g of Tris were added to 800 ml of dH_2O, pH was adjusted using HCl and total volume made up to 1 litre with dH_2O.

10% Sodium dodecyl sulphate (SDS): 10 g of electrophoresis-grade SDS were dissolved in 80 ml of dH_2O. Total volume was then made up to 100 ml.

2.5.2 Preparation of protein extracts for western blot analysis

Cells were washed twice with ice cold PBS before ice cold lysis buffer was added (100 µl/well in a 24well plate; 150 µl/well in a 6 well plate). After which cells were scraped off and transferred to an Eppendorf tube. Samples were then incubated on ice for 30 min (if required samples were then stored at -80°C for later processing). Lysates were then cleared by centrifugation at maximum speed in a table-top centrifuge for 5 min at 4ºC. Supernatants were transferred to a fresh tube and kept at -80°C until analysed. Protein concentration was determined using a BCA (bicinchoninic acid) Protein Assay Kit (Thermo Scientific Pierce, catalogue number 23228).

2.5.3 Sodium dodecyl sulfate polyacrylamide gel electrophoresis (SDS-PAGE) and Western blot analysis

Following determination of protein concentration, an equal amount of total protein from each sample (typically 5-8 µg) was mixed with 2x Laemmli Sample loading buffer. The mixture was boiled for 5 min at 98ºC followed by a brief centrifugation. Samples were then loaded onto a SDS-PAGE gel (5% stacking gel, 12% resolving gel), together with molecular weight markers (SeeBlue® Plus2 Pre-Stained Standard, Invitrogen). Running apparatus, voltage and time setting for gel running varied and depended on gel size. Transfer of proteins from the gels onto a membrane was achieved using a wet blotting procedure: gels were equilibrated briefly in transfer buffer followed by assembly of the transfer sandwich. This was organised in the following order: fiber pad, filter paper, pre-

wetted membrane, equilibrated gel, filter paper, fiber pad. All were soaked in transfer buffer prior to use. A Hybond™ ECL™ (GE Healthcare) or Immobilon-FL (Millipore) membranes were used for ECL or immunofluorescence based membrane visualisation, respectively. Following completion of protein transfer the membrane was removed and washed briefly in dH_2O.

Two protein detection methods were used Enhanced Chemiluminescence (ECL) based detection or Near-infrared (NIR) fluorescence based detection. This dictated different procedures for blocking, antibody incubation and signal detection which are detailed below. Antibodies usage and purchase details are provided in Tables 2.2- 2.4.

2.5.3.1 Enhanced Chemiluminescence (ECL) based detection

Membranes were incubated in blocking buffer (0.1% TBS-Tween, 5% skim milk powder (Sigma)), for 1 hr at room temperature or overnight in at 4°C. They were then washed 3 times, 5 min each, with TBS-Tween. Primary antibody diluted in TBS-Tween was added and membranes were incubated for 2 hr at room temperature or overnight at 4°C. Excess antibody was washed as above. Secondary antibody diluted in blocking buffer was added and 2 hr incubation at room temperature was allowed. The membrane was then washed 3 times, 10 min each, with TBS-Tween. Finally, proteins were detected using the Amersham ECL™ Western Blotting Detection Reagents (Amersham, catalogue number RPN2109), X-ray film RX NIF (FujiFilm) and the OPTIMAX X-Ray Film Processor (GmbH & Co).

2.5.3.2 Near-infrared (NIR) fluorescence based detection

Membranes were incubated in PBS for several minutes followed by blocking with Odyssey blocking buffer (Li-Cor Biosceinces) diluted 1:1 in PBS, for 1 hr at room temperature. Primary antibodies diluted in Odyssey blocking buffer + 0.1% Tween-20 were then added and a 2 hr at room temperature or overnight at 4°C incubation was allowed. Membranes were then washed 4 times, 5 min each, with 0.1% Tween PBS. All following steps were performed while protecting the antibody vials and membrane from light. Fluorescently-labelled secondary antibodies were diluted (typically 1:15,000) in Odyssey blocking buffer + 0.1% Tween-20 followed by a 60 min incubation at room temperature. The membranes were then washed 4 times, 5 min each, with 0.1% Tween PBS. Finally the membranes were rinsed with PBS and visualised using the Odyssey® Infrared Imaging System (Li-Cor Biosceinces). Images were analysed using the Odyssey Application Software version 3.0 (Li-Cor Biosciences): integrated fluorescence intensity was calculated for each protein band (defined as the sum of the intensity values for all pixels enclosed by a shape, i.e. a rectangle encompassing a single protein band, multiplied by the area of the shape (units are counts-mm^2)). Quantification of the loading control protein (β- Actin or total p38) was used as a reference to normalize the integrated fluorescence intensities of the protein of interest (IκBα or p-p38, respectively).

Table 2.2: Primary antibodies used for Western blot analysis

Antibody	Host species	Dilution	Incubation time	Supplier
Chroma 101; detects the MCMV protein ie1	Mouse	1:1000	Overnight, 4°C	A kind gift from Prof. Stipan Jonjic (Riejka University, Croatia)
Chroma 103; detects the MCMV protein e1	Mouse	1:1000	2 hr, room temperature	A kind gift from Prof. Stipan Jonjic (Riejka University, Croatia)
IkBalpha	Rabbit	1:1000	2 hr, room temperature	Sigma (# I0505)
IκBα (L35A5) Mouse mAb (Amino-terminal Antigen)	Mouse	1:1000	Overnight, 4°C	Cell Signaling Technology (# 4814)
Anti B-actin	Rabbit	1:1000	Overnight, 4°C	Cell Signaling Technology (# 4967)
anti-HA (clone 3F10)	Rat	1:1000	2 hr, room temperature	Roche (# 11867423001)
p38α (C-20)	Rabbit	1:500	Overnight, 4°C	Santa Cruz Biotechnology (# sc-535)
Phospho-p38 MAPK (Thr180/Tyr182) (28B10)	Mouse	1:1000	Overnight, 4°C	Cell Signaling Technology (# 9216)

Catalogue number

Table 2.3: Secondary antibodies used for ECL based detection

Antibody	Dilution	Incubation time	Supplier
Peroxidase conjugated Affini Pure goat anti-mouse antibody IgG (H+L)	1:3000	2 hr, room temperature	Stratech (# 115035062)
Peroxidase conjugated Affini Pure goat anti-rat antibody IgG (H+L))	1:3000	2 hr, room temperature	Stratech (# 115035062)
Anti-rabbit IgG, HRP-linked Antibody	1:2000	2 hr, room temperature	Cell Signaling Technology (# 7074)

Catalogue number

Table 2.4: Secondary antibodies near-infrared fluorescence based detection

Antibody	Dilution	Incubation time	Supplier
Anti-mouse IgG (H+L) (DyLight 800 Conjugate)	1:15,000	1 hr, room temperature	Cell Signaling Technology (# 5257)
Anti-rabbit IgG (H+L) (DyLight® 800 Conjugate)	1:15,000	1 hr, room temperature	Cell Signaling Technology (# 5151)
Alexa Fluor® 680 goat anti-rabbit IgG (H+L) *highly cross-adsorbed* *2 mg⁄mL*	1:15,000	1 hr, room temperature	Invitrogen (# A-21109)
Alexa Fluor® 680 goat anti-rat IgG (H+L) *2 mg⁄mL*	1:15,000	1 hr, room temperature	Invitrogen (# A-21096)
Alexa Fluor® 680 goat anti-mouse IgG (H+L) *highly cross-adsorbed* *2 mg⁄mL*	1:15,000	1 hr, room temperature	Invitrogen (# A-21058)

Catalogue number

2.6 Enzyme-Linked Immunosorbent Assay (ELISA)

Cytokine levels in cell culture supernatant were determined using ELISA kits in accordance with manufacturer's instructions (R&D Systems Ltd, DuoSet ELISA Development Systems: Mouse TNFα catalogue number- DY410 and mouse IL-6 catalogue number- DY406). In brief: a 96 well plate (96 well EIA/RIA Plate, Costar) was coated with capture antibody and incubated overnight at room temperature. On the following day wells were washed 3 times with wash buffer (0.05% Tween-20 in PBS). Samples or cytokine standard (100 µl) were then applied and incubated for 2 hr at room temperature. Plates were then washed as above and detection antibody added for an additional 2 hr incubation. Wells were again washed followed by addition of horseradish peroxidase (HRP) - conjugated streptavidin. After removal of non-bound HRP conjugate, the substrate solution was added and colour was allowed to develop for 20 min. Colour development was then stopped by addition of 2 N H_2SO_4 solution. Absorbance was recorded using a POLARstar OPTIMA microplate Reader (BMG LabTech, UK).

2.7 Immunofluorescence

BMDM were seeded at a density of $1x10^5$ cells/well onto BD Falcon CultureSlides (8 chamber polystyrene vessel, BD Bioscience) and incubated overnight at 5% CO_2 atmosphere, 37°C. The next day cells were infected and treated as required then washed twice with PBS and fixed in 4% paraformaldehyde (PFA) for 15 min. Fixative was

removed by washing 3 times, 5 min each, with PBS and slides stored at 4°C until used. Preparation of cells for staining: cells were incubated with 50mM NH_4CL in PBS for 10min and washed twice, 5 min each, with PBS. Permeabilization was achieved by incubation with 0.5% Triton X-100 for 3 minutes followed by two washes with PBS. Immunostaining: cells were incubated in blocking buffer (PBS; 5% normal goat serum (Cell Signalling Technology, catalogue number 5425); 0.3% Triton X-100 (Sigma)) for 1 hr. Primary antibodies diluted in antibody dilution buffer (1% BSA in PBS) were applied and overnight incubation at 4°C allowed. Cells were then washed 3 times, 5 min each, in PBS. This was followed by 2 hr incubation at room temperature with secondary antibodies also diluted in antibody dilution buffer. Excess antibody was removed by washing 3 times, 5 min each, with PBS. Finally slides were mounted using ProLong® Gold antifade reagent with DAPI (Invitrogen, catalogue number P-36931) and coverslips. The primary antibodies used were: NF-kB p65 (C22B4) (Cell Signaling Technology, catalogue number 4764) and Chroma 101 (see details in Table 2.2). The secondary antibodies used were: Alexa Fluor® 488 F(ab')2 fragment of goat anti-rabbit IgG (H+L) (Invitrogen, catalogue number catalogue number A-11070) and Alexa Fluor® 594 F(ab')2 fragment of goat anti-mouse IgG (H+L) or Alexa Fluor® 488 Goat Anti-Mouse IgG (H+L) (Invitrogen, catalogue number catalogue number A-11001) and Alexa Fluor® 594 Goat Anti-Rabbit IgG (H+L) (Invitrogen, catalogue number catalogue number A-11012). Slides were analysed using the Leica SP5 confocal microscop with a x63 objective, numerical aperture 1.4. Microscope was operated and images acquired by Shonna Johnston, Optical Imaging Manager at the CALM - Confocal and Advanced Light Microscopy Facility, Queens' Medical Research Institute, MRC Centre for

Inflammation Research, The University of Edinburgh. Images were prepared for print using ImageJ (Rasband, W.S., ImageJ, U. S. National Institutes of Health, Bethesda, Maryland, USA, http://imagej.nih.gov/ij/, 1997-2011)

2.8 DNA methods

2.8.1 Cloning

ORF M45 was derived from a previously described clone collection of the MCMV orfeom (MCMV strain Smith) (Fossum et al., 2009). This clone library makes use of the Gateway® Technology system (Invitrogen) which is based on the recombination properties of bacteriophage lambda. It includes an array of plasmids containing different *att* sites which are DNA recombination sequences recognised by proteins that mediate a recombination reaction (Clonase™ enzyme mix). This allows for a rapid and efficient transfer of genes of interest from an initial vector into which they were cloned (pDONR™ 207) into a variety of destination plasmids such as expression vectors. Two expression vectors were used: pCR3DEST and pCR3DESTHA. Both are derivatives of the pCR3 plasmid (Invitrogen) which have been previously adapted for use with the Gateway Technology system. The pCR3DESTHA plasmid includes an influenza virus hemagglutinin (HA) epitope tag at a N-terminal position. Transfer of M45 from pDONR™ 207 into pCR3DEST and pCR3DESTHA was achieved using an LR recombination reaction: 1 µl of pDONR™ 207, 1 µl of expression vector at a concentration of 300 ng/µl, 1 µl H_2O, 1 µl LR clonase, quick spin, 2 hr incubation at room temperature. A schematic representation of an LR reaction and resulting plasmids

is shown in Figure 2.3. Following completion of the LR reaction transformation into chemically competent bacteria was performed. DNA from resulting colonies was isolated and analysed by restriction endonuclease digestion.

Figure 2.3: Schematic representation of LR reaction. An LR reaction facilitates recombination of an attL substrate (entry clone = pDONR™ 207) with an attR substrate (destination vector = pCR3DEST or pCR3DESTHA) to create an attB-containing expression clone. This reaction is catalyzed by LR Clonase™ enzyme mix. For more information regarding the ccdB gene see section 2.9.2 (adapted from the Gateway® Technology manual, Invitrogen).

2.8.2 Purification of plasmid DNA

For isolation of plasmid DNA, a single colony was selected from a LB plate and transferred to a 15 ml tube containing 3 ml of LB broth with the same antibiotic selection as the agar. The culture was incubated over night at 37°C with ~250 rpm shaking. The next day plasmid DNA was isolated using the QIAprep Spin mini prep kit (Qiagen). Alternatively, overnight culture was diluted 1:500 to inoculate 200 ml of growth media to be cultured overnight at 37°C with ~250 rpm shaking. This was used for preparation of larger DNA quantities using the Pureyield Plasmid Midiprep System (Promega). The concentration and purity of the purified DNA was determined by

measuring the UV absorbance at 260 and 280 nm (NanoDrop Spectrophotometer (ND-1000), NanoDrop).

2.8.3 Restriction endonuclease digestion

Restriction enzymes EcoRV, HindIII, XbaI, corresponding buffers and BSA were purchased from New England BioLabs and used according to manufacturer's recommendations. Typically a digestion mixture included: 5 µl of plasmid DNA isolated by mini-prep (see section 2.8.3), 20 U of each enzyme used, 1x enzyme appropriate buffer, 5 µg BSA, adjusted to a total volume of 30 µl with dH_2O and incubated for 2 hr at 37°C.

2.8.4 Agarose gel electrophoresis

Agarose gels were used to analyze DNA fragments and plasmids. Gels (1% concentration) were made and run in 1xTAE buffer supplemented with ethidium bromide (final concentration 0.25 µg/ml). A 1 kb DNA ladder (Generuler, Fermentas Ltd) was used to evaluate band size.

2.9 Bacterial methods

2.9.1 Buffers and solutions for bacterial methods

Luria-Bertani (LB) broth and agar plates: 10 g Tryptone (BD Biosceinces), 5 g Yeast extract (BD Biosceinces), 10 g NaCl (Sigma) and dH_2O were mixed to a total volume of 1 litre, autoclaved and kept at 4ºC. For plate preparation 15 g of agar (Sigma) was added and the mixture poured onto plastic plates (Sterilin limited, UK).

Antibiotics: Gentamycin (final concentration 15 μg/ml), Ampicillin (final concentration 100 μg/ml), Chloramphenicol (final concentration 150 μg/ml) and Kanamycin (final concentration 50 μg/ml) were all purchased from Sigma.

2.9.2 Bacteria

Expression (destination) vectors used contain a *ccd*B gene which allows for negative selection of cells that have taken up unreacted destination and by-product vectors (see section 2.8.2 and Figure 2.3). This is due to the fact that the CccB protein inhibits the growth of most Escherichia Coli (*E.coli)* strains such as DH5α. Therefore, prior to insertion of the gene of interest these plasmids were propagated in the *E. coli* strain DB3.1 which is resistant to the CcdB effects. Following LR reaction (see section 2.8.2) plasmids were transformed into *E.Coli* strain DH5α to allow for negative selection. Both

strains were grown in LB medium or on LB agar plates at 37°C with constant shaking (~250 rpm) in the case of liquid media.

2.9.3 Preparation of chemical competent bacteria

A single colony of DH5α.bacteria was picked and grown over night in 10 ml of LB. The next day 5 ml of this starter culture was used to inoculate 1 litre of LB. Inoculated culture was incubated at 37°C with shacking and bacterial growth assessed by measuring optical density at 600 nm (OD_{600}). Once an OD_{600} of ~0.5 was reached the exponential growth of the bacteria was stopped by swirling vigorously on ice for 10 min. The culture was then divided into two and centrifuged (4°C, 10 min at 4000 g-force) followed by re-suspension in 30 ml of sterile, ice cold 100 mM $CaCl_2$ per pellet. This was followed by a 30 min incubation on ice and an additional centrifugation. Each pellet was gently re-suspended in 5 ml ice cold sterile 100 mM $CaCl_2$ supplemented with 15% glycerol (w/v). Resulting cells were aliquoted (50 µl), snap frozen in liquid nitrogen and stored at -80°C.

2.9.4 Transformation of chemical competent bacteria

Plasmid DNA (1 µl of LR reaction (see section 2.8.2)) was mixed with 50 µl chemical competent bacteria and sequential incubation steps were conducted: 30 min on ice, 1.5 min in 42°C water bath, 2 min on ice. Then LB media (800 µl) was added and the

mixture incubated for 1 hr, with shaking (950 rpm) on a hot block followed by spreading on appropriate selection plates.

2.10 Statistical analysis

Statistical analysis was performed using Microsoft Excel 2007 software.

3 Chapter 3

MCMV inhibits IL-1β induced IκBα degradation

3.1 Introduction

The cytokine IL-1β plays a key role in initiation and modulation of inflammation and additionally contributes to the shaping of adaptive immune responses (Sims and Smith, 2010). IL-1β binding to its receptor leads to recruitment of MyD88 followed by IRAK1 and IRAK4, TRAF6, TAK1 and finally the IKK complex. The IKK complex phosphorylates the NF-κB-inhibitor IκBα leading to its degradation and thus to activation of NF-κB (Weber et al., 2010). This MyD88 to NF-κB axis is also activated by TLRs (all except TLR3) (Kawai and Akira, 2010). Several TLRs, including TLR2, TLR7 and TLR9, have been shown to detect MCMV and contribute to host response against this pathogen (Tabeta et al., 2004) (Krug et al., 2004) (Zucchini et al., 2008) (Barbalat et al., 2009). Considering that MCMV is known to manipulate multiple other aspects of host anti-viral defence (Mocarski, 2002), it was hypothesised that MCMV specifically perturbs TLR- and IL-1β-induced signalling along the MyD88 to NF-κB pathway. To begin addressing this question this chapter aims to examine whether MCMV infection modulates the degradation of IκBα, the hallmark of NF-κB activation, following IL-1β stimulation.

3.2 Results

3.2.1 System characterisation

Fibroblasts are fully permissive to infection with MCMV, and constitutively express the IL-1β receptor. Therefore, MCMV infection of the fibroblast cell line NIH/3T3 followed by IL-1β treatment was chosen to evaluate the possible modulation of IL-1β signalling by this virus. Initially, basic characterisation of this system was carried out including preliminary examination of the effect of IL-1β on MCMV growth in NIH/3T3 cells and evaluation of IκBα degradation kinetics following cytokine stimulation in these cells.

3.2.1.1 Effect of IL-1β on MCMV growth in NIH/3T3 cells

To gain insight into the interplay between IL-1β and MCMV in the experimental system used, the effect of this cytokine on viral replication was examined. To this end a GFP expressing virus, MCMV-GFP (described in Chapter 2 section 2.3.1), was used. NIH/3T3 cells were treated with a range of concentrations of IL-1β prior to infection as well as maintained in cytokine containing media following infection. IFNβ treatment was used as positive control. Viral growth was monitored by microscopy (Figure 3.1a) as well as by measuring GFP signal (fluorescence intensity) over time (Figure 3.1b). As shown in Figure 3.1a, at day 2 post-infection only a small number of cells appear infected in non-treated cultures. This is followed by a rapid spread of infection with the majority of cells expressing GFP by day 4 post-infection. As expected, IFNβ treatment markedly reduced viral spread throughout the period examined. In IL-1β treated

cultures, at all time points evaluated, the number of infected cells appears equivalent or slightly higher than in non-treated cultures. Fluorescent signal measurements (Figure 1b) reflect these qualitative results. In comparison to non-treated cells, measured GFP expression is significantly lower in IFNβ treated wells. In contrast, no difference is observed following inclusion of IL-1β in the culture media up to 72 hr post-infection. At this time point a trend towards higher GFP intensity is seen in IL-1β treated wells in comparison to non-treated cultures. It is unclear if this is due to stronger GFP expression in individual infected cells or increased viral replication.

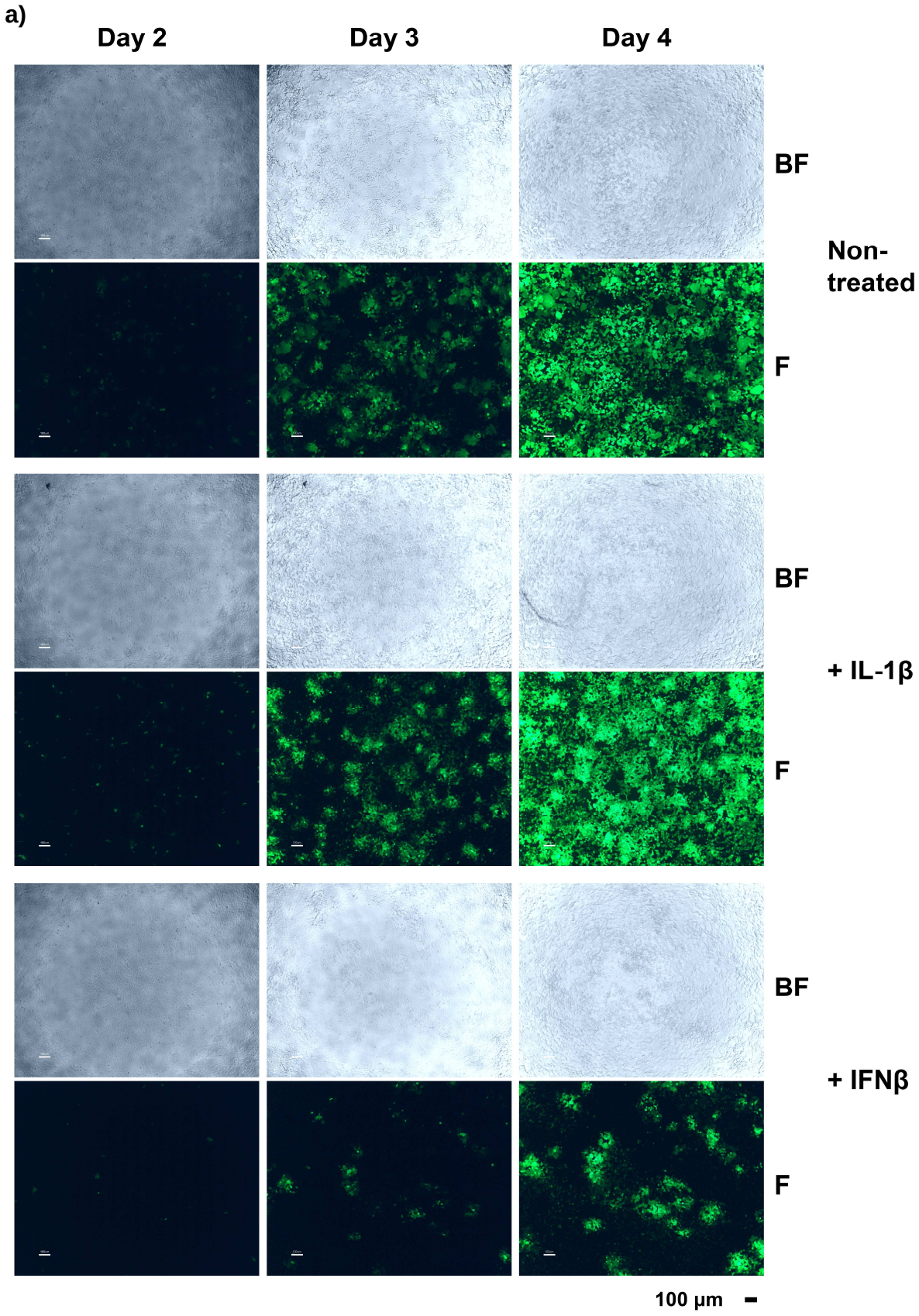
a)
Day 2
Day 3
Day 4
BF
Non-
treated
F
BF
+ IL-1β
F
BF
+ IFNβ
F
100 µm

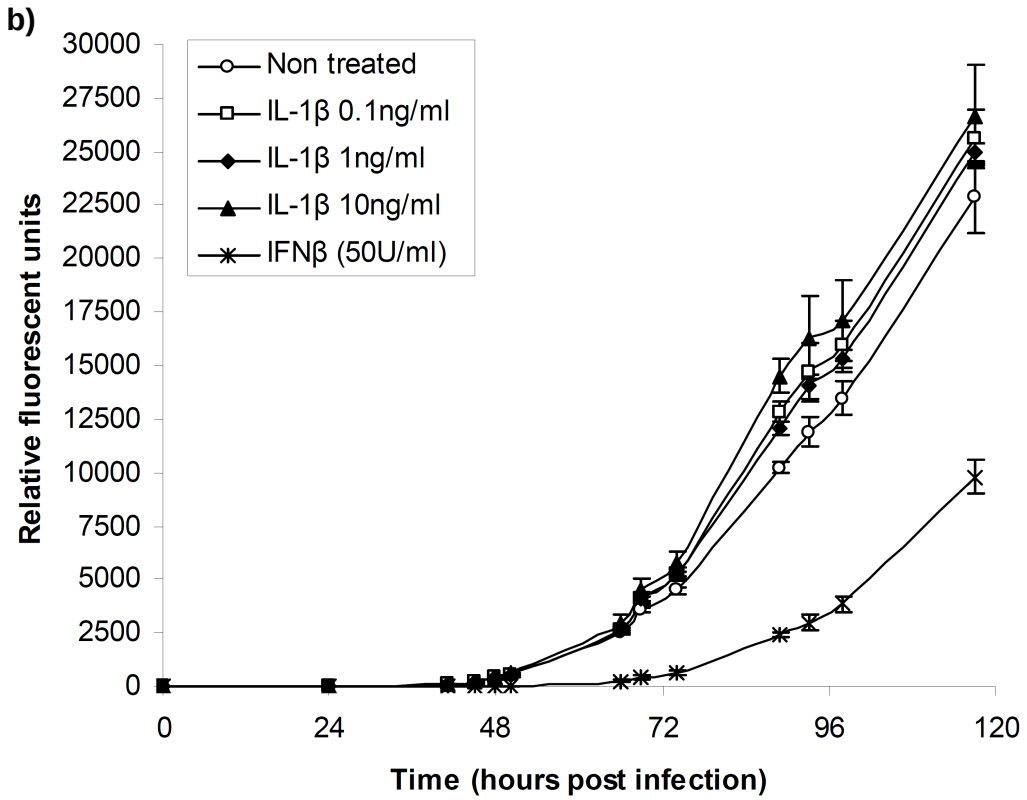

Figure 3.1: Effect of IL-1β on MCMV growth in NIH/3T3 cells. NIH/3T3 cells were treated with IL-1β at 0.1, 1 or 10 ng/ml or IFNβ at 50 U/ml for 8 hr followed by infection with MCMV-GFP (MOI = 0.02). Following infection cells were maintained in the presence of cytokines as per pre-infection treatment. (a) Whole well views of cell treated with IL-1β (10 ng/ml) or IFNβ (50 U/ml) were acquired at 2, 3 and 4 day post-infection. A representative experiment of three performed is shown (BF = Bright field; F = Fluorescence). (b) Viral replication was determined as a measure of GFP fluorescence. A representative experiment of three performed is shown. Each data point represents the average and standard deviation from six independent wells.

* Image acquisition for section (a) of this figure was performed by Kimberly Martin at the Division of Pathway Medicine.

3.2.1.2 IκBα degradation kinetics following cytokine stimulation in NIH/3T3 cells

The aim of this chapter is to examine whether MCMV infection modulates IL-1β-induced IκBα degradation. To establish a temporal frame work for measuring IL-1β-induced IκBα degradation, the kinetics of this response were initially evaluated in non-infected cells. As TNFα-induced IκBα degradation is known to be inhibited by MCMV (Le et al., 2008) (Mack et al., 2008), stimulation with this cytokine was included as a positive control throughout this chapter. Therefore, the kinetics of TNFα-induced IκBα degradation were also evaluated. NIH/3T3 cells were treated with a range of IL-1β or TNFα concentrations. Whole cell lysates were collected at 15, 30 and 45 min following stimulation and analysed by Western blotting. Stimulation with IL-1β resulted in almost complete IκBα degradation by 15 min post stimulation. Thereafter, increasing IκBα amounts were observed with IκBα levels at 45 min post-treatment being comparable to pre-stimulation levels (Figure 3.2a). Treatment with TNFα resulted in almost identical degradation kinetics (Figure 3.2b). These results are in accordance with previously published kinetics of cytokine stimulated IκBα degradation in fibroblasts (Huang et al., 2004) (Hoffmann et al., 2002). IκBα degradation kinetics were comparable between the different concentrations used, probably due to system saturation. Overall, at 15 min post IL-1β/ TNFα stimulation IκBα is largely degraded. The very low levels of IκBα at this time point provide an ideal background against which to measure any inhibition in IκBα degradation. It was therefore decided to use 15 min of cytokine treatment as the experimental time point in later experiments.

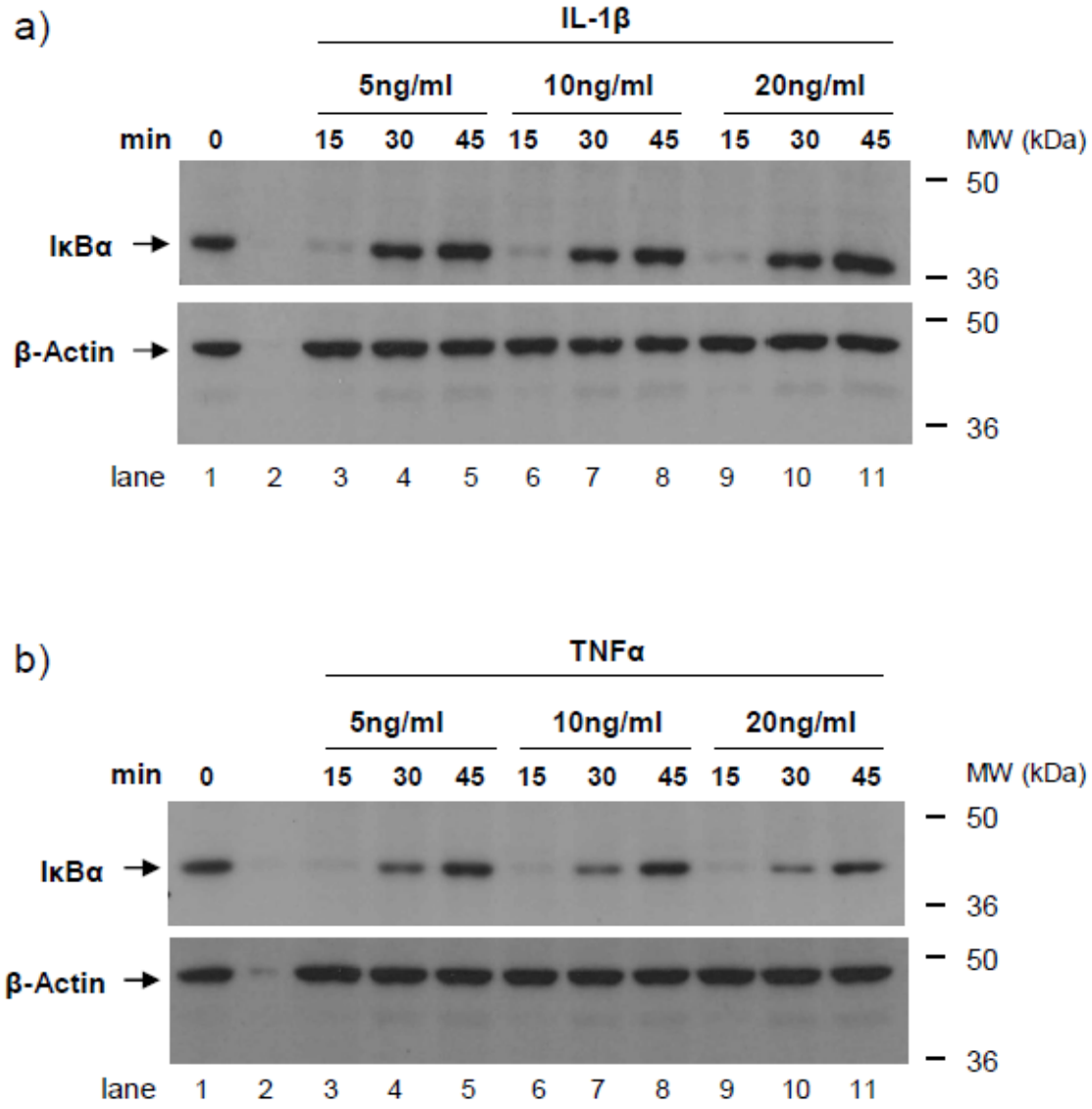

Figure 3.2: IκBα degradation kinetics following cytokine stimulation in NIH/3T3 cells. Cells were treated with different concentrations of TNFα (*a*) or IL-1β (*b*) for the indicated periods of time. Whole cell lysates were harvested and analysed using SDS-PAGE and immunoblotting with primary antibodies against either IκBα or β-Actin. No sample was loaded in lane 2 (n = 2).

3.2.2 IκBα degradation following IL-1β stimulation is inhibited in MCMV-infected cells

The aim of this chapter is to examine whether MCMV infection modulates the degradation of IκBα, the hallmark of NF-κB activation, following IL-1β stimulation. To begin examining this hypothesis, NIH/3T3 cells were mock treated or infected with MCMV, and at 7 hpi stimulated with IL-1β or TNFα. Whole cell lysates were prepared and analysed by Western blotting (Figure 3.3a). The time point used for cytokine stimulation, i.e. 7 hpi, was chosen for the following reasons: a) MCMV, as well as HCMV, attachment to the cell surface as well as infection initiate extensive cellular responses within minutes and hours (Yurochko et al., 1997) (Yurochko and Huang, 1999) (Le et al., 2008) (Browne et al., 2001). It is of great interest to establish the interplay between the virus and these early cellular responses to infection. Early detection of infection is attributed at least in part to TLRs (Boehme et al., 2006). MCMV putative inhibition of TLRs as well as IL-1β signalling (the latter being the subject matter of this chapter) forms the central hypothesis for this thesis. It was therefore of interest to examine this hypothesis within early times post infection; b) this chapter focuses on IκBα levels as a measurement for signal transduction by IL-1β. It has previously been shown that at 7 hpi IκBα levels in infected cells are comparable to those in mock-infected cells (Le et al., 2008). Indeed, in experiments presented here, prior to further stimulation, comparable IκBα levels were observed in mock- and MCMV-infected cells. In accordance with published data (Le et al., 2008), while TNFα

stimulation of non-infected cells caused a drastic decrease in IκBα levels, MCMV infection inhibited the degradation of IκBα following treatment with this cytokine. Importantly, in infected cells treated with IL-1β levels of IκBα remained equivalent to those in infected but non-treated cells. To test whether this observation was due to inhibition of IκBα degradation or a kinetic change in the breakdown of this protein, mock and MCMV infected cells were treated with IL-1β for 15, 30 or 60 min (Figure 3.3b). In non-infected cells cytokine stimulation resulted in almost complete degradation of IκBα at 15 min, followed by a slight recovery at 30 min and a return to steady state levels at 60 min post treatment. In contrast, in MCMV-infected cells IκBα levels appear stable through out the time course with only a slight decrease observed at 15 min post treatment. These results indicate that IκBα degradation following IL-1β stimulation is inhibited in MCMV-infected cells.

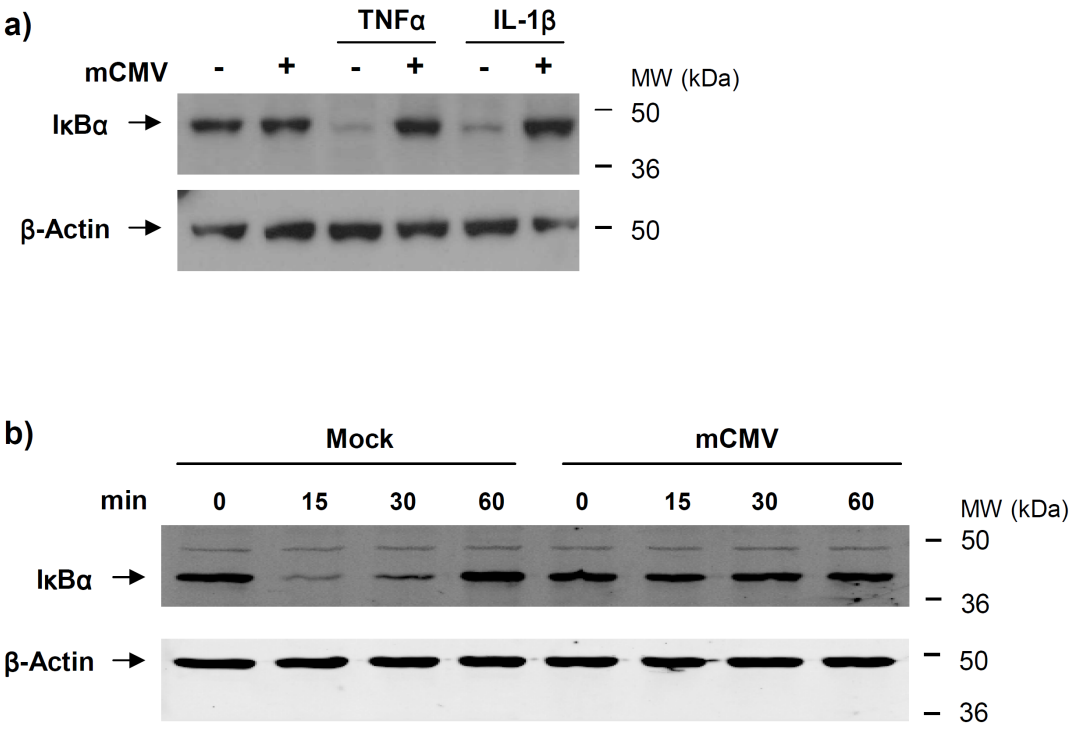

Figure 3.3: IκBα degradation following IL-1β stimulation is inhibited in MCMV-infected cells. a) NIH/3T3 cells were mock infected or infected with MCMV (MOI = 5) and at 7 hpi stimulated with IL-1β (10 ng/ml) or TNFα (10 ng/ml) for 15 min. Whole cell lysates were harvested and analysed using SDS-PAGE and immunoblotting with primary antibodies against either IκBα or β-Actin (n = 3). b) NIH/3T3 cells were mock infected or infected with MCMV (MOI = 5) and at 7hpi stimulated with IL-1β (10 ng/ml) for 15, 30 or 60 min. Cell lysates were analysed as described for (a) (n = 1).

3.2.3 De-novo viral gene expression is required for MCMV modulation of IκBα degradation following IL-1β stimulation

In the previous section (3.2) it was demonstrated that in MCMV infected cells IL-1β stimulation does not result in a decrease in IκBα levels. To test whether this is dependent on de-novo viral gene expression, the MCMVdie3 mutant virus, which lacks the fifth exon of the *ie1/ie3* transcription-unit, was used (for genomic map see Chapter 2). Gene expression of this mutant is limited to immediate-early genes *ie1* and *ie2*, rendering the virus extremely growth deficient. Replication can be rescued by growing the virus on a complementary cell line (Bam25) expressing both IE1 and IE3 (Angulo et al., 2000) (Lacaze et al., 2011). The most commonly used methods to test the involvement of viral products in processes observed in infected cells are application of Cycloheximide (CHX) or infection with ultraviolet (UV)-inactivated virus. CHX blocks the translation of both cellular and viral proteins and thus would not have been the method of choice for the work presented here, as it was preferable to isolate viral protein production without altering cellular protein synthesis. UV- inactivation damages viral DNA and thus renders the virus incapable of gene expression and DNA replication. The use of the MCMVdie3 mutant virus in comparison to UV-inactivation offers the advantage of a phenotype reversal as MCMVdie3 mutant is able to grow on Bam25 cells.

The growth characteristics of MCMVdie3 were re-evaluated in comparison to MCMV using PFU based single step (MOI = 2) growth curves. While infection of NIH/3T3 cells with MCMV resulted in productive infection, no viral growth for MCMVdie3 was

detectable in these cells (Figure 3.4a). Infection of Bam25 cells with the mutant virus resulted in recovery of viral replication although to somewhat attenuated levels in comparison to the wild type virus (Figure 3.4b). This is in agreement with previously published data and shows that MCMVdie3 is a viable virus if the IE3 protein is provided in *trans.* Additionally, the kinetics of IκBα degradation in response to cytokine stimulation were tested in the Bam25 cell line. Cells were treated with IL-1β or TNFα and following stimulation for 15, 30, 45 and 60 min whole cell lysates were collected to be analysed by Western blotting (Figure 3.5). IκBα degradation kinetics did not differ following stimulation with either cytokine. IκBα was quickly and drastically reduced (to 10% of pre-stimulation levels) at 15 min post treatment. A slight recovery was recorded at 30 min (20% of pre-stimulation levels) with IκBα levels at 45 min post stimulation being comparable to those in non-treated. These results are similar to data obtained from NIH/3T3 cells. In both cell lines drastic degradation of IκBα was observed at 15 min post cytokine stimulation and recovery of protein levels observed thereafter. These results demonstrate that IκBα degradation in Bam25 cells is normal and additionally excludes a role for IE3 as well as IE1 in IL-1β signal inhibition

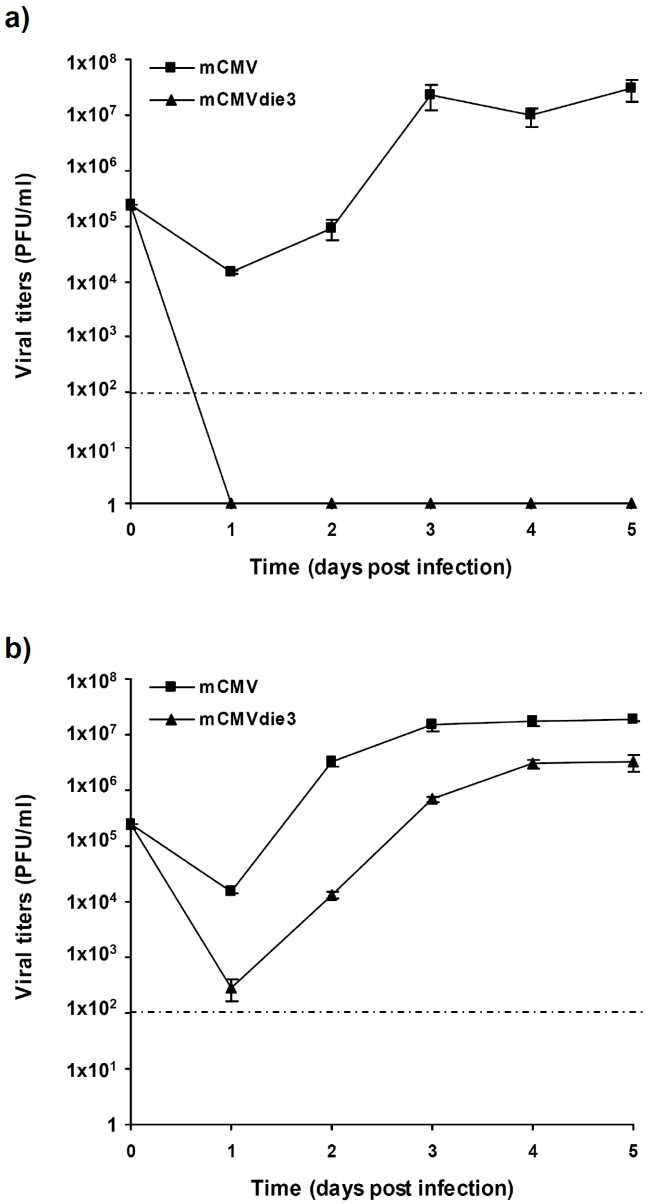

Figure 3.4: Growth kinetics of MCMV and MCMVdie3 on NIH/3T3 and Bam25 cells. NIH/3T3 (*a*) or Bam25 (*b*) cells were infected at MOI = 2 with MCMV or MCMVdie3. At indicated time points post infection (days post infection) supernatants from the infected cultures were harvested and titered on Bam25 monolayers. Error bars indicate the standard deviation from three separate wells. Dotted line represents the limit of detection (100 PFU/ml) (n = 2).

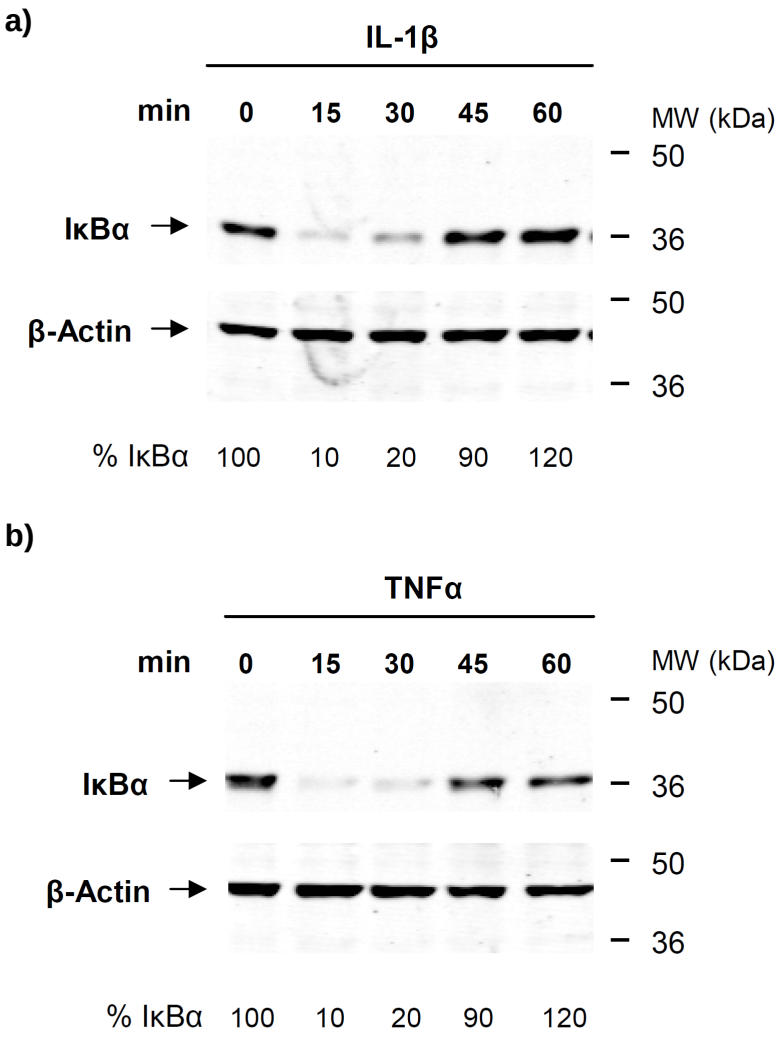

Figure 3.5: IκBα degradation kinetics following cytokine stimuli in Bam25 cells. Cells were treated with IL-1β (10 ng/ml) (*a*) or TNFα (10 ng/ml) (*b*) for the indicated periods of time. Whole cell lysates were harvested and analysed using SDS-PAGE and immunoblotting with primary antibodies against either IκBα or β-Actin. Integrated fluorescence intensity was calculated (see Chapter 2 section 2.5.3.2) for IκBα protein bands, normalised to corresponding β-Actin levels and expressed as percentage of IκBα at min 0 (n = 1).

Next, viral modulation of IL-1β induced IκBα degradation was compared in NIH/3T3 cells infected with MCMV or MCMVdie3. To this end, cells were mock, MCMV or MCMVdie3 infected and at 7 hpi treated with either IL-1β or TNFα for 15 min. Whole cell lysates were prepared and analysed by Western blotting. As shown in Figure 3.3 an MOI of 5 was used for the initial experiment to ensure a maximum number of infected cells. However, in order to optimise the use of reagents, namely viral stocks, it was considered whether a lower MOI would produce comparable levels of infection in this cell culture system. NIH/3T3 fibroblasts are a fully permissive cell line commonly used in MCMV research (Ghazal et al., 2003). For a fully infection-permissive cell line such as NIH/3T3 fibroblasts it is possible to use a formula based on the Poisson distribution to calculate the fraction of the culture that is infected by a certain number of virus particles and also to estimate the total number of cells infected for a specific MOI (S. J. Flint, 2009). For example, it is estimated that ~ 95% and ~ 99% of cells will be infected when MOI of 3 and 5 are used, respectively (calculation was done by Muhamad Fairus .B.N. Hassim from The Division of Pathway Medicine, The University of Edinburgh, UK). Hence both a MOI of 3 and MOI of 5 would result in ≥ 95% of the culture infected. Therefore an MOI of 3 was considered sufficient for all subsequent experiments in this thesis. MCMVdie3 infection results in *ie1* expression, therefore, infection with both MCMV and MCMVdie3 could be confirmed by detection of IE1. Expression of IE1 was readily detectable in cells infected with wild type or mutant virus (indeed somewhat higher levels of IE1 were seen in MCMVdie3 infected cells than in MCMV infected cells) (Figure 3.6a + b). Stimulation of mock-infected cells resulted in a dramatic decrease in IκBα levels to ~10% of non-treated levels. This was inhibited to a

large degree in MCMV-infected cells in which post-stimulation IκBα levels were five times higher (~50%) of those in non-treated cells. The decrease in IκBα in MCMVdie3 infected cells was the same as that observed in mock infected samples with a drop to ~10% of pre-treatment IκBα levels. This was true for stimulation with IL-1β (Figure 3.6a) as well as with TNFα (Figure 3.6b). These results indicate that immediate early genes *ie1* and *ie2*, which are expressed following infection with MCMVdie3, do not play a role in modulation of IκBα degradation following cytokine stimulation of infected cells. Thus, in contrast to cells infected with MCMV, IL-1β stimulation of MCMVdie3 infected cells does result in IκBα degradation.

Finally, it was tested whether the MCMVdie3 virus is able to inhibit IL-1β signalling in the Bam25 cell line. To this end Bam25 cells were mock treated or infected with either MCMV or MCMVdie3 for 7 hr followed by stimulation with IL-1β or TNFα for 15 min. Whole cell lysates were collected and analysed by Western blotting. The results obtained from mock or MCMV infected cells were equivalent to those seen in NIH/3T3 cells (Figure 3.6). MCMVdie3 infection resulted in inhibition of IκBα degradation in a similar or even higher degree to that observed for infection with MCMV. IE1 was detected in both infected and non-infected cells as Bam25 cells stably express this protein (Figure 3.7).

Taken together these results indicate that IL-1β-induced IκBα degradation is inhibited in MCMV infected cells, in a manner dependent on de-novo viral protein expression.

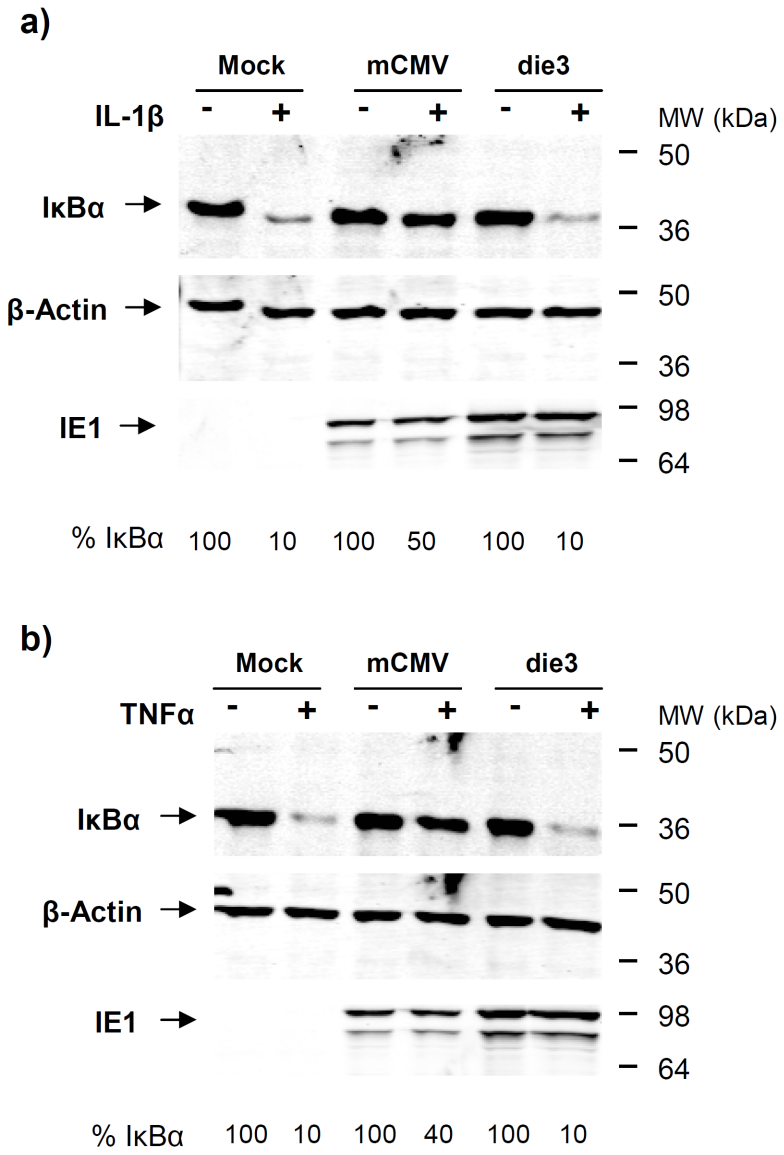

Figure 3.6: MCMVdie3 does not inhibit IκBα degradation in IL-1β stimulated NIH/3T3 cells. NIH/3T3 cells were mock infected or infected with MCMV or MCMVdie3 (MOI = 3). At 7 hpi cells were stimulated with IL-1β (10 ng/ml) (a) or TNFα (10 ng/ml) (b) for 15 min. Whole cell lysates were harvested and analysed using SDS-PAGE and immunoblotting with primary antibodies against IκBα, β-Actin or IE1. Integrated fluorescence intensity was calculated (see Chapter 2 section 2.5.3.2) for IκBα protein bands, normalised to corresponding β-Actin levels and expressed as percentage of IκBα in non-stimulated cultures (n = 2).

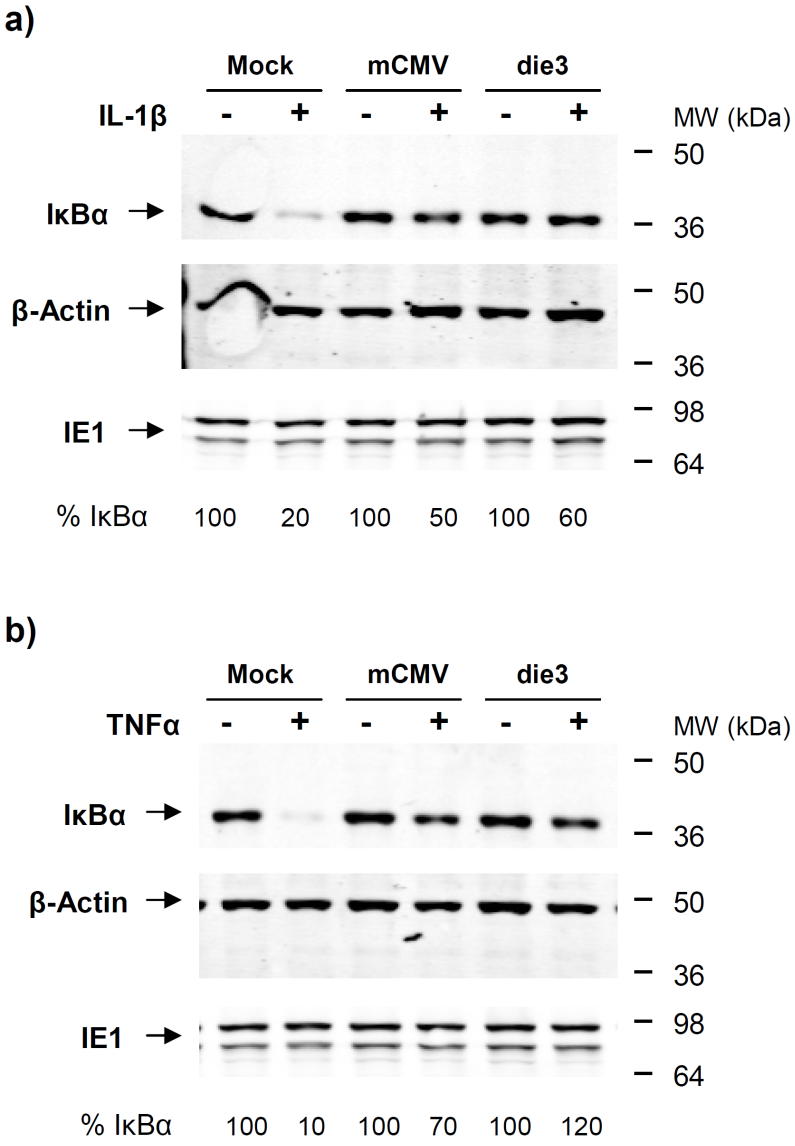

Figure 3.7: MCMVdie3 inhibits IκBα degradation in IL-1β stimulated Bam25 cells. Bam25 cells were mock infected or infected with MCMV or MCMVdie3 (MOI = 3). At 7 hpi cells were stimulated with IL-1β (10 ng/ml) (a) or TNFα (10 ng/ml) (b) for 15 min. Whole cell lysates were harvested and analysed using SDS-PAGE and immunoblotting with primary antibodies against IκBα, β-Actin or IE1. Integrated fluorescence intensity was calculated (see Chapter 2 section 2.5.3.2) for IκBα protein bands, normalised to corresponding β-Actin levels and expressed as percentage of IκBα in non-stimulated cultures (n = 2).

Discussion

CMVs have co-evolved with their hosts and accordingly acquired multiple strategies for modulation of host immunity. Various TLRs including TLR2, TLR7 and TLR9 are now known to contribute to the initiation of host response to CMV infection (Tabeta et al., 2004) (Krug et al., 2004) (Zucchini et al., 2008) (Barbalat et al., 2009). Signalling pathways activated by these TLRs as well as by the key pro-inflammatory cytokine IL-1β are characterised in great detail. However, little is known about the modulation of these signalling events during CMV infection. Work presented in this chapter examined whether IL-1β induced IκBα degradation is modulated in MCMV-infected cells.

Initial characterisation of the interplay between IL-1β and MCMV included examination of the effect of this cytokine on viral replication in 3T3/NIH fibroblasts (Figure 3.1). IL-1β has been previously shown to inhibit the growth of HCMV in human foreskin fibroblasts (HFF) and marrow stromal cell lines (Iwata et al., 1999) (Randolph-Habecker et al., 2002). Additionally, pre-treatment of mouse embryonic fibroblasts (MEFs) with IL-1β was found to reduce MCMV virus titre at day 5 post infection in comparison to control cells (van der Meer et al., 1989). However, data presented here do not indicate IL-1β inhibition of MCMV replication. The disparity between these findings and previously published data could be due to the different cell types examined and/or cytokine treatment regimes used or the methods chosen to measure viral replication. It would be of interest to conduct further experiments utilising various cytokine-treatment

regimes and cell types as well to evaluate viral growth using plaque assay based growth curves.

Data presented in this chapter show that in fibroblasts infected with MCMV the degradation of IκBα following IL-1β stimulation is inhibited in a manner dependent on de-novo viral gene expression (Figures 3.3, 3.6 and 3.7). It is noteworthy that the inhibition of IκBα degradation in infected cells was not complete i.e. a reduction in IκBα levels following cytokine stimulation was observed although markedly less than that seen in non-infected cells. In this regards the MOIs used and therefore the proportion of the culture expected to be and was actually infected should be considered. In the experiments shown (with the exception of Figure 3.3) an MOI of 3 was used which, as outlined above, is predicted to result in ~ 95% of cells being infected. Conversely, it is expected that a proportion of cells remain non-infected (~ 5% is predicted under optimal conditions but this percentage is presumably higher in culture and remains to be determined experimentally). In this cell population IL-1β stimulation will lead to IκBα degradation and this may account for at least a part of the observed reduction in IκBα levels following cytokine stimulation of infected cultures. The following approaches could be taken to further explore this possibility: - Determine the proportion of cells infected in the cell culture system used when different MOIs are applied (for example, by using the MCMV-GFP virus combined with flow cytometry analysis to establish the percentage of infected cells); - Compare IL-1β- induced IκBα degradation between cultures infected with various MOIs (for example, MOI of 1, 3 and 5). Importantly, IL-1β can induce IκBα dissociation from NF-κB and thus NF-κB activation in a manner

independent of IκBα degradation (Yao et al., 2007) (Yamazaki et al., 2009). Therefore, further experiments are needed to establish how observations presented here correlate with NF-κB nuclear translocation, DNA binding and importantly functional outcomes such as expression of NF-κB inducible genes. Finally, these data do not distinguish between specific inhibition of IL-1β signal transduction at a step upstream of NF-κB and its immediate regulatory network or a general block on NF-κB activation imposed by the virus or a combination of the two. Interestingly, Le *et al* showed that MCMV extends the stability of IκBα, under CHX treatment, beginning at approximately 5 hpi (Le et al., 2008). The significance of this observation, how it may correlate with the data presented here and whether it indicates viral modulation of the function of IκBα and therefore of NF-κB remains to be seen.

HCMV has previously been shown to suppress IL-1β as well as TNFα induction of cytokine and chemokines expression (Jarvis et al., 2006) (Montag et al., 2006). Interestingly, this was found to be distinctly regulated. In HCMV infected cells IL-1β failed to induce IκBα phosphorylation and degradation as well as NF-κB nuclear translocation. In contrast, IκBα processing following TNFα stimulation did take place albeit with retarded kinetics. As IL-1β and TNFα signal through distinct pathways converging on the IKK complex, it was concluded that HCMV alters signal transduction by these cytokines upstream of IKK activation in a pathway specific manner. However, the viral proteins mediating this effect or the underlying mechanism were not defined (Jarvis et al., 2006). In the work presented here viral inhibition of TNFα signalling was used as a positive control since MCMV has been shown to modulate this pathway prior

to IKK activation via disruption of RIP1 function (Mack et al., 2008). As RIP1 is not known to function in the context of the IL-1β signalling pathway it is unlikely that this mechanism explains the observation made here. However, this does not exclude the existence of additional viral mechanisms altering both TNFα and IL-1β signalling. Finally, both HCMV and MCMV have previously been shown to down regulate the expression of TNFR1 (Montag et al., 2006) (Popkin and Virgin, 2003). It remains to be tested whether expression of the IL-1β receptor is modulated by MCMV infection.

Overall, a previously unknown MCMV modulation of IκBα degradation following IL-1β stimulation is shown in this chapter, establishing an experimental framework in which to further test the hypothesis of this thesis.

4 Chapter 4

The MCMV protein M45 inhibits IκBα degradation following IL-1β stimulation

4.1 Introduction

The MCMV protein M45 inhibits PRR and pro-inflammatory cytokine signalling as well as serving as a key suppressor of both intrinsic and extrinsic cell death mechanisms (Brune et al., 2001) (Mack et al., 2008) (Upton et al., 2010). Mutation of this gene renders MCMV effectively avirulent in SCID mice including failure to replicate in target organs (Lembo et al., 2004). To date, M45 functions in modulation of cellular responses have been attributed to its binding of receptor interacting protein (RIP) family members, namely RIP1 and RIP3 (Mack et al., 2008) (Upton et al., 2010). RIP proteins are serine/threonine kinases activated in response to cellular stress signals such as PRR activation, death receptor ligation and DNA damage. Activation of RIP proteins results in stimulation of cellular transcription factors such as NF-κB and MAPKs as well as in induction of cell death (Festjens et al., 2007) (Declercq et al., 2009) (Meylan and Tschopp, 2005). M45 was initially described as a cell tropism determinant, required for inhibition of cell death in endothelial cells (Brune et al., 2001). Further studies demonstrated that M45 inhibits infection-induced RIP3-dependent necrosis and is therefore required for viral growth in RIP3 expressing cells (Upton et al., 2010). In addition, M45 abrogates TNFα-induced programmed necrosis, also termed necroptosis,

a process dependent on both RIP1 and RIP3 (Mack et al., 2008) (Upton et al., 2010). Upton *et al* mapped the RIP1/3 interaction domain on M45 to a RIP homotypic interaction motif (RHIM) domain, present in all three proteins (RIP1, RIP3 and M45) (Upton et al., 2008). A mutant virus M45*mut*RHIM, carrying alanine substitutions disrupting the RHIM domain, was found incapable of inhibiting virus-induced RIP3-dependent cell necrosis as well as necroptosis. Importantly, the attenuated in-vivo phenotype of M45*mut*RHIM (as measured by lack of footpad swelling and inability to recover replicating virus from salivary-glands) is reversed in RIP3 knock-out animals, thus demonstrating that RHIM-dependent M45 interactions specifically target RIP3 function (Upton et al., 2010). In addition to the above mentioned inhibition of TNFα mediated necroptosis, M45 also disrupts NF-κB and p38 activation by this cytokine (Mack et al., 2008). This M45 function was attributed to M45 binding to RIP1, which is necessary for TNFα signal transduction (Mack et al., 2008) (Kelliher et al., 1998) (Lee et al., 2003). In contrast to the finding by Upton *et al* described above, Mack et al found M45 binding with RIP1 to be independent of RHIM interactions (Mack et al., 2008). Finally, M45 inhibits TLR3 and DAI induced NF-κB activation, presumably via interaction with RIP1 and RIP3 (Mack et al., 2008) (Rebsamen et al., 2009). RIP1 participates in the TLR3 signalling pathway following recruitment to the TRIF, itself a RHIM domain containing protein (Cusson-Hermance et al., 2005). Two RHIM domains are present in DAI and serve to bind both RIP1 and RIP3 (Kaiser et al., 2008). The significance of these observations to *in vivo* viral pathogenesis remains to be examined.

In the previous chapter, MCMV infection was shown to modulate the degradation of IκBα following stimulation with IL-1β. Experiments were performed at 7 hpi, a time point at which M45 is expressed in infected cells (albeit to lower levels than at later times post infection) (Lacaze et al., 2011) (Upton et al., 2010). M45 has been shown to inhibit NF-κB activation by TNFα and other PRRs all of which utilise RIP1 as an obligatory signalling module. While RIP proteins do not play a role in IL-1β signalling (Weber et al., 2010) (Meylan et al., 2004), they are, interestingly, related to IRAK family members, which perform a key role in the IL-1β pathway (Meylan and Tschopp, 2005) (Manning et al., 2002). The aim of this chapter is to examine whether M45 plays a role in the observed inhibition of IL-1β-induced IκBα degradation.

4.2 Results

4.2.1 M45 inhibits IL-1β induced IκBα degradation

To test whether M45 plays a role in MCMV inhibition of IL-1β-induced IκBα degradation, NIH/3T3 cells were mock treated or infected with MCMV, a M45 deletion mutant (ΔM45) or complement virus into which M45 has been re-introduced (CM45). Mock treated and infected cells were stimulated with IL-1β, at 7 hpi, for 15 min. Whole cell lysates were prepared and analysed by Western blotting (Figure 4.1a). Expression of IE1 was equivalent following infection with all three viruses. IκBα levels prior to IL-1β stimulation were comparable between non-infected cells and cells infected with any of the three viruses. This is in agreement with previously published data (Mack et al., 2008). IκBα levels decreased dramatically following IL-1β treatment of mock infected cells but remained stable in MCMV or CM45 infected cells. In ΔM45-infected cells, the fall in IκBα levels was equivalent to that in non-infected cells. Thus, M45 is necessary for inhibition of IκBα degradation following IL-1β stimulation of MCMV infected cells. It was then asked whether M45 is sufficient to block IL-1β-induced IκBα degradation. Cells were transfected with M45 or HA-M45 expression vectors followed by stimulation with IL-1β. Whole cell lysates were prepared and analysed by Western blotting (Figure 4.1b). IL-1β stimulation of cells transfected with empty or a GFP expression vector resulted in almost complete degradation of IκBα. However, in cells transfected with vectors expressing M45 or tagged M45, IκBα degradation was markedly inhibited. The partial decrease in IκBα levels observed in M45 or tagged M45 transfected cells may

represent non-transfected cells. Taken together, these results show that M45 is necessary and likely sufficient to block IL-1β-induced IκBα degradation.

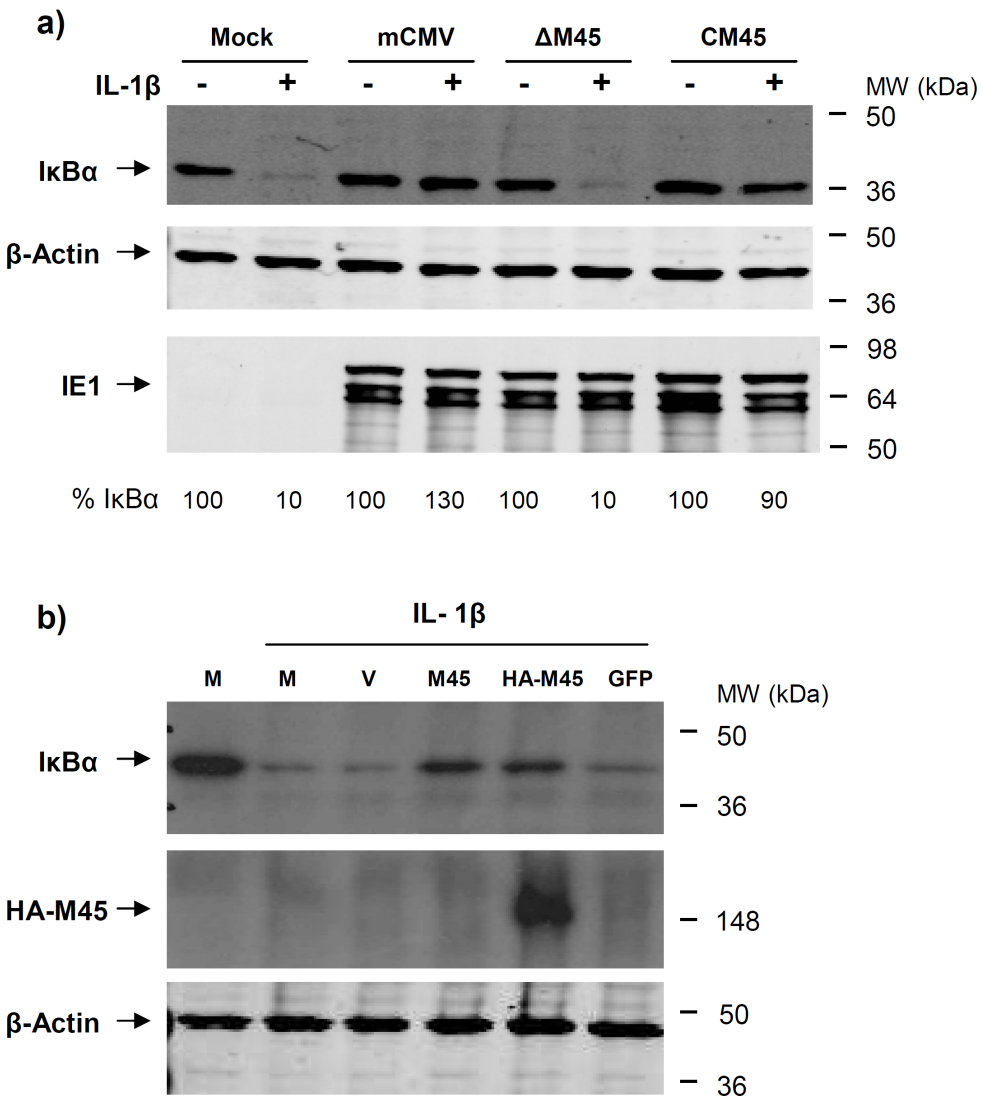

Figure 4.1: M45 inhibits IL-1β induced IκBα degradation. a) NIH/3T3 cells were mock treated or infected with MCMV, ΔM45 or CM45 (MOI = 3). At 7 hpi cells were stimulated with IL-1β (10 ng/ml) for 15 min. Whole cell lysates were harvested and analysed by using SDS-PAGE and immunoblotting with primary antibodies against IκBα, β-Actin or IE1. Data shown are representative of at least three independent experiments. Integrated fluorescence intensity was calculated (see Chapter 2 section 2.5.3.2) for IκBα protein bands, normalised to corresponding β-Actin levels and expressed as percentage of IκBα in non-stimulated cultures (n = 3). b) NIH/3T3 cells were mock treated (M), or transfected with empty vector (V), GFP, M45 or HA-M45 expression vectors. At 12 hr post transfection cells were treated with IL-1β (10 ng/ml) for 15 min. Whole cell lysates were harvested and analysed by using SDS-PAGE and immunoblotting with primary antibodies against IκBα, β-Actin or HA (n = 1).

4.2.2 p38 phosphorylation in MCMV infected cells following IL-1β stimulation

IL-1β activates MAPKs cascades as well as NF-κB (Weber et al., 2010). IL-1β stimulation leads to activation of TAK1, a MAPK kinase kinase, which in addition to its interaction with the IKK- NF-κB system also activates MAPK kinases. In turn, MAPK kinases, namely MEK3/MEK6 and MEK4/MEK7, phosphorylate and thus activate p38 and JNK family members, respectively. In view of the observation that M45 inhibits IL-1β-induced IκBα degradation, it was asked whether M45 also modulates the phosphorylation of p38 to p-p38.

The kinetics of p38 phosphorylation in response to IL-1β stimulation of NIH/3T3 cells were initially examined. Whole cell lysates were collected at 0, 4, 8, 12, 16 and 20 min following IL-1β treatment and analysed by Western blotting. Phosphorylation of p38 increased significantly within 4 min of stimulation and continued to rise at 8 min of cytokine treatment. Thereafter, phosphorylation levels dropped (Figure 4.2).

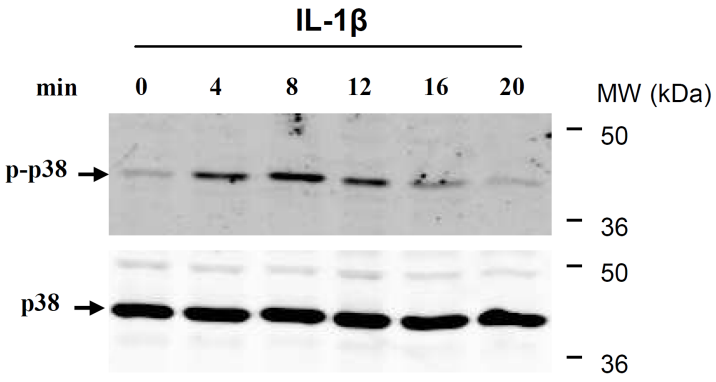

Figure 4.2: p38 phosphorylation kinetics following IL-1β stimulation in NIH/3T3 cells. NIH/3T3 cells were treated with IL-1β (10 ng/ml) for the indicated periods of time. Whole cell lysates were harvested and analysed using SDS-PAGE and immunoblotting with primary antibodies against either p-38 or p-p38 (n = 2).

Next, p38 phosphorylation following IL-1β stimulation was tested in MCMV infected cells. NIH/3T3 cells were mock treated or infected with MCMV, ΔM45 or CM45 and at 7 hpi treated with IL-1β for 0, 4, 8, 12 and 16 min. Whole cell lysates were prepared and analysed by Western blotting (Figure 4.3a and 4.3b). p38 phosphorylation followed a similar pattern in mock treated cells or cells infected with either wild-type or mutant viruses: levels of p-p38 quickly rose in response to IL-1β, peak phosphorylation was observed at 8 to 12 min post-stimulation with comparable fold change increase observed for all conditions (mock infection or infection with the different viruses), followed by a drop in p-p38 levels. It should be noted that the kinetics of phosphorylation and dephosphorylation did differ between experiments. Importantly, however, within each experiment the rate of p38 phosphorylation/dephosphorylation was similar under all conditions (mock infection or infection with the different viruses) (with exception of ΔM45-infected cells in Figure 4.3a in which dephosphorylation of p-p38 appears to be of slower kinetics than in mock-, wild-type- or CM45- infected cells). Finally, p38 phosphorylation following IL-1β stimulation was compared in cells productively or non-productively infected with MCMV. NIH/3T3 cells were mock treated or infected with MCMV or MCMVdie3 and at 7 hpi treated with IL-1β for 0, 4, 8, 12 and 16 min. Whole cell lysates were prepared and analysed by Western blotting (Figure 4.3c). IL-1β induced p-38 phosphorylation kinetics were highly similar in mock, MCMV or MCMVdie3 infected cells: levels of p-p38 quickly rose in response to IL-1β, peak phosphorylation (~ 3 fold increase in comparison to mock non-stimulated cells) was observed at 8 min post-stimulation, followed by a drop in p-p38 levels. Finally, results obtained for mock and MCMV infected cells in the three independent experiments

shown in Figure 4.3a-c were statistically analysed (Figure 4.3d). It was found that IL-1β induced p-38 phosphorylation kinetics does not differ, at least at the time post infection examined, in MCMV infected cells in comparison to non-infected cells. Taken together, these results indicate that MCMV, and specifically M45, do not inhibit the phosphorylation of p38 in response to IL-1β.

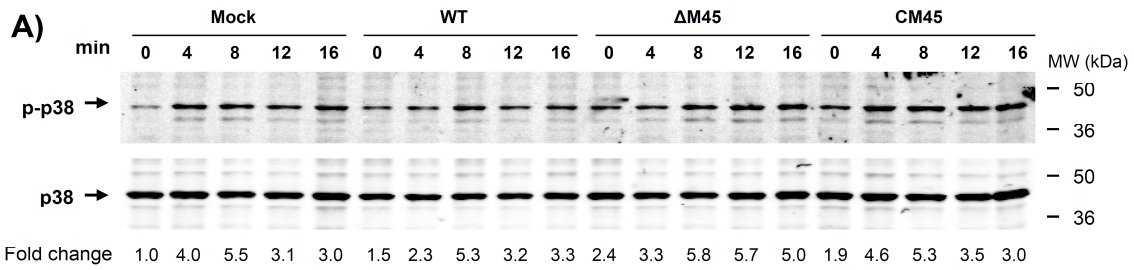
A)
Mock
WT
ΔM45
CM45
min
0 4 8 12 16 0 4 8 12 16 0 4 8 12 16 0 4 8 12 16
MW (kDa)
p-p38
50
36
p38
50
36
Fold change 1.0 4.0 5.5 3.1 3.0 1.5 2.3 5.3 3.2 3.3 2.4 3.3 5.8 5.7 5.0 1.9 4.6 5.3 3.5 3.0

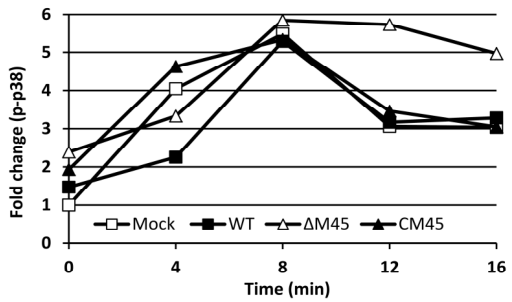
Fold change (p-p38)
Mock
WT
ΔM45
CM45
Time (min)

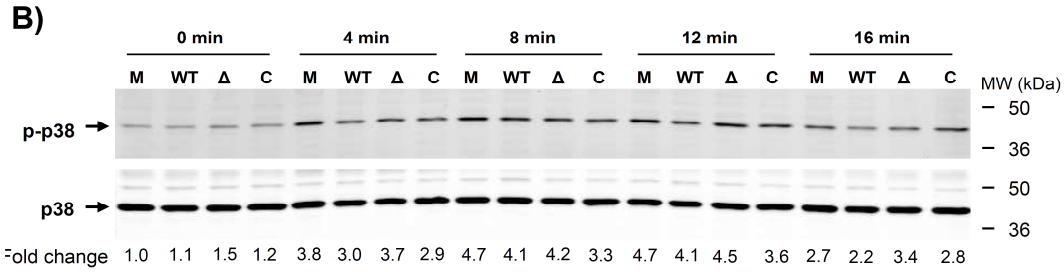
B)
0 min
4 min
8 min
12 min
16 min
M WT Δ C M WT Δ C M WT Δ C M WT Δ C M WT Δ C
MW (kDa)
p-p38
50
36
p38
50
36
Fold change 1.0 1.1 1.5 1.2 3.8 3.0 3.7 2.9 4.7 4.1 4.2 3.3 4.7 4.1 4.5 3.6 2.7 2.2 3.4 2.8

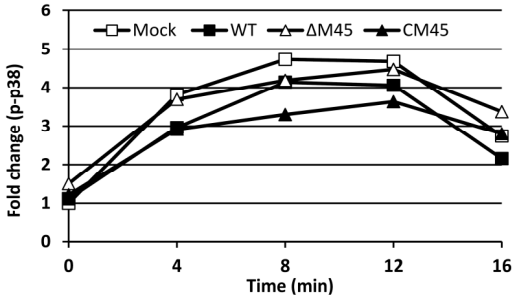
Mock
WT
ΔM45
CM45
Fold change (p-p38)
Time (min)

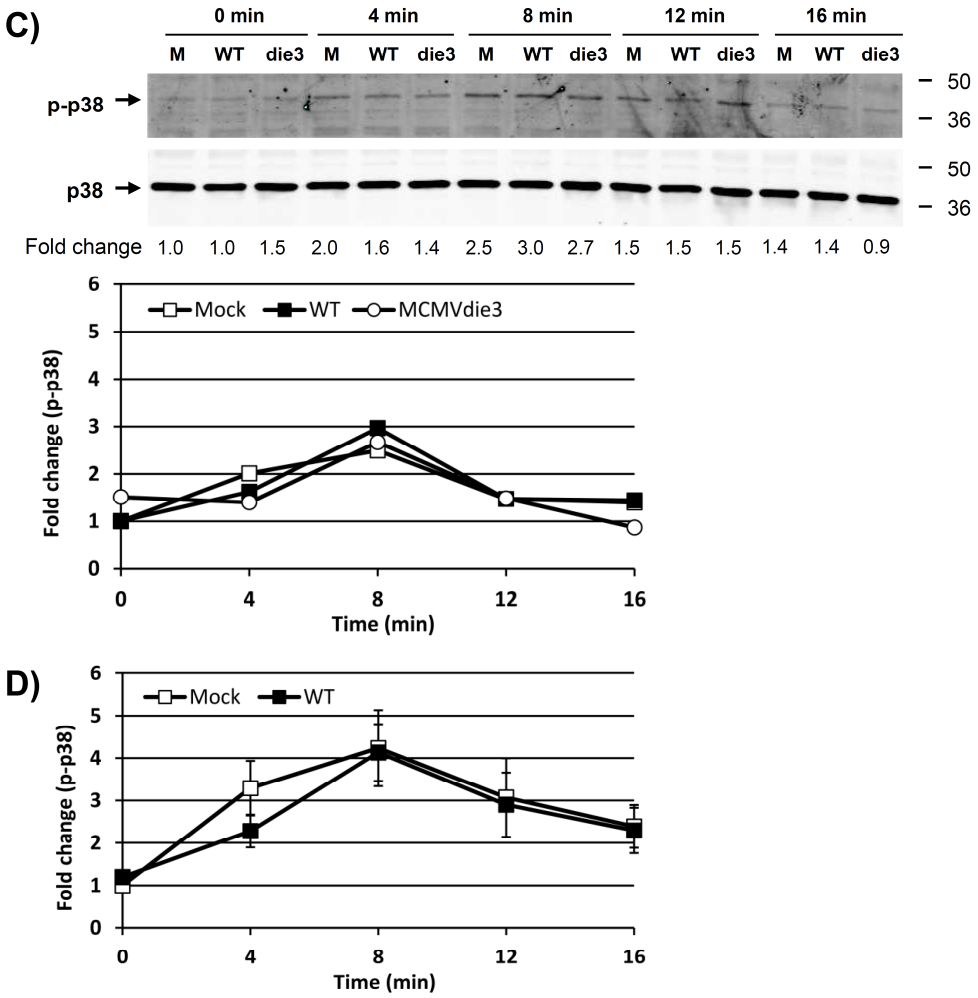

Figure 4.3: p38 phosphorylation in MCMV infected cells following IL-1β stimulation. a) and b) NIH/3T3 cells were mock infected or infected with MCMV, ΔM45 or CM45 (MOI = 3). At 7 hpi cells were stimulated with IL-1β (10 ng/ml) for indicated periods of time. Whole cell lysates were harvested and analysed by using SDS-PAGE and immunoblotting with primary antibodies against p38 and p-p38. Integrated fluorescence intensity was calculated (see Chapter 2 section 2.5.3.2) for p-p38 protein bands, normalised to corresponding p38 levels and expressed as fold change as compared with non-infected cells at min 0. Calculated fold change in p-p38 levels is shown below gel images and plotted in accompanying graphs (n = 2). c) NIH/3T3 cells were mock infected or infected with MCMV or MCMVdie3 (MOI = 3). At 7hpi cells were stimulated with IL-1β (10 ng/ml) for indicated periods of time. Whole cell lysates were harvested and analysed as described above (n = 1). d) Graph showing average fold change in p-p38 levels calculated for IL-1β- treated mock and MCMV infected cells in the three independent experiments shown in a – c (error bars indicate standard error).

4.3 Discussion

In the previous chapter IL-1β-induced IκBα degradation was found to be modulated in MCMV infected cells. Data presented in the current chapter demonstrates that MCMV protein M45 mediates this effect.

M45 is shown here to inhibit IL-1β-induced IκBα degradation (Figure 4.1). M45 has previously been shown to inhibit both innate-immune receptor signalling (namely TNFα, TLR3, DAI) as well as cell death induced by infection. These M45 functions were attributed to its ability to bind and modulate the function of cellular-stress signal transducers RIP1 and RIP3 (Mack et al., 2008) (Upton et al., 2010). RIP proteins are not known to take part in the IL-1β pathway (Weber et al., 2010) (Meylan et al., 2004). Therefore, M45 inhibition of signalling events described here likely represents a novel function of this protein. Further experiments are required to substantiate this conclusion by establishing the underlying protein-protein interactions and mechanism.

M45 does not appear to inhibit p38 phosphorylation in response to IL-1β (Figure 4.3). IL-1β binding to its receptor induces, via IRAKs and TRAF6, the activation of TAK1. At this point the signalling pathway bifurcates as TAK1 activates the IKK complex followed by NF-κB, as well as phosphorylates MAPK kinases resulting in p38 and JNKs phosphorylation/activation. It was therefore of interest to establish whether M45 perturbs only one or both arms of the pathway. Interestingly, IL-1β-induced p38 phosphorylation was not found to differ between non-infected and MCMV-infected cells

regardless of viral gene expression including M45 (Figure 4.3). It should be noted that p38 phosphorylation kinetics differed somewhat between the experiments conducted. Importantly, however, within each experiment the rate of p38 phosphorylation/dephosphorylation was similar under all conditions (mock infection or infection with the different viruses). Differences observed could be resolved with further repetition of experiments shown as well as by using more sensitive techniques such as ELISA. In this regards the MOIs used and therefore the proportion of the culture expected to be infected should also be considered. In the experiments presented here a MOI of 3 was used which is predicted to result in the grand majority of cells being infected. Conversely, it is expected that a small proportion of cells remain non-infected (this question of the ratio between these populations of infected and non-infected cells is discussed in more detail in Chapter 3). In the non-infected cell population IL-1β stimulation will lead to p38 phosphorylation and thus contribute to the proportion of p-p38 observed following cytokine stimulation of infected cultures. It would be of interest to compare the levels of IL-1β- induced p38 phosphorylation between cultures infected with various MOIs (for example, MOI of 1, 3 and 5). This said, NIH/3T3 is a fully infection-permissive cell line and a MOI of 3 is expected to result in the predominant portion of cells being infected. Therefore, it is safe to conclude that the IL-1β- induced increase in p-p38 observed in infected cultures does indeed represent p38 phosphorylation occurring in infected cells.

p38 activation, following IL-1β stimulation, is considered entirely dependent on TAK1 (Sato et al., 2005) (Weber et al., 2010). Thus, the finding that p38 is phosphorylated

suggests, that in the experimental settings used, TAK1 is activated. This in turn may indicate that the observed inhibition of IκBα degradation is a result of M45 interference with a signalling step between TAK1 activation and IκBα degradation. Possible points of viral interference include: inhibition of TAK1 phosphorylation of the IKK complex, modulation of the IKK complex itself (for example the abundance of IKKα, IKKβ or IKKγ) or its activity (for example blockage of kinase functions) or interference with IκBα processing for degradation (at or after its ubiquitination). In other words, these results may indicate that M45 modulates the function of the immediate regulatory circuit of NF-κB.

It is also possible that the activation of NF-κB and p38 is differentially modulated by the virus. Activated p38, through phosphorylation of multiple and diverse substrates, regulates various cellular processes including protein degradation and localization, mRNA stability, endocytosis, apoptosis and cytoskeleton dynamics (Cargnello and Roux, 2011) (Cuadrado and Nebreda, 2010). The overall outcome of p38 driven processes or that of a subset of them might contribute to a formation of a favourable cellular environment for viral replication. This in turn may have selected for either virus non-interference with or even potentiation of p38 activation. An interesting example is that of vaccinia virus protein A52R. In transfection experiments this protein inhibits NF-κB activation by multiple TLRs via interaction with IRAK2, presumably disrupting the ability of IRAK2 to engage its cellular interaction partners (Keating et al., 2007) (Harte et al., 2003) (Bowie et al., 2000). At the same time, by binding to TRAF6, A52R potentiates the activation of p38 and JNK upon TLR stimulation. It has been

hypothesised that by A52R can selectively induce downstream signalling by TRAF6 (that is, A52R may induce p38 phosphorylation without affecting NF-κB activation) (Maloney et al., 2005). This differential effect reflected in A52R modulation of LPS-induced gene expression such that NF-κB-dependent expression of IL-8 was inhibited while p-38 dependent expression of IL-10 was enhanced (Maloney et al., 2005). In the case of MCMV and M45, it is noteworthy that M45 does inhibit TNFα-induced p38 phosphorylation (Mack et al., 2008). M45 modulation of TNFα signalling is thought to be due to M45 binding to RIP1 (Mack et al., 2008). RIP1 is a regulator of several cellular stress responses including those originating from activation of PRRs and by death receptor ligation and DNA damage (Meylan and Tschopp, 2005). Hence M45 modulation of RIP1 function can be considered as viral interference with a hub of cellular signalling. Inhibition of TNFα-induced RIP1-dependent p38 activation can therefore be viewed as an inevitable consequence of M45 targeting RIP1 rather than a result of M45 primarily targeting p38.

The inter-relationship between HCMV/MCMV and NF-κB has been previously studied in some detail. Infection with either HCMV or MCMV induces NF-κB activation. HCMV infection results in rapid translocation of NF-κB to the nucleus, stimulation of NF-κB DNA binding activity and transcription initiation (Kowalik et al., 1993) (Yurochko et al., 1997) (Yurochko and Huang, 1999). Indeed, viral envelope glycoproteins gH and gB alone have been shown to elicit the activation of NF-κB, potentially through detection by TLR2 (Yurochko et al., 1997) (Yurochko and Huang, 1999) (Boehme et al., 2006). Similarly, MCMV infection induces IκBα degradation, NF-

κB DNA-binding activity and associated transcriptional regulation (Gribaudo et al., 1996) (Le et al., 2008). NF-κB activation following infection is attributed, at least partially, to stimulation by PRRs including TLR induced NF-κB activation (Tabeta et al., 2004) (Zucchini et al., 2008) (Krug et al., 2004).

It has been previously suggested that one way CMVs may have adapted to the activation of NF-κB is by harnessing its transcriptional activity to augment viral gene expression and replication (Sambucetti et al., 1989). In both HCMV and MCMV the enhancer of the major immediate-early enhancer promoter (MIEP), which regulates immediate-early gene expression, contains binding sites for cellular transcription factors including NF-κB, AP1 and CREB/ATF (Stinski and Isomura, 2008). Additionally, NF-κB complexes have been shown to bind to HCMV enhancer derived sequences and up-regulate the expression of reporter genes (Sambucetti et al., 1989) (Prosch et al., 1995). It was therefore hypothesised that NF-κB activation is required for the initiation of viral immediate-early gene transcription and therefore viral replication. However, disruption of the NF-κB binding sites with the HCMV enhancer does not alter IE1 expression or viral growth kinetics in cultured cells (Gustems et al., 2006). These data are supported by *in vivo* investigations. An intact HCMV enhancer or an enhancer in which the NF-κB binding sites were silenced were used to replace the MCMV enhancer, resulting viruses were named hMCMV-ES and hMCMV-ES.NF-κB, respectively (an enhancer swap approach was used due to prohibitive to manipulation properties of the MCMV enhancer on one hand and the need for in-vivo investigation on the other hand). In an in-vivo model of neonatal infection no difference was found between the growth of the

hMCMV-ES and hMCMV-ES.NF-κB viruses (Isern et al., 2011). Importantly, in the same model system an enhancer swap virus in which both NF-κB and AP1 enhancer binding sites were mutated showed significant attenuated growth (Isern et al., 2011). In addition, serum response factor (SRF) and est-like gene-1 (Elk-1) binding sites have been shown to compensate for NF-κB mediated activation of MIEP (Caposio et al., 2010). This suggests that enhancer usage of various cellular transcription factors allows for robustness such that elimination of input by one transcription factor is compensated by others (Caposio et al., 2010) (Isern et al., 2011). This is turn implies that the role of NF-κB in activation of immediate-early viral gene transcription can only be understood in the context of a complex fine-tuned "conversation" between the CMV-MIEP enhancer and the transcriptional response to infection (Stinski and Isomura, 2008). Finally, impairment of the canonical NF-κB pathway, using an IκBα dominant negative mutant, a IKKβ dominant negative mutant or p65 knock-out cells, did not affect HCMV or MCMV replication in-vitro (Benedict et al., 2004) (Caposio et al., 2007). Indeed, at low MOI (0.02) replication of MCMV on p65-deficient fibroblasts was enhanced (Benedict et al., 2004). Interestingly, expression of an IKKβ dominant negative mutant did block HCMV replication in quiescent cells (Caposio et al., 2007). Overall, in cultured cells NF-κB activation appears to have a neutral, if not inhibitory, role in CMV replication although additional work is required to assess its contribution to the viral life cycle in quiescent cells and *in-vivo* relevant cell types such as endothelial and primary monocyte/macrophage cells.

HCMV, in addition to the above discussed activation of NF-κB, has been shown to disrupt NF-κB activation and function. Taylor *et al* have demonstrated that IE86, the HCMV immediate-early 2 gene product, blocks NF-κB binding to DNA (although it does not affect IκBα degradation or NF-κB nuclear translocation). This results in inhibition of infection-induced expression of IFNβ as well as inflammatory genes (*TRAIL, IL-6*). TNFα-induced NF-κB DNA binding and upregulation of inflammatory genes (*IL-8* and *RANTES*) expression is also inhibited by IE86. Interestingly, IE86 was not found to bind to NF-κB subunits p50 or p65. It was hypothesised by the authors that modulation of NF-κB function by IE86 is achieved by binding to a NF-κB interaction partner or by modulation of pathways controlling the post-transcriptional modification of p65 (Taylor and Bresnahan, 2006). In addition, NF-κB activation following stimulation with IL-1β or TNFα is inhibited in HCMV infected cells (Montag et al., 2006) (Jarvis et al., 2006). This inhibition occurs upstream of IL-1β and TNFα signalling pathways convergence on NF-κB and appears to be pathway specific rather than a result of viral modulation of NF-κB function (Montag et al., 2006) (Jarvis et al., 2006).

MCMV has also been shown modulate NF-κB activation. As discussed above, MCMV protein M45 inhibits several signalling pathways leading to NF-κB activation by binding to cellular proteins RIP1 and RIP3 (Mack et al., 2008) (Upton et al., 2008). Examination of NF-κB activation kinetics following MCMV infection showed that IκBα degradation and NF-κB DNA-binding activity were induced following infection, however, both were dampened by 6 hpi (i.e. by this time point both cytoplasmic IκBα and nuclear NF-κB-DNA complexes returned to pre-infection levels) (Le et al., 2008). Additionally,

stimulation of infected cells with TNFα at 7 hpi did not result in IκBα degradation. Interestingly, under cycloheximide treatment IκBα intrinsic half-life increased significantly in infected cells versus controls (Le et al., 2008). The authors concluded that these finding indicate that NF-κB activation is controlled by MCMV. However, the underlying mechanism or viral product/s mediating this effect were not elucidated (Le et al., 2008). Considering that M45 is expressed at 6 hpi (Lacaze et al., 2011) (Upton et al., 2010) and the above suggested hypothesis that M45 modulates NF-κB activation, it would be of interest to examine infection-induced NF-κB activation (nuclear translocation, DNA binding and transcriptional activation of target genes) over time in cells infected with wild type versus UV-inactivated virus and the M45 deletion mutant.

Overall, data presented here identifies M45 as the MCMV protein mediating viral inhibition of IL-1β induced IκBα degradation. Additionally, preliminary observations suggest that M45 directly modulates the immediate NF-κB regulatory circuit. Although the interaction between HCMV/MCMV infection and NF-κB activation has been researched in some detail there is much to learn. Indeed, much of the research described in the literature (as briefly reviewed above) explored the overall effect of NF-κB activation or lack thereof on CMV replication. Alternatively, NF-κB activation was used as marker in investigations into viral modulation of signalling by cytokines or PRRs. However, little is known about direct CMV targeting of NF-κB as a major cellular signalling hub synthesising signals from multiple pathways (this is with the exception of the study by Taylor *et al*). In the case of MCMV, previous studies alluded to the fact that NF-κB activation might be controlled by the virus. However, the underlying mechanism

or viral product/s mediating this effect were not elucidated (Le et al., 2008). Thus the findings presented here, which identify M45 as a potential direct modulator of NF-κB function, can form the basis for detailed investigations into MCMV- NF-κB interplay. Thus, allowing research in this field to progress from observational to mechanistic studies which put this key signalling factor, namely NF-κB, at the heart of the research effort. This may include more detailed mapping of temporal regulation during infection and the resulting differential effects on gene expression, detailed understating of M45 interaction with the NF-κB network and identification of additional viral products affecting the function of NF-κB.

5 Chapter 5

MCMV modulates NF-κB activation following TLR7 or TLR9 stimulation in bone marrow-derived macrophages

5.1 Introduction

TLR7 and TLR9 are intracellular TLRs capable of detecting nucleic acids (Blasius and Beutler, 2010). TLR9 is often quoted as recognising hypo/unmethylated CpG-rich DNA that is more frequently present in the genomes of microbes than in mammalian DNA (Blasius and Beutler, 2010). However, several studies have now demonstrated that DNA recognition by TLR9 is dependent on the 2'-deoxyribosephosphate backbone. Furthermore, these studies suggest that chemical modifications and specific sequences present in synthetic CpG-oligodeoxynucleotides (ODNs) ligands used in TLR9 research actually serve to improve delivery into intracellular compartments of TLR9 expression rather than facilitating the ligand-TLR9 interaction itself (Haas et al., 2008) (Yasuda et al., 2005) (Yasuda et al., 2006). TLR7 detects ssRNA as well as the low molecular weight synthetic compounds called imidazoquinolines, for example resiquimod (R-848), and guanine analogs (Hemmi et al., 2002) (Diebold et al., 2004) (Heil et al., 2004) (Lund et al., 2004). Both TLR7 and TLR9 localize to an endosomal compartment and are activated only in acidified endolysosomal compartments (Blasius and Beutler, 2010). It is thought that this particular localization/activation profile is important in

discrimination between self and non-self nucleic acids as host DNA is usually excluded from these intracellular bodies (Barton and Kagan, 2009) (Blasius and Beutler, 2010).

TLR7 and TLR9 induced responses are cell-type dependent. In conventional dendritic cells (cDCs) and macrophages stimulation of these TLRs leads to MyD88-dependent activation of NF-κB and MAPK pathways resulting in secretion of inflammatory cytokines. This occurs via the IRAKs-TRAF6-TAK1 signalling cascade. NF-κB activation is enabled via TAK1 activation of the IKK complex followed by phosphorylation and degradation of NF-κB-inhibitor IκBα (reviewed in Chapter 1). In plasmacytoid dendritic cells (pDCs) activation of TLR7 and TLR9 leads, in addition to NF-κB and MAPKs activation, to secretion of type I IFN (Blasius and Beutler, 2010).

As reviewed in Chapter 1, both TLR9 and TLR7 have been shown to play a role in host response to MCMV. MCMV infection of TLR9 knock-out (TLR9-/-) mice or mice with a non-functional TLR9 receptor results in increased mortality and elevated viral titres in the spleen in comparison to wild type animals. This correlates with impaired cytokine responses and diminished activation of NK cells (Delale et al., 2005) (Krug et al., 2004) (Tabeta et al., 2004). A study by Zucchini et al suggested an overlapping function for TLR7 and TLR9 in the detection of MCMV. Higher susceptibility to MCMV-induced death, increased viral load in the spleen and significantly lower serum levels of IFNα were found in TLR9-/-TLR7-/- double knock-out mice in comparison to TLR9 or TLR7 single knock-out animals. Indeed, the phenotype of TLR9-/-TLR7-/- animals with

regards to susceptibility to MCMV-induced death recapitulated that of MyD88-/- mice (Zucchini et al., 2008).

HCMV and MCMV infect monocytes and macrophages both in-vivo and in-vitro, with permissiveness to infection depending on cellular differentiation state (such that non-productive versus productive replication is supported in monocytes and macrophages, respectively) (Mocarski, 2006) (L.K.Hanson, 2006). Infection of monocytes/macrophages by CMVs is considered to play a key role in viral dissemination during acute infection, potentially through tissue infiltration of non-actively infected monocytes followed by differentiation into macrophage thus stimulating productive infection and viral spread (Collins et al., 1994) (Stoddart et al., 1994) (Hanson et al., 1999) (Smith et al., 2004) (Mocarski, 2006). Macrophages, monocytes and their progenitor cells have also been implicated as a site of latency (Reddehase et al., 2002).

In previous chapters MCMV, and more specifically MCMV protein M45, were shown to modulate IL-1β-induced IκBα degradation. Following binding of their cognate ligands TLR9, TLR7 and the IL-1β receptor induce a largely overlapping MyD88-dependent pathway leading to IκBα degradation and NF-κB activation. It would therefore be expected that M45 inhibits TLR9- and TLR7- induced NF-κB activation. As outlined above, TLR9 and TLR7 have previously been shown to play a role in MCMV detection and initiation of anti-viral immune responses. TLR7 and TLR9 are not expressed by

fibroblasts in which experiments shown in the previous chapters were performed. However, Bone marrow-derived macrophages (BMDM) have previously been found to constitutively express TLR7. In addition, TLR9 was found to be expressed at low levels in resting BMDM and to be upregulated upon MCMV infection (P.Lacaze, Division of Pathway Medicine, Personal communication). Importantly, as discussed above, macrophages are considered to play a key role in CMV pathogenesis. Considering the roles of TLR7, TLR9 and macrophages in CMV biology it is of interest to examine whether, as suggested above, M45 indeed inhibits TLR9- and TLR7- induced NF-κB activation in the context of BMDM. This is the aim of the following chapter.

5.2 Results

5.2.1 TLR7 and TLR9-induced IκBα degradation is inhibited in MCMV infected BMDM

In previous chapters MCMV was shown to modulate IL-1β-induced IκBα degradation. As TLR7/9 utilise a signalling pathway largely overlapping that of IL-1β leading to IκBα degradation, it was asked whether MCMV also modulates TLR7/9-mediated IκBα degradation in BMDM. Initial experiments tested viral modulation of TLR7-induced IκBα degradation since, as mentioned above, TLR7 has previously been found to be constitutively expressed in the BMDM model used here. BMDM were mock-treated or infected with MCMV, ΔM45 or CM45. At 8 hpi mock-treated and infected cells were stimulated with the TLR7 ligand R-848. Whole cell lysates were collected at 0, 10, 30 and 60 min post stimulation and analysed by Western blotting (Figure 5.1a). In mock-infected cells treated with R-848, IκBα levels decreased rapidly and were nearly abolished (to ~ 5% of IκBα levels in non-stimulated cells) by 30 min post-treatment. At 60 min post-stimulation IκBα levels were restored to ~ 77% of levels in non-stimulated cells. In contrast, in MCMV infected cells treated with R-848 only a very small decrease in IκBα levels, to ~ 88% of those in non-treated cells, was seen at 30 min post stimulation. This was followed by recovery to pre-stimulation levels by 60 min post treatment. The IκBα degradation profile following TLR7 stimulation of ΔM45 infected cells paralleled that seen in non-infected cells. R-848 stimulation of CM45 infected cells resulted in a marked decrease in IκBα levels (~ 28% of IκBα amount measured in non-stimulated cells at 30 min post treatment), followed by an increase in IκBα levels at

60 min post treatment (~ 72% of IκBα amount measured in non-stimulated cells). Thus the CM45 virus exhibited an intermediate phenotype between wild-type and ΔM45 viruses (for example, at 30 min post R-848 treatment IκBα levels in CM45 infected cells were lower than those in wild-type virus infected cells but higher in comparison to ΔM45 infected cells).

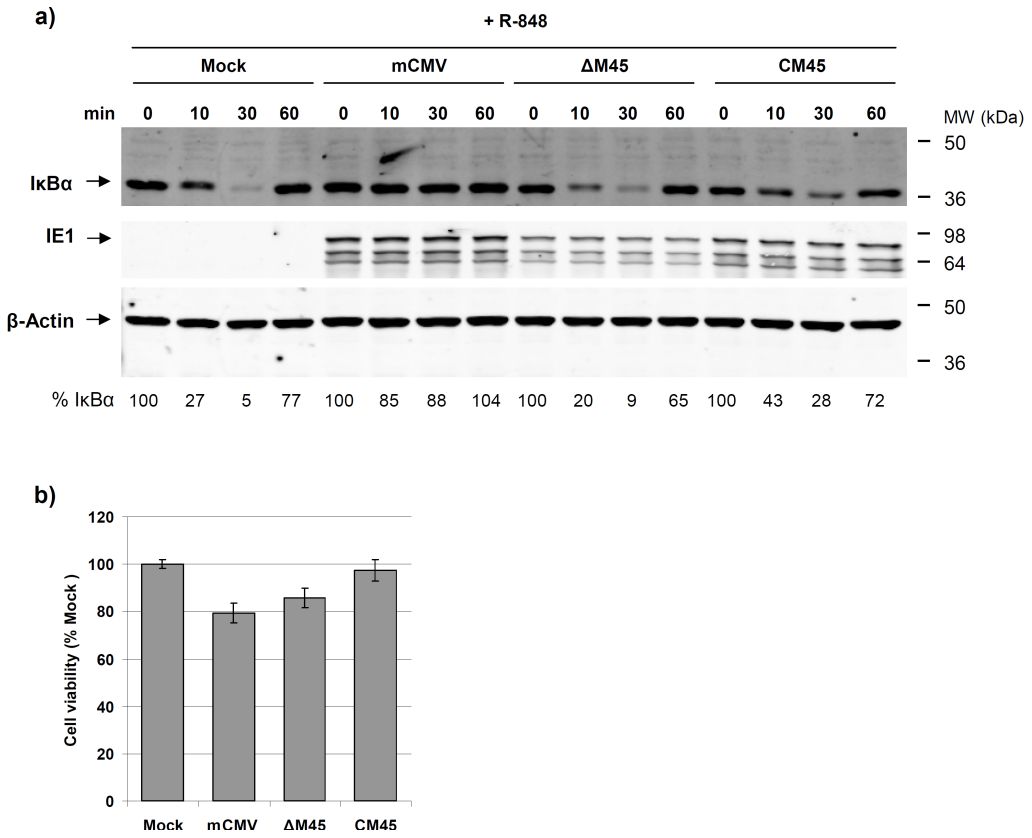

Figure 5.1: MCMV modulates IκBα degradation following TLR7 stimulation. a) BMDM were mock infected or infected with MCMV, ΔM45 or CM45 (MOI =3). At 8 hpi cells were stimulated with R-848 (0.1 μM) for the indicated periods of time. Whole cell lysates were harvested and analysed by using SDS-PAGE and immunoblotting with primary antibodies against IκBα, IE1 or β-Actin. Integrated fluorescence intensity was calculated (see Chapter 2 section 2.5.3.2) for IκBα protein bands, normalised to corresponding β-Actin levels and expressed as percentage of IκBα at min 0 (n = 3).b) BMDM were mock infected or infected with MCMV, ΔM45 or CM45 (MOI = 3). At 8 hpi cell viability was determined using the Cell Titer-Blue assay and is expressed as percentage of fluorescent signal in comparison to mock infected cells. Data is representative of at least two experiments (each experiment included 6 replicates, mean values and standard error (SE) bars shown) (n = 2).

Infection equivalency, examined by measuring IE1 expression, showed IE1 levels in ΔM45 and CM45 infected cells to be ~ 55% and ~ 75% that of wild type-virus infected cells, respectively. One possible reason for the low IE1 expression measured in ΔM45-infected cultures is that M45 deletion mutants have previously been found to grow poorly on a macrophage cell line, presumably due to failure to inhibit virus-induced cell death (Brune et al., 2001). Hence cell viability following infection with the wild type, ΔM45 or CM45 viruses was evaluated (Figure 5.1b). Cell viability of infected BMDM was found comparable between the three viruses. It is noteworthy that, IκBα levels, at 30 min post-stimulation, adjusted to IE1 expression are ~ 88, 17 and 37% in wild-type, ΔM45 and CM45 infected cultures, respectively. Hence, differences in infection equivalency alone, as indicated by IE1 expression, are unlikely to explain the different competencies of the wild-type, ΔM45 and CM45 viruses to inhibit TLR7-induced IκBα degradation. Overall, these data show a strong inhibition of TLR7-induced IκBα degradation by MCMV in BMDM.

Next it was tested whether MCMV infection modulates TLR9-induced IκBα degradation. BMDM were mock treated or infected with MCMV and at 8 hpi stimulated with TLR9 the ligand ODN 1668. Whole cell lysates were collected at 0, 10, 30 and 60 min post stimulation and analysed by Western blotting (Figure 5.2). Stimulation of mock infected cells resulted in IκBα levels falling to ~ 38% and ~ 34% of pre-treated levels within 30 and 60 min, respectively. Stimulation of MCMV infected cells resulted in a markedly smaller decrease in IκBα levels to ~ 70% and 60% of pre-treated levels at 30

and 60 min post-treatment, respectively. These data indicate that MCMV inhibits TLR9, as well as TLR7-induced IκBα degradation in BMDM, albeit to a lesser extent.

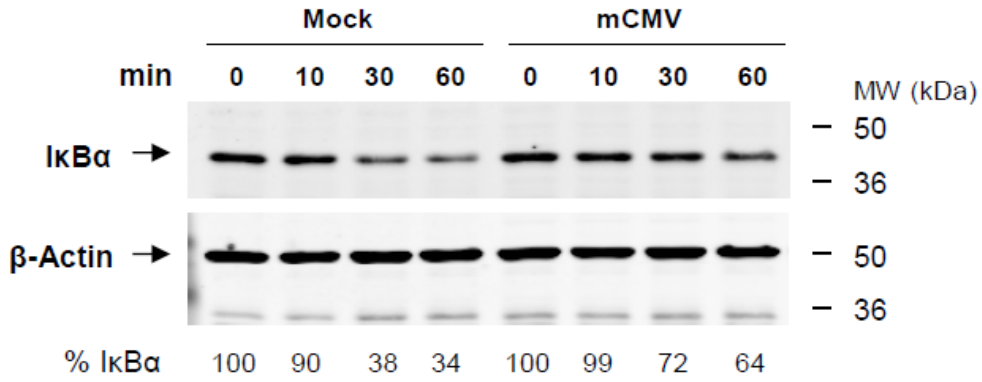

Figure 5.2: MCMV modulates IκBα degradation following TLR9 stimulation. BMDM were mock infected or infected with MCMV (MOI = 3). At 8 hpi cells were stimulated with TLR9 ligand ODN 1668 (1 μM) for the indicated periods of time. Whole cell lysates were analysed by using SDS-PAGE and immunoblotting with primary antibodies against IκBα or β-Actin. Integrated fluorescence intensity was calculated (see Chapter 2 section 2.5.3.2) for IκBα protein bands, normalised to corresponding β-Actin levels and expressed as percentage of IκBα at min 0 (n = 2).

5.2.2 TLR7 and TLR9 induced NF-κB nuclear translocation is inhibited in MCMV infected BMDM

Results presented in the previous section show that TLR7- and TLR9-induced IκBα degradation is inhibited in MCMV infected cells. IκBα sequesters NF-κB in the cytoplasm, and stimulation induced degradation of IκBα leads to NF-κB translocation into the nucleus. It was therefore asked whether MCMV infection of BMDM inhibits TLR7/9-induced NF-κB nuclear translocation. Initially, TLR7 induced NF-κB nuclear translocation in MCMV infected cells was examined. BMDM were mock-infected or infected with MCMV, and stimulated with TLR7-ligand R-848 before subcellular localization of NF-κB was analyzed by immunofluorescence (Figure 5.3a). Prior to stimulation of mock-infected or infected cells NF-κB localized to the cytoplasm. As expected, R-848 stimulation of mock infected cells resulted in NF-κB translocation to the nucleus. In contrast, NF-κB was retained in the cytoplasm of infected cells following stimulation. Next, the subcellular localization of NF-κB was examined in cells stimulated with either a TLR7 agonist (Figure 5.3b) or TLR9 agonist (Figure 5.3c) following mock infection or infection with wild type, ΔM45 or CM45 viruses (note that in figure sections 5.3b and 5.3c NF-κB and IE1 staining differs from that presented in section 5.3a). Mock-infected, ΔM45- or CM45-infected cells stimulated with TLR7 agonist all exhibited nuclear localization of NF-κB. As described above, TLR7 stimulation did not result in NF-κB nuclear translocation in wild-type virus infected cells. As with TLR7, mock-infected cells responded to TLR9 stimulation by re-localizing NF-κB to the nucleus, while infection with in wild-type MCMV restricted

NF-κB to the cytoplasm. In contrast, in cells infected with ΔM45 or CM45 followed by TLR9 stimulation, NF-κB localized to the nucleus. Overall, these results suggest that TLR7 and TLR9 induced NF-κB nuclear translocation is inhibited in MCMV infected cells.

Figure 5.3: TLR7 and TLR9 induced NF-κB nuclear translocation is inhibited in MCMV infected BMDM. a) BMDM were mock infected or infected with MCMV (MOI = 1). At 8 hpi cells were mock treated or stimulated with R-848 (0.1 µM) for 30 min. Cell were then fixed and subcellular localization of NF-κB p65 subunit was analyzed by confocal immunofluorescence. b + c) BMDM were mock infected or infected with MCMV, ΔM45 or CM45 (MOI = 1). At 8 hpi cells were stimulated with R-848 (0.1 µM) (b) or ODN 1668 (1 µM) (c) for 30 min. Cells were then fixed and subcellular localization of NF-κB p65 subunit was analyzed by immunofluorescence.

a)

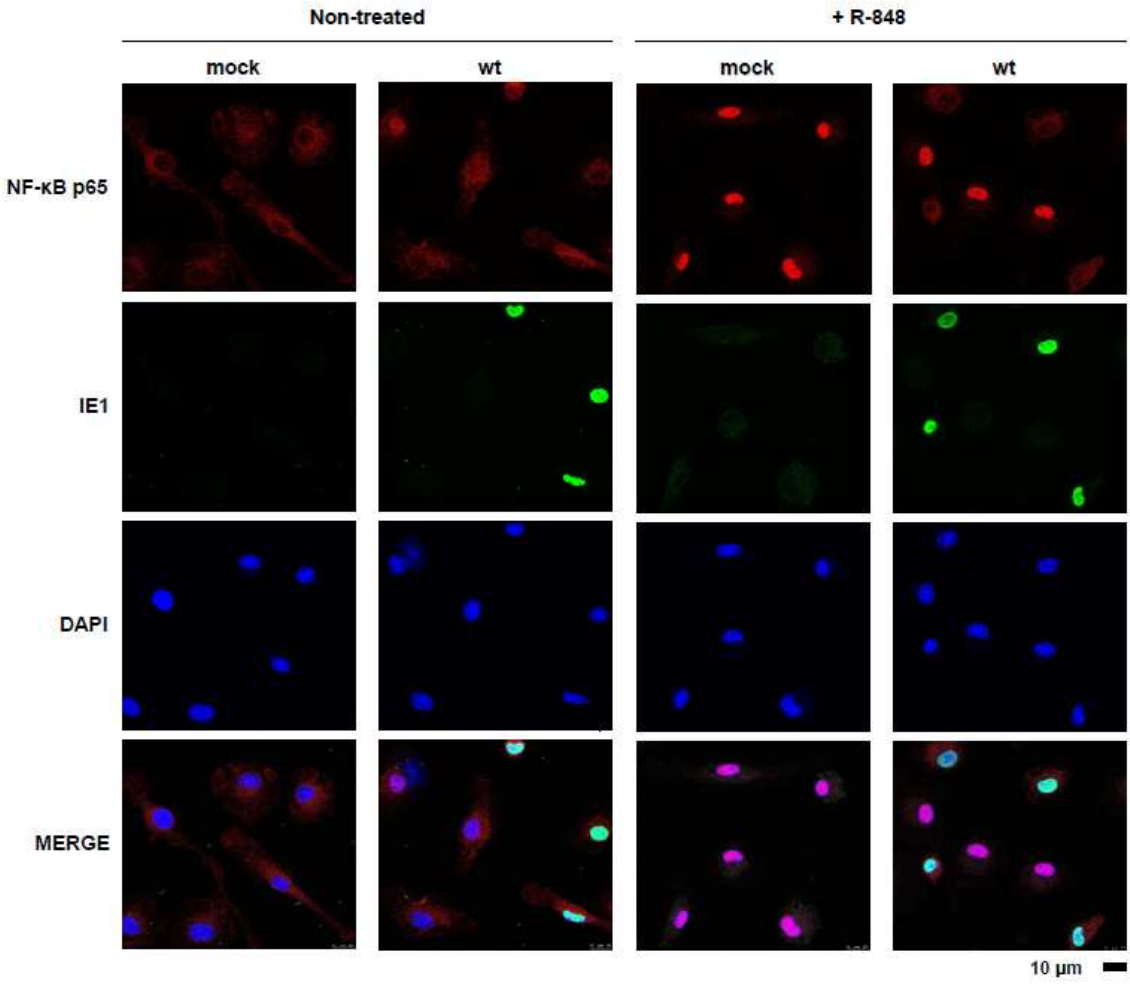

b)

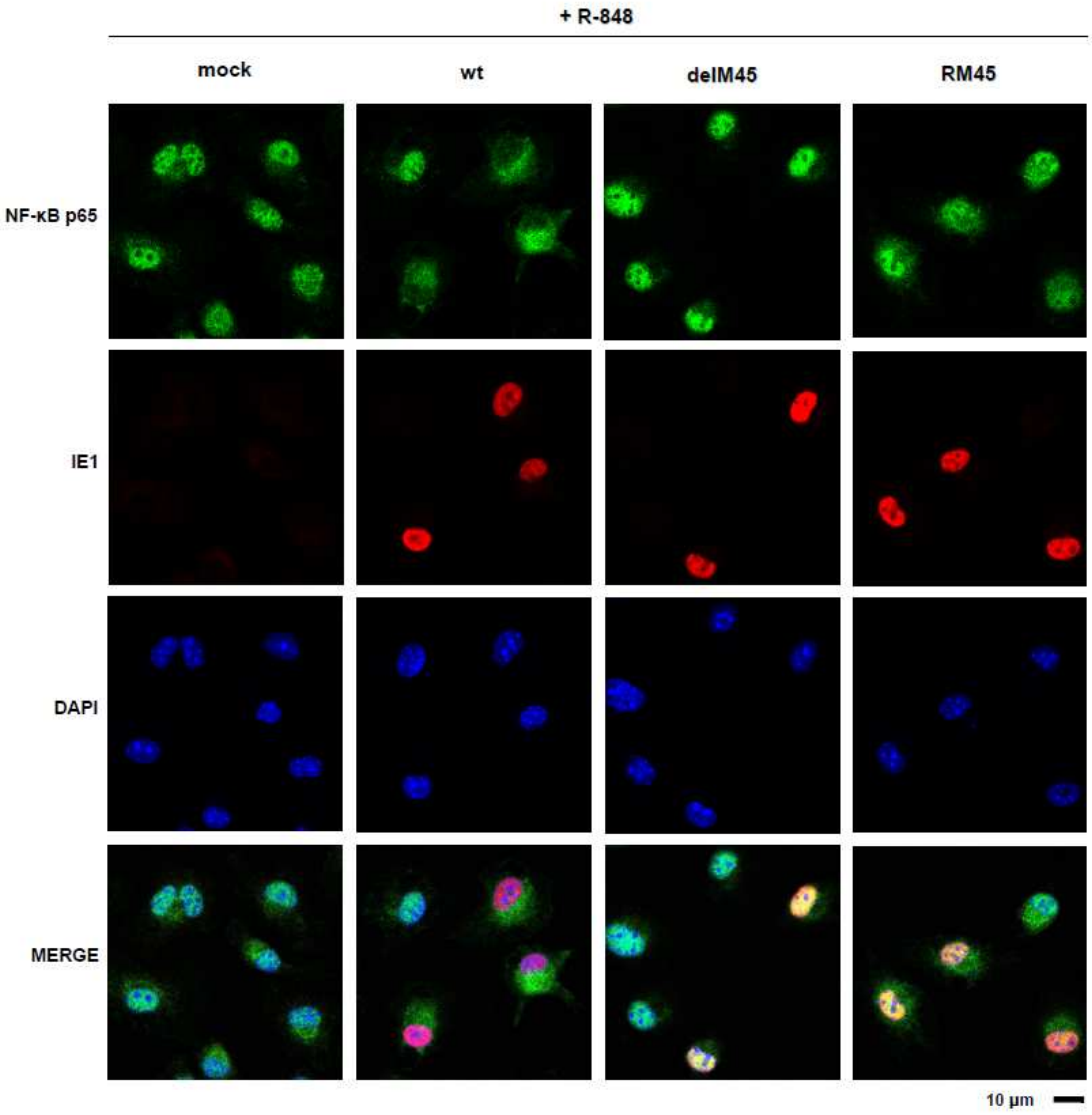

c)

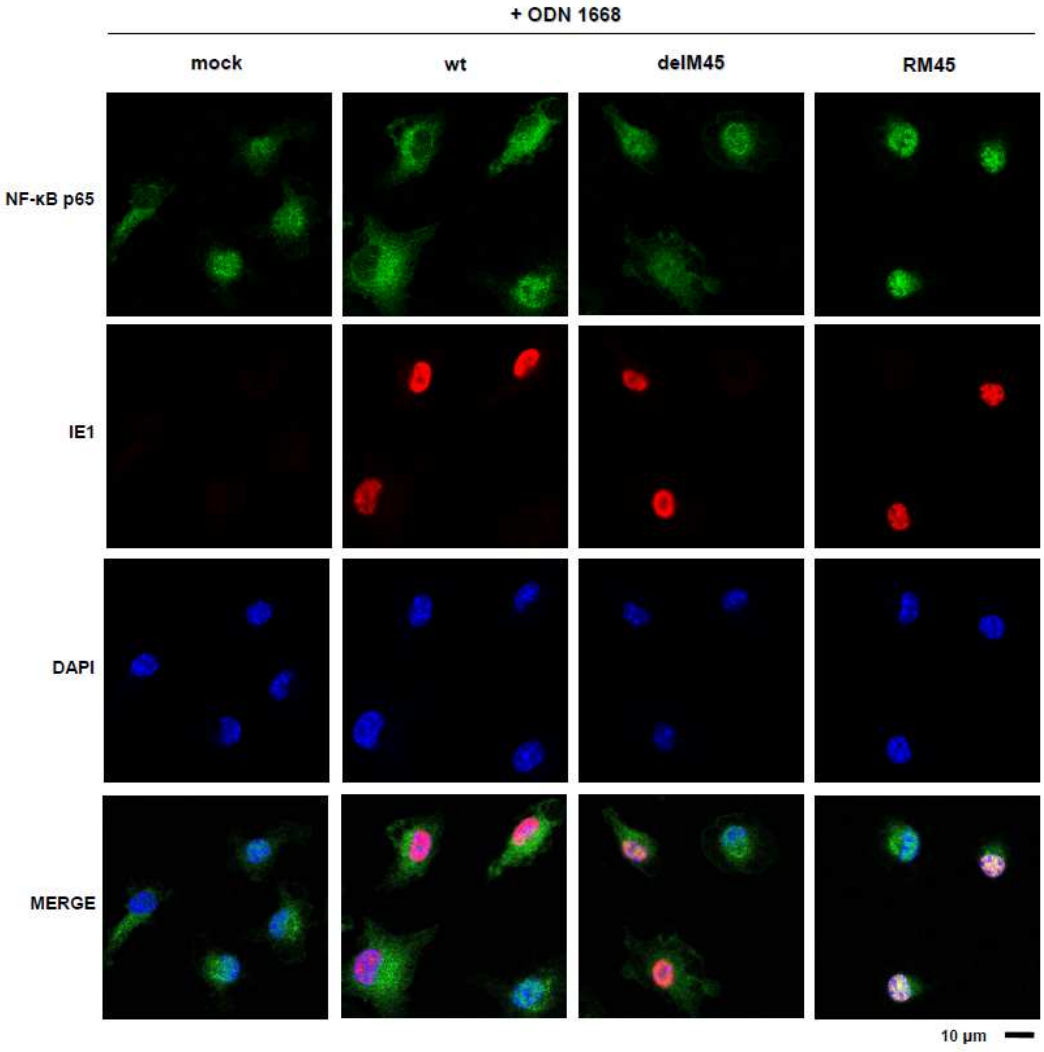

5.2.3 TLR7-induced cytokine secretion in inhibited in MCMV-infected BMDM

Results presented in the previous sections show that TLR7-induced IκBα degradation as well as NF-κB nuclear translocation are inhibited in MCMV infected cells. It was therefore tested whether these observations correlate with inhibition of NF-κB upregulation of cytokine expression. BMDM were mock infected or infected with MCMV, ΔM45 or CM45. Cells were then stimulated with TLR7 ligand R-848, supernatants were harvested and the concentrations of IL-6 and TNFα determined by ELISA (Figure 5.4). Wild-type virus or CM45 infected cells stimulated with R-848 secreted less IL-6 and TNFα than mock infected cells stimulated in the same manner. Cells infected with ΔM45 and treated with R-848 secreted more IL-6 and TNFα than wild-type virus or CM45 infected cells stimulated in the same manner. Overall, a trend towards reduced cytokine secretion was observed in MCMV infected cells treated with R-848 in comparison to mock infected cells.

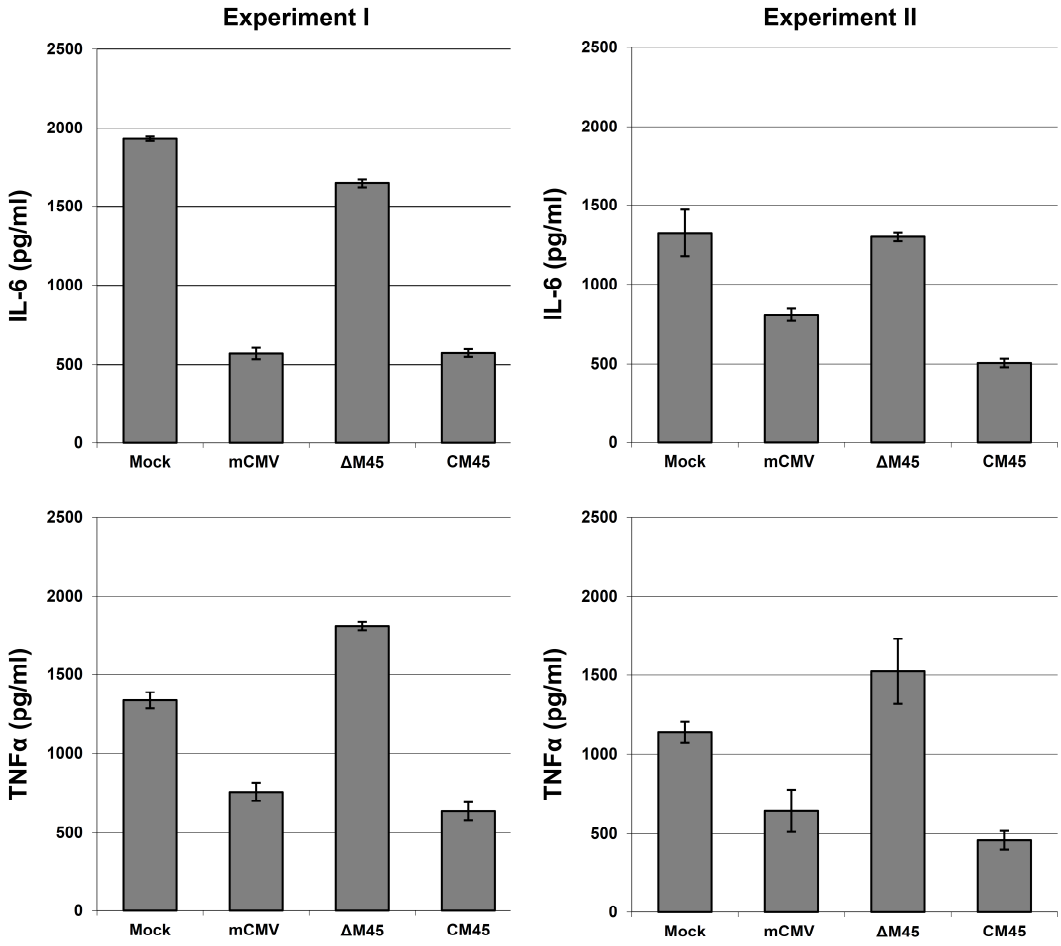

Figure 5.4: TLR7-induced cytokine secretion in inhibited in MCMV-infected BMDM. BMDM were mock-infected or infected with MCMV, ΔM45 or CM45 (MOI = 3). At 8 hpi cells were stimulated with the TLR7 ligand R-848 (0.1 µM). After 16 h of stimulation supernatants were harvested and the concentrations of IL-6 and TNFα determined by ELISA (Data from two experiments performed is shown; each experiment included 3 replicates, mean values and standard error (SE) bars shown).

5.3 Discussion

Results presented in this chapter show that TLR7- and TLR9-induced IκBα degradation and NF-κB nuclear translocation as well as TLR7 mediated upregulation of IL-6 and TNFα secretion are modulated in MCMV infected BMDM.

Firstly, TLR7- and TLR9-induced IκBα degradation was shown to be curbed in MCMV infected cells (Figures 5.1 and 5.2). This inhibitory effect was stronger in the case of TLR7 (with peak IκBα degradation of 5% versus 88% in non-infected and infected cells, respectively (Figure 5.1)) in comparison to TLR9 (with peak IκBα degradation of 34% versus 64% in non-infected and infected cells, respectively (Figure 5.2)). The reason for this is unclear, however one possible explanation is that it results from inherent, i.e. independent of infection, variations in TLR7 and TLR9 induced IκBα degradation kinetics. In non-infected cells, TLR7 stimulation leads to a rapid and almost complete IκBα degradation, whereas TLR9 stimulation results in a slightly delayed and less exhaustive IκBα degradation (Figures 5.1 and 5.2). These observations are compatible with published data on IκBα degradation following TLR7/9 stimulation in BMDM (Wan et al., 2011). It is noteworthy that the agonists used (R-848 and ODN 1668 for TLR7 and TLR9, respectively) are commonly used and adequately characterised specific ligands of TLR7 and TLR9. Moreover, these ligands have previously been shown to induce NF-κB activation and cytokine secretion in macrophages (Hemmi et al., 2000) (Hemmi et al., 2002) (Heil et al., 2004). Indeed, a central question in NF-κB research is to understand the mechanisms controlling the subtle variation in NF-κB activation profiles induced by

various receptors including different TLRs (Sen and Smale, 2010) (Bode et al., 2009). In turn, it would be of interest to explore viral-host interactions in this context.

Secondly, TLR7 and TLR9 induced NF-κB nuclear translocation was shown to be inhibited in MCMV infected cells (Figures 5.3a and 5.3c). These results are in full agreement with the observed inhibition of IκBα degradation.

Thirdly, MCMV infected cells treated with a TLR7 agonist were found to secrete less IL-6 and TNFα than non-infected cells equally stimulated (Figure 5.4). Cytokine secretion in the absence of TLR7 stimulation was not measured. However, it has been previously shown that resting BMDM secrete no detectable amounts of IL-6 and TNFα and that secretion of these cytokines is upregulated upon infection (Dr P.Lacaze, DPM, Personal communications). In results presented here, in the presence of TLR7 simulation MCMV-infected cells secreted less of these cytokines in comparison to mock-infected cells, indicating that TLR7-induced secretion of IL-6 and TNFα is curbed in MCMV infected BMDM. Taken together, these results suggest that TLR7/9-induced NF-κB activation is inhibited during MCMV infection of BMDM.

It is noteworthy that BMDM are semi-permissive to infection (L.K.Hanson, 2006). At the MOI used in the experiments presented, namely a MOI = 3, ~ 50 -70% of BMDM will be productively infected (assessed by flow cytometry measurements of GFP-positive cells in a population of MCMV-GFP infected BMDM, M.F.B.N. Hassim, DPM, Personal communications). That is, a significant proportion of cells in infected cultures

are non-productively infected. It would therefore be of interest to utilise methods which allow for assays of interest to be performed only on the infected portion of the cell population, these include: - immunofluorescence analysis (as shown above); - flow cytometry combined with infection with GFP expressing viruses or staining for a viral protein thus allowing gating of infected cells and measurement (by a second staining) of, for example, a protein of interest within this selected population; - similarly Fluorescence-Activated Cell Sorting (FACS) combined with infection with GFP expressing viruses or staining for a viral protein could be used to isolate productively infected cells to be assayed in a chosen downstream application.

The role of the MCMV protein M45 in mediating the above shown inhibition of TLR7/9-induced NF-κB activation in infected cells was also examined. TLR7-induced IκBα degradation, NF-κB nuclear translocation and cytokine secretion in ΔM45 infected cells was found comparable to that observed in mock infected cells (Figures 5.1-5.4). However interpretation of these results is confounded by the following factors:

1) In experiments examining the modulation of IκBα degradation, IE1 expression, used as an indicator of infection, was considerably lower in ΔM45-infected cultures in comparison to wild-type virus-infected cells. It is therefore possible that the seemingly different ability of the two viruses (wild type and ΔM45) to inhibit TLR7 induced IκBα degradation, is at least partially due to varying infection levels. M45 deletion mutants have previously been shown to grow poorly on a macrophage cell line, presumably due to failure to inhibit virus-induced cell death, at least in a proportion of the cells, in the

absence of M45 (Brune et al., 2001). This might contribute to the low IE1 expression observed in ΔM45 infected cultures. Preliminary examination of cell viability following infection with wild-type virus and ΔM45 was conducted with no difference in cell viability between cells infected with the two viruses observed (Figure 5.1). However, this should be further examined using additional methods for assessment of cell viability and cell death. Furthermore, additional testing of infection equivalency is required as well as examination of the relationship between any such variation and the differing IκBα degradation profiles measured. Alternatively, techniques which allow examination of IκBα levels, or NF-κB function for that matter, at a single cell level (as opposed to the cell population view given by Western blotting) should be used in future work. One example for this is immunofluorescence analysis of NF-κB subcellular localisation as presented in Figure 5.3. Interestingly, in ΔM45 infected cells treated with TLR7/9 agonists, NF-κB was localised in the nucleus, in contrast to the cytoplasmic localisation seen in wild-type virus infected cells. This result indicates a role for M45 in inhibition of NF-κB nuclear translocation.

2) The phenotype exhibited by the CM45 virus did not fully replicate the phenotype of the wild-type virus. In cells infected with CM45, IκBα degradation following TLR7 stimulation was only partially inhibited, while an almost complete inhibition of this response was observed in wild type virus infected cells (Figure 5.1). This differs from observations made in fibroblast cells (Chapter 4) where inhibition of IL-1β-induced IκBα degradation was comparable in wild type virus and CM45 infected cells. In this regards it should be noted that the *M45* gene is expressed in the CM45 virus from a

different locus than in the wild-type virus (Jurak and Brune, 2006) (Mack et al., 2008). It is possible that resulting subtle variations, for example, in expression levels of M45 lead to functional differences between wild type and CM45, which are more apparent in some cell types (macrophages) than in others (fibroblasts). It would be of interest to construct a ΔM45 revertant virus in which deleted sequences are reintroduced in the correct genomic context, and examine its function in experiments such as the ones presented here. Additionally, regardless of the comparison to the wild type virus, the function of the CM45 virus in the experiments conducted was somewhat complex. The CM45 virus seemed not to or only partially inhibit TLR7 induced IκBα degradation and NF-κB nuclear translocation. However, cytokine secretion from CM45 infected cells stimulated with a TLR7 ligand was comparable to that observed in wild type infected cells (Figures 5.1-5.3). The reason for this discrepancy is not clear. One possibility is that the partial inhibition of IκBα degradation, measured in Western blot analysis, was not clearly appreciable (i.e. visible) in the immunofluorescence analysis of NF-κB subcellular localisation (that is, NF-κB nuclear translocation in CM45 infected cells stimulated with TLR7/9 agonists seems complete although a small but potentially significant proportion of NF-κB remained cytoplasmic). In turn it is conceivable that even a partial inhibition of NF-κB activation results in markedly dampened upregulation of cytokine secretion. To conclude, some indications exist to suggest a role for M45 in modulation of TLR7/9 activation of NF-κB in BMDM, however further investigations are required to validate such a conclusion.

Overall, data presented in this chapter show that TLR7/9-induced NF-κB activation is inhibited in MCMV infected BMDM. Experiments presented here used exogenous stimulation of TLR7/9 i.e. addition of TLR7/9 ligands to infected cells. Future research should examine the significance of this observation in the context of infection induced activation of TLR7/9.

6 Chapter 6

Concluding discussion

CMVs, like all viruses, are obligate parasites which have evolved to harness host cellular processes to drive viral replication. However, to be able to replicate, disseminate and, in the case of CMVs, establish latent infection these viruses must contend with host defence mechanisms. These include intrinsic cellular defences as well as innate and adaptive immune responses. Co-evolution of CMVs with their hosts has allowed these viruses to develop an extensive range of strategies to evade, subvert and manipulate the host immune response (Mocarski, 2002) (Loewendorf and Benedict, 2010). Understanding viral mechanisms of immune modulation is crucial to our understanding of pathogenesis, may enhance future therapeutic strategies and can teach us valuable lessons about the host response itself.

The key role played by pattern recognition receptors (PRRs) in initiating and shaping the host response to infection in general and CMVs in particular is now recognised. Multiple PRRs have been implicated in sensing CMVs including TLR-family members TLR2, TLR7 and TLR9. NF-κB and MAPK activation pathways utilised by these receptors largely overlap signalling cascades induced by the key pro-inflammatory cytokine IL-1β. While activation of NF-κB and MAPKs by TLRs and IL-1β is well characterised, little is known about the modulation of these signalling events during CMV infection. The central hypothesis posed for this thesis was that a viral counter-measure by MCMV

involves specific targeting of TLR- and IL-1β-induced signalling along the MyD88 to NF-κB pathway.

To begin addressing this hypothesis, it was asked whether MCMV infection modulates IL-1β-induced signalling along the MyD88 to NF-κB pathway, more specifically, experiments were conducted to evaluate IL-1β-induced degradation of IκBα, the hallmark of NF-κB activation, in MCMV infected cells. It was found that IL-1β-induced IκBα degradation is, indeed, inhibited in MCMV infected cells in a manner dependent on de-novo viral protein expression (Chapter 3). These observations are in agreement with the central hypothesis in that IL-1β-induced NF-κB activation (as least as far as indicated by IκBα degradation) is inhibited following MCMV infection. Moreover, the requirement for de-novo viral gene expression strongly suggests that the observed inhibition is, as hypothesised, a result of a viral function and not part of the cellular response to infection.

Importantly the above discussed results do not address two key elements in the hypothesis. a) It was hypothesised that the IL-1β to NF-κB signalling pathway is modulated during infection as a result of specific viral function. To confirm this element of the hypothesis evidence needed to be provided showing that the observed inhibition of IκBα degradation is a result of a viral mechanism for modulating cellular signalling, and not part of the cell's own response to infection. The requirement for de-novo viral gene expression did imply viral targeting of cellular responses. However, it could not have been excluded that IκBα degradation is inhibited in productively infected cells and not in non-productively infected cells due to cellular responses initiated by productive

but not abortive infection. b) It was hypothesised that MCMV specifically targets IL-1β-induced signalling. However, it has not been elucidated whether the observed inhibition of IκBα degradation is a result of a specific block in IL-1β signalling or rather a general inhibition of IκBα degradation regardless of the initiating signal. To address these questions several lines of investigation were possible, including: 1) Identification of the viral product/s mediating the observed effect, thus addressing article (a) above; 2) Identification of the cellular signalling event targeted by the virus leading to inhibition of IκBα degradation, thus addressing article (b) above.

In accordance with this, investigations next focused on determining which viral product mediated the observed inhibition of NF-κB activation. This led to the identification of viral protein M45 as the viral protein modulating the degradation of IκBα following IL-1β stimulation (Chapter 4). Importantly, this represents a potential novel function of this protein. Moreover, this finding proves that the observed inhibition of IL-1β-induced IκBα degradation in MCMV-infected cells is, as hypothesised, a result of a viral function.

Research then turned to begin elucidating which signalling event/s in the IL-1β pathway is targeted by M45. This was done by examining whether p38 as well as NF-κB activation is modulated by M45. IL-1β binding to its receptor induces, via IRAKs and TRAF6, the activation of TAK1. At this point the signalling pathway bifurcates as TAK1 activates the IKK complex followed by NF-κB, as well as phosphorylates MAPK kinases resulting in p38 phosphorylation/activation. Therefore M45 modulation of a signalling event upstream or at TAK1 activation would be expected to result in

inhibition of activation of both NF-κB and MAPK kinases, whereas M45 modulation of a signalling event downstream of TAK1 activation would be expected to result in inhibition of NF-κB but not MAPK kinases. Thus through examining whether M45 perturbs only one or both arms of the pathway it was possible to begin dissecting which part of the IL-1β pathway is modulated by M45, as a first step toward identification of specific IL-1β-induced signalling events modulated by this protein. Interestingly, it was found that IL-1β-induced p38 phosphorylation is not modulated by M45 or by MCMV infection for that matter (Chapter 4). As outlined above, this suggests that M45 interferes with a signalling event downstream of TAK1 activation i.e. the function of NF-κB and its immediate regulatory circuit. Possible points of viral interference include: inhibition of TAK1 phosphorylation of the IKK complex, modulation of the IKK complex itself (for example, the abundance of IKKα, IKKβ, IKKγ) or its activity (for example, blockage of kinase functions) or interference with IκBα processing for degradation. As multiple signalling pathways converge at this level of NF-κB activation, this result implies that M45 functions to employ a general block on NF-κB activation. That is to say, that in contrast to the original hypothesis, M45 does not specifically target the IL-1β pathway (as discussed further below).

Finally, research efforts were extended to include TLR signalling, more specifically, TLR7/9 signalling in the context of MCMV infection of BMDM. It was shown that, in agreement with data presented for IL-1β, TLR7/9-induced NF-κB activation is curbed in MCMV infected cells (Chapter 5). Furthermore, viral protein M45 was indicated to mediate this effect.

Overall, data presented in this thesis indicate a previously unrecognised MCMV inhibition of NF-κB activation mediated by MCMV protein M45. This research began with the hypothesis that MCMV specifically targets TLR- and IL-1β-induced signalling along the MyD88 to NF-κB pathway. MCMV, more specifically MCMV protein M45, was indeed shown to modulate TLR- and IL-1β-induced NF-κB activation. Initial studies suggest that this is due to a viral block of NF-κB activation independently of the nature of the stimulus provided. This is in contrast to the original hypothesis, which predicted viral modulation of signalling events unique to the TLR- and IL-1β- NF-κB activation pathway. Further research is required into the arising hypothesis that - MCMV, more specifically MCMV protein M45, inhibits NF-κB activation by targeting its immediate regulatory circuit i.e. the function of the IKK complex and IκB proteins. Experiments to test this hypothesis could begin with the following: - Examining NF-κB activation in MCMV infected cells, or cells expressing M45, in response a range of stimuli which utilise various signalling pathways prior to conversion on the TAK1-IKK-IκB regulatory subunit (although care should be taken when choosing stimulating compounds and with interpretation of such experiments as M45 has previously been shown to inhibit signalling, including NF-κB activation, by RIP family members and thus pathways utilising RIP proteins). – Examination of the abundance and phosphorylation state of IKK complex subunits and IκB proteins in non-treated versus M45 expressing cells (whether through infection or transfection), in presences or absence of stimulation. - Examination of whether M45 directly binds to IKK complex

subunits and IκB proteins. The results of such experiments will then determine further research aimed at proving/disproving the above hypothesis.

If the above hypothesis is proven correct, that is M45 is unequivocally shown to inhibit NF-κB, the greater question presenting itself would be - what is the role of M45 inhibition of NF-κB activation in the life cycle of MCMV in vitro? Furthermore, what is the role of this M45 function in vivo i.e. its contribution to pathogenesis? As discussed in Chapter 4, M45 is known to inhibit the function of RIP3 and as a result prevents the infected cell from executing RIP3-dependent cell death. Moreover, there is evidence to suggest that M45 interaction with RIP3 is key to in vivo viral replication, dissemination and pathogenesis. Importantly, a RHIM domain has been found to mediate the M45-RIP3 interaction (Upton et al., 2010). Crucial to future research into M45 will be the identification of the precise protein domain/s underlying its inhibition of NF-κB activity. If the M45 domain required for inhibition of M45 activity is different for that required for interaction with RIP3, it would be possible to separate the two functions by creating mutant viruses with deletions targeting a specific domain and therefore function of M45. This will make it possible to study the in vivo role of NF-κB inhibition by M45 without it being confounded with the in vivo role played by M45 interaction with RIP3. It should be noted that this experiments would have to be designed and interpreted with care as it possible that M45 has additional functions yet to be discovered.

Moreover, it would be of interest to examine the function of M45 throughout the life cycle of MCMV. Research work presented here concentrated on a single time point (7-8 hpi), however M45 expression in infected cells begins at about 6 hpi and increases

thereafter throughout infection. The following question thus arises: are known M45 functions (inhibition of NF-κB activation, as suggested here, and the previously shown modulation of the function of RIP proteins) maintained throughout infection? Does M45 gain, lose or has its functions modified as the environment in the infected cell changes (for example, as the expression of yet to be identified cellular and viral protein interaction partners of M45 is up or down regulated)?

It should also be considered that the central hypothesis for this thesis, namely that MCMV specifically targets TLR- and IL-1β-induced NF-κB activation, requires further examination at times of infection not studied in the work presented here. At the time point examined in this thesis viral inhibition of IL-1β-induced NF-κB activation was shown to be M45 dependent. However, it is possible that the TLR- and IL-1β-induced NF-κB activation is targeted at earlier or later times post infection by a viral product not expressed in the time frame examined in presented experiments. It would be of interest to further study TLR- and IL-1β-induced NF-κB throughout MCMV infection using a M45 deletion mutant.

During work on this thesis it became apparent that similar work was being undertaken by Patricia M. Fliss under the supervision of Prof. Wolfram Brune (Heinrich Pette Institute, Hamburg, Germany). Their research agrees with the findings of this thesis i.e. that M45 inhibits IL-1β- and TLR-induced NF-κB activation. Furthermore, it confirms that, as hypothesised above, this is achieved by M45 disruption of the NF-κB-regulatory module. More specifically, M45 was found to bind to the IKKγ (NEMO) subunit of the

IKK complex, leading to the re-direction of IKKγ to autophagosomes for subsequent degradation in lysosomes (Fliss et al., 2012).

Considering the key role played by NF-κB in mediating intra-cellular- and immune-responses to infection surprisingly little is known about how NF-κB function is modulated by MCMV, or by HCMV for that matter. This study and crucially the identification of the specific viral protein, namely M45, modulating the function of this key transcription factor significantly improves and expands current knowledge regarding CMV- NF-κB interplay. That said the key importance of these finding is that they can serve to assist the dissecting of the role of NF-κB controlled host responses in controlling infection. Moreover, this work together with previous studies identifies M45 as crucial mediator of viral pathogenesis. Thus M45 is marked as a specific target for drug design. Indeed, the ultimate challenge is to translate the insights provided by such research into understanding of viral induced pathogenesis and devising ways to prevent it.

7 Bibliography

Akira, S., and Takeda, K. (2004). Toll-like receptor signalling. Nat Rev Immunol *4*, 499-511.

Angulo, A., Ghazal, P., and Messerle, M. (2000). The major immediate-early gene ie3 of mouse cytomegalovirus is essential for viral growth. J Virol *74*, 11129-11136.

Barbalat, R., Lau, L., Locksley, R.M., and Barton, G.M. (2009). Toll-like receptor 2 on inflammatory monocytes induces type I interferon in response to viral but not bacterial ligands. Nat Immunol *10*, 1200-1207.

Barksby, H.E., Lea, S.R., Preshaw, P.M., and Taylor, J.J. (2007). The expanding family of interleukin-1 cytokines and their role in destructive inflammatory disorders. Clin Exp Immunol *149*, 217-225.

Barton, G.M. (2008). A calculated response: control of inflammation by the innate immune system. J Clin Invest *118*, 413-420.

Barton, G.M., and Kagan, J.C. (2009). A cell biological view of Toll-like receptor function: regulation through compartmentalization. Nat Rev Immunol *9*, 535-542.

Bauernfeind, F., Ablasser, A., Bartok, E., Kim, S., Schmid-Burgk, J., Cavlar, T., and Hornung, V. (2011). Inflammasomes: current understanding and open questions. Cell Mol Life Sci *68*, 765-783.

Benedict, C.A., Angulo, A., Patterson, G., Ha, S., Huang, H., Messerle, M., Ware, C.F., and Ghazal, P. (2004). Neutrality of the canonical NF-kappaB-dependent pathway for human and murine cytomegalovirus transcription and replication in vitro. J Virol *78*, 741-750.

Blasius, A.L., and Beutler, B. (2010). Intracellular toll-like receptors. Immunity *32*, 305-315.

Bodaghi, B., Slobbe-van Drunen, M.E., Topilko, A., Perret, E., Vossen, R.C., van Dam-Mieras, M.C., Zipeto, D., Virelizier, J.L., LeHoang, P., Bruggeman, C.A., and Michelson, S. (1999). Entry of human cytomegalovirus into retinal pigment epithelial and endothelial cells by endocytosis. Invest Ophthalmol Vis Sci *40*, 2598-2607.

Bode, K.A., Schmitz, F., Vargas, L., Heeg, K., and Dalpke, A.H. (2009). Kinetic of RelA activation controls magnitude of TLR-mediated IL-12p40 induction. J Immunol *182*, 2176-2184.

Boeckh, M., and Geballe, A.P. (2011). Cytomegalovirus: pathogen, paradigm, and puzzle. J Clin Invest *121*, 1673-1680.

Boehme, K.W., Guerrero, M., and Compton, T. (2006). Human cytomegalovirus envelope glycoproteins B and H are necessary for TLR2 activation in permissive cells. J Immunol *177*, 7094-7102.

Bowie, A., Kiss-Toth, E., Symons, J.A., Smith, G.L., Dower, S.K., and O'Neill, L.A. (2000). A46R and A52R from vaccinia virus are antagonists of host IL-1 and toll-like receptor signaling. Proc Natl Acad Sci U S A *97*, 10162-10167.

Bresnahan, W.A., and Shenk, T. (2000). A subset of viral transcripts packaged within human cytomegalovirus particles. Science *288*, 2373-2376.

Brocchieri, L., Kledal, T.N., Karlin, S., and Mocarski, E.S. (2005). Predicting coding potential from genome sequence: application to betaherpesviruses infecting rats and mice. J Virol *79*, 7570-7596.

Brown, R.A., Gralewski, J.H., and Razonable, R.R. (2009). The R753Q polymorphism abrogates toll-like receptor 2 signaling in response to human cytomegalovirus. Clin Infect Dis *49*, e96-99.

Browne, E.P., Wing, B., Coleman, D., and Shenk, T. (2001). Altered cellular mRNA levels in human cytomegalovirus-infected fibroblasts: viral block to the accumulation of antiviral mRNAs. J Virol *75*, 12319-12330.

Brune, W., Menard, C., Heesemann, J., and Koszinowski, U.H. (2001). A ribonucleotide reductase homolog of cytomegalovirus and endothelial cell tropism. Science *291*, 303-305.

Brune, W., Nevels, M., and Shenk, T. (2003). Murine cytomegalovirus m41 open reading frame encodes a Golgi-localized antiapoptotic protein. J Virol *77*, 11633-11643.

Busche, A., Angulo, A., Kay-Jackson, P., Ghazal, P., and Messerle, M. (2008). Phenotypes of major immediate-early gene mutants of mouse cytomegalovirus. Med Microbiol Immunol *197*, 233-240.

Cannon, M.J., Schmid, D.S., and Hyde, T.B. (2010). Review of cytomegalovirus seroprevalence and demographic characteristics associated with infection. Rev Med Virol *20*, 202-213.

Cao, Z., Xiong, J., Takeuchi, M., Kurama, T., and Goeddel, D.V. (1996). TRAF6 is a signal transducer for interleukin-1. Nature *383*, 443-446.

Caposio, P., Luganini, A., Bronzini, M., Landolfo, S., and Gribaudo, G. (2010). The Elk-1 and serum response factor binding sites in the major immediate-early promoter of human cytomegalovirus are required for efficient viral replication in quiescent cells and compensate for inactivation of the NF-kappaB sites in proliferating cells. J Virol *84*, 4481-4493.

Caposio, P., Luganini, A., Hahn, G., Landolfo, S., and Gribaudo, G. (2007). Activation of the virus-induced IKK/NF-kappaB signalling axis is critical for the replication of human cytomegalovirus in quiescent cells. Cell Microbiol *9*, 2040-2054.

Cardin, R.D., Abenes, G.B., Stoddart, C.A., and Mocarski, E.S. (1995). Murine cytomegalovirus IE2, an activator of gene expression, is dispensable for growth and latency in mice. Virology *209*, 236-241.

Cargnello, M., and Roux, P.P. (2011). Activation and function of the MAPKs and their substrates, the MAPK-activated protein kinases. Microbiol Mol Biol Rev *75*, 50-83.

Carpenter, S., and O'Neill, L.A. (2009). Recent insights into the structure of Toll-like receptors and post-translational modifications of their associated signalling proteins. Biochem J *422*, 1-10.

Collins, T.M., Quirk, M.R., and Jordan, M.C. (1994). Biphasic viremia and viral gene expression in leukocytes during acute cytomegalovirus infection of mice. J Virol *68*, 6305-6311.

Compton, T., Kurt-Jones, E.A., Boehme, K.W., Belko, J., Latz, E., Golenbock, D.T., and Finberg, R.W. (2003). Human cytomegalovirus activates inflammatory cytokine responses via CD14 and Toll-like receptor 2. J Virol *77*, 4588-4596.

Cuadrado, A., and Nebreda, A.R. (2010). Mechanisms and functions of p38 MAPK signalling. Biochem J *429*, 403-417.

Cusson-Hermance, N., Khurana, S., Lee, T.H., Fitzgerald, K.A., and Kelliher, M.A. (2005). Rip1 mediates the Trif-dependent toll-like receptor 3- and 4-induced NF-{kappa}B activation but does not contribute to interferon regulatory factor 3 activation. J Biol Chem *280*, 36560-36566.

Declercq, W., Vanden Berghe, T., and Vandenabeele, P. (2009). RIP kinases at the crossroads of cell death and survival. Cell *138*, 229-232.

DeFilippis, V.R., Alvarado, D., Sali, T., Rothenburg, S., and Fruh, K. (2010a). Human cytomegalovirus induces the interferon response via the DNA sensor ZBP1. J Virol *84*, 585-598.

DeFilippis, V.R., Sali, T., Alvarado, D., White, L., Bresnahan, W., and Fruh, K.J. (2010b). Activation of the interferon response by human cytomegalovirus occurs via cytoplasmic double-stranded DNA but not glycoprotein B. J Virol *84*, 8913-8925.

Delale, T., Paquin, A., Asselin-Paturel, C., Dalod, M., Brizard, G., Bates, E.E., Kastner, P., Chan, S., Akira, S., Vicari, A., *et al.* (2005). MyD88-dependent and -independent murine cytomegalovirus sensing for IFN-alpha release and initiation of immune responses in vivo. J Immunol *175*, 6723-6732.

Deng, L., Wang, C., Spencer, E., Yang, L., Braun, A., You, J., Slaughter, C., Pickart, C., and Chen, Z.J. (2000). Activation of the IkappaB kinase complex by TRAF6 requires a dimeric ubiquitin-conjugating enzyme complex and a unique polyubiquitin chain. Cell *103*, 351-361.

Diebold, S.S., Kaisho, T., Hemmi, H., Akira, S., and Reis e Sousa, C. (2004). Innate antiviral responses by means of TLR7-mediated recognition of single-stranded RNA. Science *303*, 1529-1531.

Dinarello, C.A. (1996). Biologic basis for interleukin-1 in disease. Blood *87*, 2095-2147.

Dinarello, C.A. (2009). Immunological and inflammatory functions of the interleukin-1 family. Annu Rev Immunol *27*, 519-550.

Dinarello, C.A. (2011a). A clinical perspective of IL-1beta as the gatekeeper of inflammation. Eur J Immunol *41*, 1203-1217.

Dinarello, C.A. (2011b). Interleukin-1 in the pathogenesis and treatment of inflammatory diseases. Blood *117*, 3720-3732.

Dudding, L., Haskill, S., Clark, B.D., Auron, P.E., Sporn, S., and Huang, E.S. (1989). Cytomegalovirus infection stimulates expression of monocyte-associated mediator genes. J Immunol *143*, 3343-3352.

Festjens, N., Vanden Berghe, T., Cornelis, S., and Vandenabeele, P. (2007). RIP1, a kinase on the crossroads of a cell's decision to live or die. Cell Death Differ *14*, 400-410.

Flannery, S., and Bowie, A.G. (2010). The interleukin-1 receptor-associated kinases: critical regulators of innate immune signalling. Biochem Pharmacol *80*, 1981-1991.

Fliss, P.M., Jowers, T.P., Brinkmann, M.M., Holstermann, B., Mack, C., Dickinson, P., Hohenberg, H., Ghazal, P., and Brune, W. (2012). Viral mediated redirection of NEMO/IKKgamma to autophagosomes curtails the inflammatory cascade. PLoS Pathog *8*, e1002517.

Fossum, E., Friedel, C.C., Rajagopala, S.V., Titz, B., Baiker, A., Schmidt, T., Kraus, T., Stellberger, T., Rutenberg, C., Suthram, S., *et al*. (2009). Evolutionarily conserved herpesviral protein interaction networks. PLoS Pathog *5*, e1000570.

Gandhi, M.K., and Khanna, R. (2004). Human cytomegalovirus: clinical aspects, immune regulation, and emerging treatments. Lancet Infect Dis *4*, 725-738.

Ghosh, S., and Hayden, M.S. (2008). New regulators of NF-kappaB in inflammation. Nat Rev Immunol *8*, 837-848.

Gilliet, M., Cao, W., and Liu, Y.J. (2008). Plasmacytoid dendritic cells: sensing nucleic acids in viral infection and autoimmune diseases. Nat Rev Immunol *8*, 594-606.

Gribaudo, G., Ravaglia, S., Guandalini, L., Cavallo, R., Gariglio, M., and Landolfo, S. (1996). The murine cytomegalovirus immediate-early 1 protein stimulates NF-kappa B activity by transactivating the NF-kappa B p105/p50 promoter. Virus Res *45*, 15-27.

Gustems, M., Borst, E., Benedict, C.A., Perez, C., Messerle, M., Ghazal, P., and Angulo, A. (2006). Regulation of the transcription and replication cycle of human cytomegalovirus is insensitive to genetic elimination of the cognate NF-kappaB binding sites in the enhancer. J Virol *80*, 9899-9904.

Haas, T., Metzger, J., Schmitz, F., Heit, A., Muller, T., Latz, E., and Wagner, H. (2008). The DNA sugar backbone 2' deoxyribose determines toll-like receptor 9 activation. Immunity *28*, 315-323.

Hanson, L.K., Slater, J.S., Karabekian, Z., Virgin, H.W.t., Biron, C.A., Ruzek, M.C., van Rooijen, N., Ciavarra, R.P., Stenberg, R.M., and Campbell, A.E. (1999). Replication of murine cytomegalovirus in differentiated macrophages as a determinant of viral pathogenesis. J Virol *73*, 5970-5980.

Harte, M.T., Haga, I.R., Maloney, G., Gray, P., Reading, P.C., Bartlett, N.W., Smith, G.L., Bowie, A., and O'Neill, L.A. (2003). The poxvirus protein A52R targets Toll-like receptor signaling complexes to suppress host defense. J Exp Med *197*, 343-351.

Heil, F., Hemmi, H., Hochrein, H., Ampenberger, F., Kirschning, C., Akira, S., Lipford, G., Wagner, H., and Bauer, S. (2004). Species-specific recognition of single-stranded RNA via toll-like receptor 7 and 8. Science *303*, 1526-1529.

Hemmi, H., Kaisho, T., Takeuchi, O., Sato, S., Sanjo, H., Hoshino, K., Horiuchi, T., Tomizawa, H., Takeda, K., and Akira, S. (2002). Small anti-viral compounds activate immune cells via the TLR7 MyD88-dependent signaling pathway. Nat Immunol *3*, 196-200.

Hemmi, H., Takeuchi, O., Kawai, T., Kaisho, T., Sato, S., Sanjo, H., Matsumoto, M., Hoshino, K., Wagner, H., Takeda, K., and Akira, S. (2000). A Toll-like receptor recognizes bacterial DNA. Nature *408*, 740-745.

Hoffmann, A., Levchenko, A., Scott, M.L., and Baltimore, D. (2002). The IkappaB-NF-kappaB signaling module: temporal control and selective gene activation. Science *298*, 1241-1245.

Hokeness-Antonelli, K.L., Crane, M.J., Dragoi, A.M., Chu, W.M., and Salazar-Mather, T.P. (2007). IFN-alphabeta-mediated inflammatory responses and antiviral defense in

liver is TLR9-independent but MyD88-dependent during murine cytomegalovirus infection. J Immunol *179*, 6176-6183.

Huang, Q., Yang, J., Lin, Y., Walker, C., Cheng, J., Liu, Z.G., and Su, B. (2004). Differential regulation of interleukin 1 receptor and Toll-like receptor signaling by MEKK3. Nat Immunol *5*, 98-103.

Isaacson, M.K., Juckem, L.K., and Compton, T. (2008). Virus entry and innate immune activation. Curr Top Microbiol Immunol *325*, 85-100.

Isern, E., Gustems, M., Messerle, M., Borst, E., Ghazal, P., and Angulo, A. (2011). The activator protein 1 binding motifs within the human cytomegalovirus major immediate-early enhancer are functionally redundant and act in a cooperative manner with the NF-{kappa}B sites during acute infection. J Virol *85*, 1732-1746.

Ishii, K.J., Koyama, S., Nakagawa, A., Coban, C., and Akira, S. (2008). Host innate immune receptors and beyond: making sense of microbial infections. Cell Host Microbe *3*, 352-363.

Iwata, M., Vieira, J., Byrne, M., Horton, H., and Torok-Storb, B. (1999). Interleukin-1 (IL-1) inhibits growth of cytomegalovirus in human marrow stromal cells: inhibition is reversed upon removal of IL-1. Blood *94*, 572-578.

James H. Strauss, E.G.S. (2008). DNA-containing viruses In Viruses and Human Disease (Academic Press).

Janeway, C.A., Jr., and Medzhitov, R. (2002). Innate immune recognition. Annu Rev Immunol *20*, 197-216.

Jarvis, M.A., Borton, J.A., Keech, A.M., Wong, J., Britt, W.J., Magun, B.E., and Nelson, J.A. (2006). Human cytomegalovirus attenuates interleukin-1beta and tumor necrosis factor alpha proinflammatory signaling by inhibition of NF-kappaB activation. J Virol *80*, 5588-5598.

Jurak, I., and Brune, W. (2006). Induction of apoptosis limits cytomegalovirus cross-species infection. EMBO J *25*, 2634-2642.

Kaiser, W.J., Upton, J.W., and Mocarski, E.S. (2008). Receptor-interacting protein homotypic interaction motif-dependent control of NF-kappa B activation via the DNA-dependent activator of IFN regulatory factors. J Immunol *181*, 6427-6434.

Kalejta, R.F. (2008). Tegument proteins of human cytomegalovirus. Microbiol Mol Biol Rev *72*, 249-265, table of contents.

Kawagoe, T., Sato, S., Matsushita, K., Kato, H., Matsui, K., Kumagai, Y., Saitoh, T., Kawai, T., Takeuchi, O., and Akira, S. (2008). Sequential control of Toll-like receptor-dependent responses by IRAK1 and IRAK2. Nat Immunol *9*, 684-691.

Kawai, T., and Akira, S. (2010). The role of pattern-recognition receptors in innate immunity: update on Toll-like receptors. Nat Immunol *11*, 373-384.

Kawai, T., and Akira, S. (2011). Toll-like receptors and their crosstalk with other innate receptors in infection and immunity. Immunity *34*, 637-650.

Keating, S.E., Maloney, G.M., Moran, E.M., and Bowie, A.G. (2007). IRAK-2 participates in multiple toll-like receptor signaling pathways to NFkappaB via activation of TRAF6 ubiquitination. J Biol Chem *282*, 33435-33443.

Kelliher, M.A., Grimm, S., Ishida, Y., Kuo, F., Stanger, B.Z., and Leder, P. (1998). The death domain kinase RIP mediates the TNF-induced NF-kappaB signal. Immunity *8*, 297-303.

Kijpittayarit, S., Eid, A.J., Brown, R.A., Paya, C.V., and Razonable, R.R. (2007). Relationship between Toll-like receptor 2 polymorphism and cytomegalovirus disease after liver transplantation. Clin Infect Dis *44*, 1315-1320.

Kowalik, T.F., Wing, B., Haskill, J.S., Azizkhan, J.C., Baldwin, A.S., Jr., and Huang, E.S. (1993). Multiple mechanisms are implicated in the regulation of NF-kappa B

activity during human cytomegalovirus infection. Proc Natl Acad Sci U S A *90*, 1107-1111.

Krmpotic, A., Bubic, I., Polic, B., Lucin, P., and Jonjic, S. (2003). Pathogenesis of murine cytomegalovirus infection. Microbes Infect *5*, 1263-1277.

Krug, A., French, A.R., Barchet, W., Fischer, J.A., Dzionek, A., Pingel, J.T., Orihuela, M.M., Akira, S., Yokoyama, W.M., and Colonna, M. (2004). TLR9-dependent recognition of MCMV by IPC and DC generates coordinated cytokine responses that activate antiviral NK cell function. Immunity *21*, 107-119.

L.K.Hanson, A.E.C. (2006). Determinants of Macrophage Tropism. In Cytomegaloviruses Molecular Biology and Immunology M. J.Reddehase, ed. (Caister Academic Press), pp. 419-443.

Lacaze, P., Forster, T., Ross, A., Kerr, L.E., Salvo-Chirnside, E., Lisnic, V.J., Lopez-Campos, G.H., Garcia-Ramirez, J.J., Messerle, M., Trgovcich, J., *et al.* (2011). Temporal profiling of the coding and noncoding murine cytomegalovirus transcriptomes. J Virol *85*, 6065-6076.

Le, V.T., Trilling, M., Zimmermann, A., and Hengel, H. (2008). Mouse cytomegalovirus inhibits beta interferon (IFN-beta) gene expression and controls activation pathways of the IFN-beta enhanceosome. J Gen Virol *89*, 1131-1141.

Lee, T.H., Huang, Q., Oikemus, S., Shank, J., Ventura, J.J., Cusson, N., Vaillancourt, R.R., Su, B., Davis, R.J., and Kelliher, M.A. (2003). The death domain kinase RIP1 is essential for tumor necrosis factor alpha signaling to p38 mitogen-activated protein kinase. Mol Cell Biol *23*, 8377-8385.

Lembo, D., Donalisio, M., Hofer, A., Cornaglia, M., Brune, W., Koszinowski, U., Thelander, L., and Landolfo, S. (2004). The ribonucleotide reductase R1 homolog of murine cytomegalovirus is not a functional enzyme subunit but is required for pathogenesis. J Virol *78*, 4278-4288.

Liu, S., and Chen, Z.J. (2011). Expanding role of ubiquitination in NF-kappaB signaling. Cell Res *21*, 6-21.

Loewendorf, A., and Benedict, C.A. (2010). Modulation of host innate and adaptive immune defenses by cytomegalovirus: timing is everything. J Intern Med *267*, 483-501.

Lomaga, M.A., Yeh, W.C., Sarosi, I., Duncan, G.S., Furlonger, C., Ho, A., Morony, S., Capparelli, C., Van, G., Kaufman, S., *et al.* (1999). TRAF6 deficiency results in osteopetrosis and defective interleukin-1, CD40, and LPS signaling. Genes Dev *13*, 1015-1024.

Lund, J.M., Alexopoulou, L., Sato, A., Karow, M., Adams, N.C., Gale, N.W., Iwasaki, A., and Flavell, R.A. (2004). Recognition of single-stranded RNA viruses by Toll-like receptor 7. Proc Natl Acad Sci U S A *101*, 5598-5603.

Mack, C., Sickmann, A., Lembo, D., and Brune, W. (2008). Inhibition of proinflammatory and innate immune signaling pathways by a cytomegalovirus RIP1-interacting protein. Proc Natl Acad Sci U S A *105*, 3094-3099.

Maloney, G., Schroder, M., and Bowie, A.G. (2005). Vaccinia virus protein A52R activates p38 mitogen-activated protein kinase and potentiates lipopolysaccharide-induced interleukin-10. J Biol Chem *280*, 30838-30844.

Manning, G., Whyte, D.B., Martinez, R., Hunter, T., and Sudarsanam, S. (2002). The protein kinase complement of the human genome. Science *298*, 1912-1934.

Manning, W.C., and Mocarski, E.S. (1988). Insertional mutagenesis of the murine cytomegalovirus genome: one prominent alpha gene (ie2) is dispensable for growth. Virology *167*, 477-484.

Masters, S.L., Simon, A., Aksentijevich, I., and Kastner, D.L. (2009). Horror autoinflammaticus: the molecular pathophysiology of autoinflammatory disease (*). Annu Rev Immunol *27*, 621-668.

McGeoch, D.J., Rixon, F.J., and Davison, A.J. (2006). Topics in herpesvirus genomics and evolution. Virus Res *117*, 90-104.

Medzhitov, R. (2007). Recognition of microorganisms and activation of the immune response. Nature *449*, 819-826.

Messerle, M., Crnkovic, I., Hammerschmidt, W., Ziegler, H., and Koszinowski, U.H. (1997). Cloning and mutagenesis of a herpesvirus genome as an infectious bacterial artificial chromosome. Proc Natl Acad Sci U S A *94*, 14759-14763.

Mettenleiter, T.C., Klupp, B.G., and Granzow, H. (2009). Herpesvirus assembly: an update. Virus Res *143*, 222-234.

Meylan, E., Burns, K., Hofmann, K., Blancheteau, V., Martinon, F., Kelliher, M., and Tschopp, J. (2004). RIP1 is an essential mediator of Toll-like receptor 3-induced NF-kappa B activation. Nat Immunol *5*, 503-507.

Meylan, E., and Tschopp, J. (2005). The RIP kinases: crucial integrators of cellular stress. Trends Biochem Sci *30*, 151-159.

Mocarski, E.S., Jr. (2002). Immunomodulation by cytomegaloviruses: manipulative strategies beyond evasion. Trends Microbiol *10*, 332-339.

Mocarski, E.S., Jr. (2004). Immune escape and exploitation strategies of cytomegaloviruses: impact on and imitation of the major histocompatibility system. Cell Microbiol *6*, 707-717.

Mocarski, E.S., Jr., Thomas Shenk, Robert F. Pass (2006). Cytomegaloviruses. In Fields Virology, P.M.H.M. David M. Knipe PhD, ed. (Lippincott Williams & Wilkins), pp. 2702-2758.

Montag, C., Wagner, J., Gruska, I., and Hagemeier, C. (2006). Human cytomegalovirus blocks tumor necrosis factor alpha- and interleukin-1beta-mediated NF-kappaB signaling. J Virol *80*, 11686-11698.

Netea, M.G., Simon, A., van de Veerdonk, F., Kullberg, B.J., Van der Meer, J.W., and Joosten, L.A. (2010). IL-1beta processing in host defense: beyond the inflammasomes. PLoS Pathog *6*, e1000661.

O'Neill, L.A. (2008). The interleukin-1 receptor/Toll-like receptor superfamily: 10 years of progress. Immunol Rev *226*, 10-18.

O'Neill, L.A., and Bowie, A.G. (2007). The family of five: TIR-domain-containing adaptors in Toll-like receptor signalling. Nat Rev Immunol *7*, 353-364.

Oeckinghaus, A., Hayden, M.S., and Ghosh, S. (2011). Crosstalk in NF-kappaB signaling pathways. Nat Immunol *12*, 695-708.

Paludan, S.R., Bowie, A.G., Horan, K.A., and Fitzgerald, K.A. (2011). Recognition of herpesviruses by the innate immune system. Nat Rev Immunol *11*, 143-154.

Pass, F.R. (2001). Cytomegaloviruses. In Fields Virology
P.M.H.M. David M. Knipe PhD, ed. (Lippincott Williams & Wilkins), pp. 2675-2705.

Philip E. Pellett, B.R. (2006). The Family Herpesviridae: A Brief Introduction. In Fields Virology, P.M.H.M. David M. Knipe PhD, ed. (Lippincott Williams & Wilkins), pp. 2479-2497.

Popkin, D.L., and Virgin, H.W.t. (2003). Murine cytomegalovirus infection inhibits tumor necrosis factor alpha responses in primary macrophages. J Virol *77*, 10125-10130.

Price, P., and Olver, S.D. (1996). Syndromes induced by cytomegalovirus infection. Clin Immunol Immunopathol *80*, 215-224.

Prosch, S., Staak, K., Stein, J., Liebenthal, C., Stamminger, T., Volk, H.D., and Kruger, D.H. (1995). Stimulation of the human cytomegalovirus IE enhancer/promoter in HL-60 cells by TNFalpha is mediated via induction of NF-kappaB. Virology *208*, 197-206.

Randolph-Habecker, J., Iwata, M., Geballe, A.P., Jarrahian, S., and Torok-Storb, B. (2002). Interleukin-1-mediated inhibition of cytomegalovirus replication is due to increased IFN-beta production. J Interferon Cytokine Res *22*, 765-772.

Rathinam, V.A., and Fitzgerald, K.A. (2010). Inflammasomes and anti-viral immunity. J Clin Immunol *30*, 632-637.

Rathinam, V.A., and Fitzgerald, K.A. (2011). Innate immune sensing of DNA viruses. Virology *411*, 153-162.

Rathinam, V.A., Jiang, Z., Waggoner, S.N., Sharma, S., Cole, L.E., Waggoner, L., Vanaja, S.K., Monks, B.G., Ganesan, S., Latz, E., *et al.* (2010). The AIM2 inflammasome is essential for host defense against cytosolic bacteria and DNA viruses. Nat Immunol *11*, 395-402.

Rawlinson, W.D., Farrell, H.E., and Barrell, B.G. (1996). Analysis of the complete DNA sequence of murine cytomegalovirus. J Virol *70*, 8833-8849.

Rebsamen, M., Heinz, L.X., Meylan, E., Michallet, M.C., Schroder, K., Hofmann, K., Vazquez, J., Benedict, C.A., and Tschopp, J. (2009). DAI/ZBP1 recruits RIP1 and RIP3 through RIP homotypic interaction motifs to activate NF-kappaB. EMBO Rep *10*, 916-922.

Reddehase, M.J., Podlech, J., and Grzimek, N.K. (2002). Mouse models of cytomegalovirus latency: overview. J Clin Virol *25 Suppl 2*, S23-36.

Ruzek, M.C., Miller, A.H., Opal, S.M., Pearce, B.D., and Biron, C.A. (1997). Characterization of early cytokine responses and an interleukin (IL)-6-dependent pathway of endogenous glucocorticoid induction during murine cytomegalovirus infection. J Exp Med *185*, 1185-1192.

Ryckman, B.J., Jarvis, M.A., Drummond, D.D., Nelson, J.A., and Johnson, D.C. (2006). Human cytomegalovirus entry into epithelial and endothelial cells depends on genes UL128 to UL150 and occurs by endocytosis and low-pH fusion. J Virol *80*, 710-722.

S. J. Flint, L.W.E., V. R. Racaniello, A. M. Skalka (2009). The infectious cycle. In Principles of virology (USA: ASM press), p. 38.

Sambucetti, L.C., Cherrington, J.M., Wilkinson, G.W., and Mocarski, E.S. (1989). NF-kappa B activation of the cytomegalovirus enhancer is mediated by a viral transactivator and by T cell stimulation. EMBO J *8*, 4251-4258.

Sato, S., Sanjo, H., Takeda, K., Ninomiya-Tsuji, J., Yamamoto, M., Kawai, T., Matsumoto, K., Takeuchi, O., and Akira, S. (2005). Essential function for the kinase TAK1 in innate and adaptive immune responses. Nat Immunol *6*, 1087-1095.

Scalzo, A.A., Corbett, A.J., Rawlinson, W.D., Scott, G.M., and Degli-Esposti, M.A. (2007). The interplay between host and viral factors in shaping the outcome of cytomegalovirus infection. Immunol Cell Biol *85*, 46-54.

Schattgen, S.A., and Fitzgerald, K.A. (2011). The PYHIN protein family as mediators of host defenses. Immunol Rev *243*, 109-118.

Scrivano, L., Esterlechner, J., Muhlbach, H., Ettischer, N., Hagen, C., Grunewald, K., Mohr, C.A., Ruzsics, Z., Koszinowski, U., and Adler, B. (2010). The m74 gene product of murine cytomegalovirus (MCMV) is a functional homolog of human CMV gO and determines the entry pathway of MCMV. J Virol *84*, 4469-4480.

Sen, R., and Smale, S.T. (2010). Selectivity of the NF-{kappa}B response. Cold Spring Harb Perspect Biol *2*, a000257.

Sims, J.E., and Smith, D.E. (2010). The IL-1 family: regulators of immunity. Nat Rev Immunol *10*, 89-102.

Sinzger, C. (2008). Entry route of HCMV into endothelial cells. J Clin Virol *41*, 174-179.

Smith, M.S., Bentz, G.L., Alexander, J.S., and Yurochko, A.D. (2004). Human cytomegalovirus induces monocyte differentiation and migration as a strategy for dissemination and persistence. J Virol *78*, 4444-4453.

Stinski, M.F., and Isomura, H. (2008). Role of the cytomegalovirus major immediate early enhancer in acute infection and reactivation from latency. Med Microbiol Immunol *197*, 223-231.

Stipan Jonjic, I.B., Astrid Krmpotic (2006). Innate Immunity to Cytomegaloviruses. In Cytomegaloviruses Molecular Biology and Immunology M. J.Reddehase, ed. (Caister Academic Press), pp. 285-319.

Stoddart, C.A., Cardin, R.D., Boname, J.M., Manning, W.C., Abenes, G.B., and Mocarski, E.S. (1994). Peripheral blood mononuclear phagocytes mediate dissemination of murine cytomegalovirus. J Virol *68*, 6243-6253.

Suzuki, N., Suzuki, S., Duncan, G.S., Millar, D.G., Wada, T., Mirtsos, C., Takada, H., Wakeham, A., Itie, A., Li, S., *et al.* (2002). Severe impairment of interleukin-1 and Toll-like receptor signalling in mice lacking IRAK-4. Nature *416*, 750-756.

Szomolanyi-Tsuda, E., Liang, X., Welsh, R.M., Kurt-Jones, E.A., and Finberg, R.W. (2006). Role for TLR2 in NK cell-mediated control of murine cytomegalovirus in vivo. J Virol *80*, 4286-4291.

Tabeta, K., Georgel, P., Janssen, E., Du, X., Hoebe, K., Crozat, K., Mudd, S., Shamel, L., Sovath, S., Goode, J., *et al.* (2004). Toll-like receptors 9 and 3 as essential components of innate immune defense against mouse cytomegalovirus infection. Proc Natl Acad Sci U S A *101*, 3516-3521.

Takaoka, A., Wang, Z., Choi, M.K., Yanai, H., Negishi, H., Ban, T., Lu, Y., Miyagishi, M., Kodama, T., Honda, K., *et al.* (2007). DAI (DLM-1/ZBP1) is a cytosolic DNA sensor and an activator of innate immune response. Nature *448*, 501-505.

Takeuchi, O., and Akira, S. (2010). Pattern recognition receptors and inflammation. Cell *140*, 805-820.

Taylor, R.T., and Bresnahan, W.A. (2006). Human cytomegalovirus IE86 attenuates virus- and tumor necrosis factor alpha-induced NFkappaB-dependent gene expression. J Virol *80*, 10763-10771.

Terhune, S.S., Schroer, J., and Shenk, T. (2004). RNAs are packaged into human cytomegalovirus virions in proportion to their intracellular concentration. J Virol *78*, 10390-10398.

Upton, J.W., Kaiser, W.J., and Mocarski, E.S. (2008). Cytomegalovirus M45 cell death suppression requires receptor-interacting protein (RIP) homotypic interaction motif (RHIM)-dependent interaction with RIP1. J Biol Chem *283*, 16966-16970.

Upton, J.W., Kaiser, W.J., and Mocarski, E.S. (2010). Virus inhibition of RIP3-dependent necrosis. Cell Host Microbe *7*, 302-313.

van der Meer, J.W., Rubin, R.H., Pasternack, M., Medearis, D.N., Lynch, P., and Dinarello, C.A. (1989). The in vivo and in vitro effects of interleukin-1 and tumor necrosis factor on murine cytomegalovirus infection. Biotherapy *1*, 227-231.

Wagner, M., Jonjic, S., Koszinowski, U.H., and Messerle, M. (1999). Systematic excision of vector sequences from the BAC-cloned herpesvirus genome during virus reconstitution. J Virol *73*, 7056-7060.

Wan, Y., Kim, T.W., Yu, M., Zhou, H., Yamashita, M., Kang, Z., Yin, W., Wang, J.A., Thomas, J., Sen, G.C., *et al.* (2011). The dual functions of IL-1 receptor-associated

kinase 2 in TLR9-mediated IFN and proinflammatory cytokine production. J Immunol *186*, 3006-3014.

Wang, C., Deng, L., Hong, M., Akkaraju, G.R., Inoue, J., and Chen, Z.J. (2001). TAK1 is a ubiquitin-dependent kinase of MKK and IKK. Nature *412*, 346-351.

Weber, A., Wasiliew, P., and Kracht, M. (2010). Interleukin-1 (IL-1) pathway. Sci Signal *3*, cm1.

Yamazaki, K., Gohda, J., Kanayama, A., Miyamoto, Y., Sakurai, H., Yamamoto, M., Akira, S., Hayashi, H., Su, B., and Inoue, J. (2009). Two mechanistically and temporally distinct NF-kappaB activation pathways in IL-1 signaling. Sci Signal *2*, ra66.

Yao, J., Kim, T.W., Qin, J., Jiang, Z., Qian, Y., Xiao, H., Lu, Y., Qian, W., Gulen, M.F., Sizemore, N., *et al.* (2007). Interleukin-1 (IL-1)-induced TAK1-dependent Versus MEKK3-dependent NFkappaB activation pathways bifurcate at IL-1 receptor-associated kinase modification. J Biol Chem *282*, 6075-6089.

Yasuda, K., Rutz, M., Schlatter, B., Metzger, J., Luppa, P.B., Schmitz, F., Haas, T., Heit, A., Bauer, S., and Wagner, H. (2006). CpG motif-independent activation of TLR9 upon endosomal translocation of "natural" phosphodiester DNA. Eur J Immunol *36*, 431-436.

Yasuda, K., Yu, P., Kirschning, C.J., Schlatter, B., Schmitz, F., Heit, A., Bauer, S., Hochrein, H., and Wagner, H. (2005). Endosomal translocation of vertebrate DNA activates dendritic cells via TLR9-dependent and -independent pathways. J Immunol *174*, 6129-6136.

Yerkovich, S.T., Olver, S.D., Lenzo, J.C., Peacock, C.D., and Price, P. (1997). The roles of tumour necrosis factor-alpha, interleukin-1 and interleukin-12 in murine cytomegalovirus infection. Immunology *91*, 45-52.

Yurochko, A.D., and Huang, E.S. (1999). Human cytomegalovirus binding to human monocytes induces immunoregulatory gene expression. J Immunol *162*, 4806-4816.

Yurochko, A.D., Hwang, E.S., Rasmussen, L., Keay, S., Pereira, L., and Huang, E.S. (1997). The human cytomegalovirus UL55 (gB) and UL75 (gH) glycoprotein ligands initiate the rapid activation of Sp1 and NF-kappaB during infection. J Virol *71*, 5051-5059.

Zucchini, N., Bessou, G., Traub, S., Robbins, S.H., Uematsu, S., Akira, S., Alexopoulou, L., and Dalod, M. (2008). Cutting edge: Overlapping functions of TLR7 and TLR9 for innate defense against a herpesvirus infection. J Immunol *180*, 5799-5803.